THESIS FOR THE DEGREE OF DOCTOR OF PHILOSOPHY

Recycling of CIGS solar cell waste materials

ANNA M. K. GUSTAFSSON

Department of Chemical and Biological Engineering

CHALMERS UNIVERSITY OF TECHNOLOGY

Gothenburg, Sweden 2014

Recycling of CIGS solar cell waste materials
ANNA M. K. GUSTAFSSON
ISBN 978-91-7597-080-6

Doktorsavhandlingar vid Chalmers tekniska högskola
Serie nr 3761
ISSN 0346-718X

Industrial Materials Recycling
Department of Chemical and Biological Engineering
Chalmers University of Technology
SE-412 96 Gothenburg
Sweden
Telephone + 46 (0)31-772 1000

Cover: Electrochemical separation of copper

Chalmers Reproservice
Gothenburg, Sweden 2014

Recycling of CIGS solar cell materials

ANNA M. K. GUSTAFSSON

Industrial materials recycling
Department of Chemical and Biological Engineering
Chalmers University of Technology

ABSTRACT

The increased interest in solar power over the last few decades has led to a constant development of existing and new types of solar cells. One type of solar cell that is making advances on the global market is copper indium gallium diselenide (CIGS) thin film solar cells. The advantage of thin film solar cells is that they require less semiconductor material than conventional silicon solar cells and as a result are more cost effective. However, the CIGS material contains the valuable and rare elements indium and gallium, which makes recycling of CIGS materials necessary in order to ensure a future supply and keep production costs down. In the future there will be a need to recycle all solar cells currently being installed, but at present the biggest issue is the large amounts of waste material that are generated from the solar cell production.

The use of recycled CIGS materials in new solar cells requires separation and purification (up to 99.999 %) of the elements. The goal of the work presented in this thesis was therefore to develop a recycling process for CIGS in which the elements are separated from each other, preferably with high enough purity to allow direct use in new solar cells without further purification.

In this work a new, innovative recycling process for CIGS material was developed. Firstly, the separation of selenium, as selenium dioxide, was achieved by oxidation of the CIGS material at elevated temperatures. The method resulted in a selenium recovery above 99 %. After reduction of the selenium dioxide the recovered selenium had a purity of 99.999 wt% with respect to scandium, titanium, vanadium, chromium, manganese, iron, cobalt, nickel and zinc, which are the elements that might decrease the solar cell efficiency.

Next the separation of the remaining elements was achieved with selective electrodeposition. Electrodeposition of copper and indium, using different potentials, resulted in an almost complete separation of the elements. High-temperature chlorination and solvent extraction was also tested for separation of copper, indium and gallium. However, electrochemical separation and was determined to be the promising separation method for future process development.

KEYWORDS: Recycling, Solar cells, CIGS, Pyrometallurgy, Hydrometallurgy

LIST OF PUBLICATIONS

This thesis is based on the work contained in the following papers:

PAPER I

Gustafsson, A.M.K., Foreman, M.R.S., and Ekberg, C. Recycling of high purity selenium from CIGS solar cell waste materials. Waste Management, 2014. DOI: http://dx.doi.org/10.1016/j.wasman.2013.12.021

PAPER II

Gustafsson, A.M.K., Steenari, B.-M., and Ekberg, C. Evaluation of high-temperature chlorination as a process for separation of copper, indium and gallium from CIGS solar cell waste materials. Separation Science and Technology, 2014. DOI: http://dx.doi.org/10.1080/01496395.2014.949350

PAPER III

Gustafsson, A.M.K., Steenari, B.-M., and Ekberg, C. Recycling of CIGS solar cell waste materials - separation of copper, indium and gallium by high-temperature chlorination reaction with ammonium chloride. Submitted for publication in Separation Science and Technology

PAPER IV

Gustafsson, A.M.K., Björefors, F., Steenari, B.-M., and Ekberg, C. Electrochemical separation of copper, indium and gallium for recycling of CIGS solar cell waste materials. Submitted for publication in Hydrometallurgy

Contribution report

Paper I-IV All experimental work, data treatment, evaluation and major part of writing of the manuscripts.

Table of Contents

1. Introduction

Solar cells are considered by many to be part of the future energy mix [1]. The amount of energy coming from the sun makes it the largest available energy source, but the question is how to best utilize that energy [2]. One way to exploit solar energy is to use solar cells, which transform solar energy into electricity. The ability of some materials to convert light into electricity is called the photovoltaic (PV) effect and was discovered by Henry Becquerel in 1839 [3]. Since then extensive work has resulted in a number of different types of solar cells that are used in a variety of applications; from terrestrial applications supplying power to the national grid to applications in space [4]. Today the importance of solar cells as a power source is growing due to the environmental advantages compared to fossil fuels [5]. New PV materials, devices and production methods are constantly being developed in order to increase cell efficiency and minimize the energy and material consumption, thereby making PV power more competitive both economically and environmentally when compared with other power sources. The progress in this area has been reviewed by several authors [5-11]. At present the most common solar cell material is silicon, but other types of PV materials, such as cadmium telluride (CdTe) and copper indium gallium diselenide (CIGS), are making advances on the global market [12]. CdTe and CIGS are used in thin film solar cells, which require much less semiconductor material than conventional silicon solar cells and as a result are more cost effective [13]. Lately the issue of recycling spent solar cells and production waste has been receiving attention, especially since most PV technologies utilize expensive, rare, or toxic elements [14]. This is definitely the case with CIGS thin film solar cells, where the utilization of the scarce and valuable metals indium and gallium makes recycling of CIGS materials necessary in order to keep production costs down [15]. In 2010 the European Commission identified both indium and gallium, along with only twelve other materials, as critical raw materials with regards to supply shortage and economic impact in the European Union [16]. In the future there will be a need to recycle all solar cells currently being installed [17], but at present the biggest issue is the large amounts of waste material that are generated from solar cell production [18]. The production of high efficiency solar cells requires the materials used in the semiconductor production to be of high purity. For CIGS solar cells this means that the recycled materials must have a purity of at least 99.999 % to be used directly in new solar cells [19]. A number of recycling processes for CIGS solar cells and production waste materials have been presented [19-25]. However, only two of the processes actually result in the separation of the elements and none of these result in recycled materials of high-purity. The goal of the work presented in this thesis has therefore been to develop a recycling process for CIGS in which the elements (copper, indium gallium and selenium) are separated from each other, preferably with high enough purity to allow direct use in new solar cells without further purification.

2. Background

2.1 Solar cells

A description of the most common types of solar cells and their construction can be found in Appendix A. These include the standard pn-junction solar cells (e.g. single crystal silicon solar cells) and thin film solar cells (e.g. CIGS and CdTe solar cells). This work is focused on CIGS and the main emphasis is therefore here.

2.1.1 CIGS solar cells

In CIGS solar cells the semiconductor layer is made from a thin film of $Cu(In,Ga)Se_2$. The advantage of thin film technologies, compared to e.g. standard silicon solar cells, is that each solar cell only contains minor amounts of the valuable semiconductor. The CIGS material consists of $CuInSe_2$ with some percentages of the indium replaced by gallium. By modifying the amount of gallium the bandwidth (see Appendix A) of the solar cell can be adjusted and a higher efficiency device can be achieved [26, 27]. The possibility to modify the composition of the CIGS absorber and produce high efficiency devices on a laboratory scale has made the technology one of the most promising thin film technologies [7, 28]. One challenge with this technology is that the CIGS material contains four different elements, which makes the system complex and production therefore demands a high level of process control [26]. The scale up to large-scale production with preserved solar cell efficiency has been difficult to achieve due to the complexity of the processes [7] and high investment costs [13]. There are several different manufacturing processes for CIGS solar cells, but the two most common approaches are (1) co-evaporation and (2) selenization [7]. In the co-evaporation process evaporation sources are heated under vacuum and the evaporated atoms are deposited on the substrate. The selenization process starts with the deposition of a film containing only copper, indium and gallium, with e.g. sputtering, followed by selenization with, for example, hydrogen selenide [29]. The co-evaporation process has been used to produce high efficiency laboratory scale solar cells, but the selenization process has been more successful in industrial scale production [14]. Another challenge is that, independent of the CIGS solar cell production method, large amounts (up to 34 %) of the starting material are lost in different waste streams [18]. The recycling of this waste material is of great importance for the future advance of the technology.

2.2 Recycling of solar cells

Interest in the recycling of solar cell modules has increased over recent years, but normally only the aluminium frame and the glass encasing the solar cells are recycled. A number of recycling methods have been described in the literature, but only a few have been commercialized [30, 31]. While this section is focused on the recycling of CIGS solar cells, a description of recycling methods for silicon and CdTe solar cells can be found in Appendix A.

2.2.1 Recycling of CIGS solar cells

Today only a small fraction of the indium and gallium used in different applications are recycled [32] and to ensure a future supply of these relatively rare elements, recycling of CIGS solar cells and waste material is necessary [16]. The literature includes some processes that only consider the removal of the CI(G)S material (with or without gallium) from the substrate for further processing [19, 22]. Menezes on the other hand developed an electrochemical method to transfer CIS material directly from an old solar cell to a new one [23]. A cyclic variation of the electrochemical potential was used to dissolve the old CIGS film and deposit the material on the new cell. A more detailed study of the mechanisms, e.g. potentials and electrolyte composition, of the process has also been done [33]. So far only two recycling processes have been presented where the elements are separated [20, 21]. Drinkard *et al.* [21] leached CIS material with nitric acid before electrochemically separating copper and selenium from indium. After dissolution of the copper/selenium deposit in sulphuric or nitric acid and evaporation of the solvent the copper and selenium was separated by distillation of the selenium dioxide formed. The indium was recovered as indium oxide after evaporation and decomposition of the copper and selenium-depleted leach solution. In the SENSE project [20] a variety of hydrometallurgical methods, including leaching, solvent extraction and precipitation, were used to separate the elements. CIGS material was leached with oxidizing acid and indium was separated using di-(2-ethylhexyl) phosphoric acid (D2EHPA). The indium was stripped from the organic phase and recovered by precipitation or electrodeposition. Recovery of selenium was achieved by reduction with sulphur dioxide followed by filtration and gallium was precipitated as gallium hydroxide. There are also some examples of companies that recycle CI(G)S. Loser Chemie are using a universal wet chemical recycling process for recycling of thin film solar cells, and solar cell waste materials, containing CI(G)S and CdTe [24, 25]. The process includes treating mechanically processed cells with 15 % hydrochloric acid with an addition of a catalytic amount of hydrogen peroxide to de-metallize the substrates. The process yields recyclable fractions of glass and/or laminating plastics along with concentrates containing metal salts, which can be further processed. In addition, the Canadian company 5N Plus recycles both CIGS and CdTe solar cells while the Belgian company Umicore recycles the elements from CIGS solar cells using a hydrometallurgical process [31]. No further details on what the recycling processes used by 5N Plus and Umicore has been found.

2.3 Purity of the recycled materials

In general the production of high efficiency solar cells requires the materials used in the semiconductor production to be of high purity. In the case of CIGS solar cells this means that the recycled materials must have a purity of at least 99.999 % to be used directly in new solar cells [19]. According to Langer and Heinrich [34] all 3d transition metal impurities might decrease the efficiency of solar cells and these elements are therefore of special interest when it comes to the purity of the recycled materials.

2.4 Copper

Copper is mainly found in low-grade sulphide (e.g. $CuFeS_2$, Cu_2S) and oxide ores (e.g. Cu_2O, $Cu_2CO_3(OH)_2$), which often contain less than 1 % copper [35-37]. One source of copper that is becoming more important is scrap copper and alloys and in 2010 the copper produced by recycling amounted to 10-15 % of the total production [36]. Sulphide ores are typically treated by pyrometallurgical methods while oxide ores are leached with sulphuric acid, purified by solvent extraction and recovered by electrodeposition [36, 37]. The pyrometallurgical treatment includes e.g. roasting, smelting and fire refining, followed by electrorefining.

2.5 Indium

Indium is a scarce element that is primarily recovered as a by-product from zinc, and in some cases lead, processing [38-40]. Since the price of indium would have to increase significantly to make direct mining of the few and small indium deposits found around the world economically feasible the availability of indium is limited by the zinc production [15]. Indium is leached from the zinc processing by-products with sulphuric or hydrochloric acid and the indium-containing solution is purified in several steps before sponge indium is precipitated by addition of zinc [38-40]. The recovery of sponge indium is then normally followed by electrorefining. The indium metal that is formed is soft, with a melting point of 156 °C and a boiling point of 2070 °C [39].

2.6 Gallium

The dominating commercial source of gallium is Bayer liquid, which is caustic liquid from the aluminium recovery industry [35, 39, 41]. Today the most common method for separation of gallium from Bayer liquid is solvent extraction [39] and the primary extractant used is Kelex 100 [41]. After the separation step gallium metal is produced by electrodeposition [39]. Further purification can be done by vacuum refining, electrorefining or fractional crystallization [39]. Another suggested purification method is halogenation where gallium is chlorinated and the formed gallium chloride is distilled [42]. Gallium has a melting point of 29.8 °C and a boiling point of 2420 °C [39].

2.7 Selenium

Selenium is a relatively rare element in the earth's crust and is mainly recovered from electrolytic copper refining slimes [35, 37]. Several different methods for selenium recovery from the slimes have been developed e.g. soda ash roasting, sulphuric acid roasting and direct volatilization of selenium dioxide [35, 37, 43]. Selenium is found in several allotropic forms [35]. The amorphous form exists in two different colours, red and black, and red selenium is transformed to black selenium when heated or by aging. The black selenium is the form most commonly used in industry. In the crystalline form selenium is found as dark red, transparent crystals and the metallic form is glossy grey [44]. Upon heating, the amorphous and crystalline allotropes are transformed into metallic selenium [35]. Selenium has a melting point of 217 °C and a boiling point of 685 °C [35]

2.8 Explored separation paths for CIGS material

The use of recycled CIGS materials in new solar cells requires separation and purification of the elements [7, 19]. The separation paths explored in this thesis are shown in Fig. 2.1. Selenium is the element in CIGS that is most unlike the other elements [29]. Thus, the separation of selenium is the best starting point for recycling. After selenium separation, several methods could potentially be used to separate the remaining elements e.g. high-temperature chlorination and, after dissolution of the solid material, solvent extraction or electrodeposition.

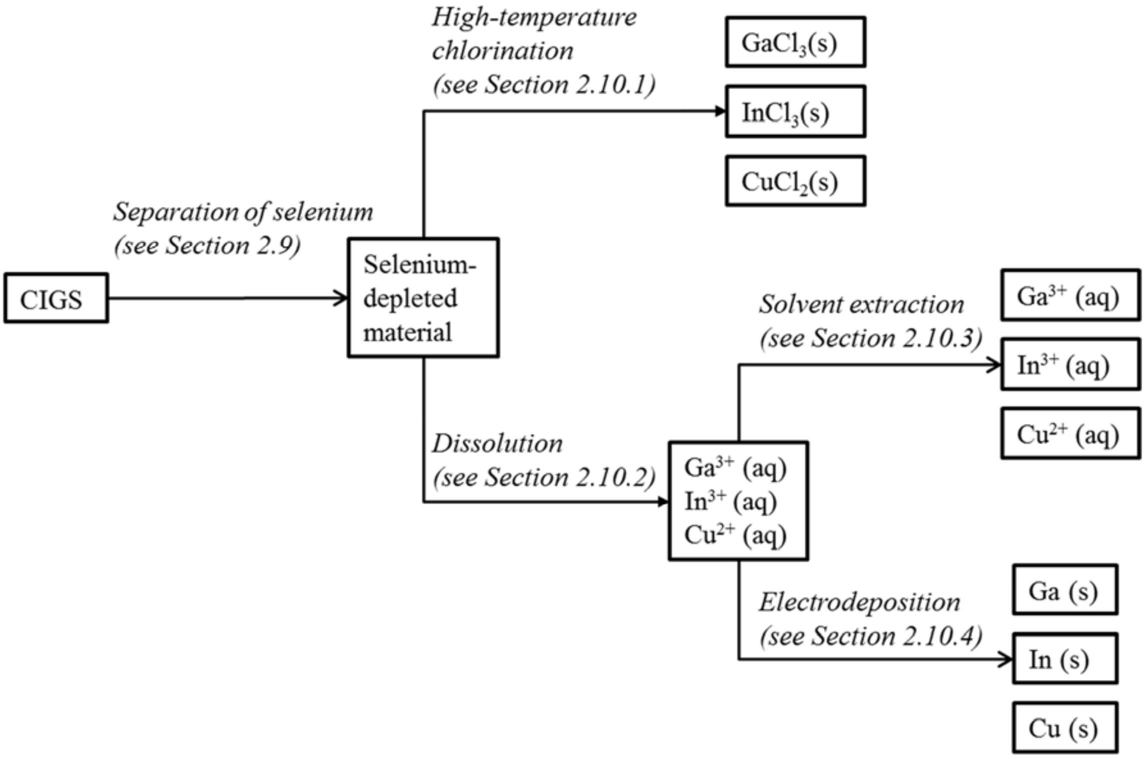

Fig. 2.1 Flow chart of the explored paths for separation of the elements in CIGS.

2.9 Separation of selenium from CIGS

There are several possible hydrometallurgical methods that could be used for the separation of selenium from CIGS e.g. electrodeposition [21] or precipitation [20] from aqueous solution, but it would be of advantage if the separation could be done in such a way that selenium could be obtained directly at high purity. Separation of selenium, or a compound thereof, in a gas phase is therefore of interest.

2.9.1 Distillation of selenium dioxide

Distillation is a well-tried method for the separation of different elements and compounds. During distillation the difference in volatility of the different compounds is utilized. An advantage with this kind of separation is that the separated element can be obtained with very high purity if optimal process parameters are used. The purification of selenium by distillation of selenium dioxide, formed by heating selenium to above 317 °C in an oxygen-containing atmosphere, has been described by several authors [45-47]. The reaction, which is catalysed by nitrogen oxides [46, 47] or alternatively by copper, chromium or magnesium oxides [45], results in the formation of gaseous selenium dioxide that upon cooling sublimes and can be collected as crystals. After reduction of the selenium dioxide the process results in high purity selenium. For separation of selenium from CIGS by oxidation to selenium dioxide the general oxidation reaction is presented in Reaction (2.1). Me_xO_y represents the different metal oxides (pure oxides of copper, indium and gallium, or mixed oxides containing two or more of the metals) that may form during the oxidation.

$$Cu(In,Ga)Se_2\ (s) + (4+1/2y)O_2\ (g) \leftrightarrows 2SeO_2\ (g) + Me_xO_y\ (s) \qquad (2.1)$$

Upon cooling, the selenium dioxide sublime according to Reaction (2.2).

$$SeO_2\ (g) \rightarrow SeO_2\ (s) \qquad (2.2)$$

Reduction of selenium dioxide to selenium can be achieved by the use of the selenium dioxide as a mild oxidizing agent for organic compounds, e.g. oxidation of a ketone to a di-ketone according to Reaction (2.3), as first described by Riley *et al.* in 1932 [48]. Since then this type of reaction has been extensively studied and used in numerous applications [49-51].

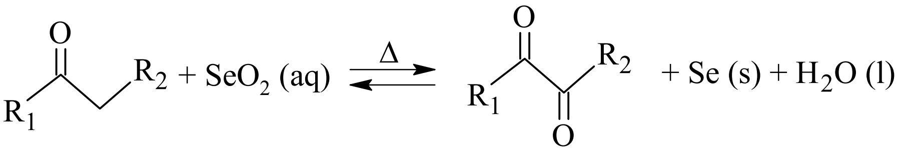

(2.3)

Selenium dioxide can also be reduced using a wide variety of inorganic reducing agents [51]. One of the reducing agents described in the literature is sulphur dioxide gas (see Reaction (2.4)) [20, 43, 46, 52].

$$SeO_2\ (aq) + 2SO_2\ (g) + 2H_2O\ (l) \leftrightarrows Se\ (s) + 2H_2SO_4\ (aq) \qquad (2.4)$$

The advantage of this reduction method is a decreased risk of contamination of the selenium produced.

2.9.2 Separation of selenium as hydrogen selenide

Under certain conditions selenium can be reduced to hydrogen selenide, which is a gas at room temperature. The reduction of the selenium to hydrogen selenide could therefore possibly be used as a method for separation of selenium from the other elements in CIGS. In addition, hydrogen selenide is used in the selenization step of the CIGS solar cell production [44]. Thus, the recycled selenium in the form of hydrogen selenide could be used directly in new solar cells. However, hydrogen selenide is a flammable and highly toxic gas [35] and the production and handling therefore require high levels of safety.

The preparation of hydrogen selenide can be done in several different ways. The most common production methods involve the reaction of water with aluminium selenide (Al_2Se_3) or the hydrolysis of iron selenide (FeSe) by a dilute mineral acid [35], but there are also methods to produce hydrogen selenide directly from selenium, either in solid state or dissolved in liquid. According to Patnaik [44], hydrogen selenide can be produced via reduction of selenium with hydrogen gas at 440 °C (see Reaction (2.5)).

$$Se\ (s\ or\ g) + H_2\ (g) \leftrightarrows H_2Se\ (g) \qquad (2.5)$$

This reaction between selenium and hydrogen in the gas phase has also been described by Greenwood [35], but here the reaction is said to be surface catalysed in the temperature range between 350 and 650° C. Sonoda *et al.* [53] prepared hydrogen selenide from metallic selenium with water and carbon monoxide gas in the presence of a mild base according to Reaction (2.6).

$$Se\ (s) + CO\ (g) + H_2O\ (l) \leftrightarrows H_2Se\ (g) + CO_2\ (g) \qquad (2.6)$$

There are some examples of sodium borohydride being used as a reducing agent for the production of hydrogen selenide for the analysis of selenium with atomic absorption spectroscopy [54, 55]. Several metals interfere with this reaction, among them copper [54]. To avoid interference the copper can be removed from the solution as copper hydroxide precipitate [55]. Some electrochemical methods have also been suggested [56, 57]. Hydrogen peroxide, although it is known for its oxidizing properties, can under certain conditions also work as a reducing agent [35, 44].

Several tests on the separation of selenium from CIGS with the methods described above have been presented in previously published work [58]. None of the tests resulted in hydrogen selenide and are therefore not discussed further in this thesis.

2.10 Separation of copper, indium and gallium from the selenium-depleted CIGS material

2.10.1 High-temperature chlorination

High-temperature chlorination is a pyrometallurgical process where the starting material (e.g. metal ore, metal oxide or metal scrap) is allowed to react with a chlorination agent at elevated temperatures (above 100 °C). This results in the formation of volatile metal chlorides that can be separated from the starting material by distillation. High-temperature chlorination has been developed for numerous applications, including metal extraction from crude ores [38, 59, 60] and slag [61], removal of heavy metal contaminants [62] and recycling of valuable metals from waste materials [63-71]. Current high interest in the method and the number of processes being developed can be attributed to several factors. These include the high reactivity of chlorine, which results in the relatively low reaction temperatures needed for the chlorination and the advantageous chemical and physical properties of the formed chlorides (e.g. a high solubility in water and a high volatility) [72]. Other advantages are the availability and comparatively low cost of the chlorination agents, such as chlorine gas, hydrogen chloride gas and ammonium chloride [72].

High temperature chlorination has been used to separate copper [59, 61, 62, 72-74], indium [67, 70, 71, 75, 76] and gallium [65, 77-79] from different materials and for purification of these metals on an industrial scale [66]. González *et al.* [77] studied the kinetics of the chlorination of gallium oxide with chlorine gas and showed that gallium chloride was formed at temperatures above 650 °C. Park *et al.* [67] used hydrogen chloride gas for the recycling of indium from the indium tin oxide used in LCD screens, while Terakado *et al.* [70] used ammonium chloride for indium extraction from similar material. In addition, Túnes *et al.* [79] showed that chlorine gas could be used for the chlorination of indium oxide above 400 °C. Similar results have been presented for the chlorination of copper oxides using chlorine gas [72, 80]. For metal oxides other than those discussed above, it has been shown that a method called carbochlorination, where an addition of carbon is made to the starting material before treating it with chlorine gas, can lower the reaction temperature needed for the chlorination [72, 81-84].

2.10.2 Dissolution

To allow hydrometallurgical separation of copper, indium and gallium in the oxidized material from the selenium separation the material has to be dissolved. The dissolution of the oxides are therefore of interest. According to the reference literature copper(II) oxide is soluble in dilute acids and ammonium hydroxide [44]. Gallium(III) oxide is soluble in both alkali and in dilute mineral acids upon heating, while indium(III) oxide is soluble only in acids and not in alkali [39]. The amorphous form of indium(III) oxide dissolves readily in mineral acids whereas the crystalline form is more difficult to dissolve [44].

Studies have shown that leaching of copper from copper(II) oxide-containing ores can been done with 1 M sulphuric acid [85] and that copper(II) oxide can be dissolved in 0.5 M hydrochloric acid, sulphuric acid or nitric acid in under 15 min [86]. In the case of gallium leaching from oxidized zinc residues with sulphuric acid at 70 to 80 °C has been reported [87, 88]. In another study good gallium recovery from coal fly ash was achieved after 1 h leaching with 2 M hydrochloric acid at room temperature [89]. It is also clear that dissolution of indium(III) oxide (or the similar material, indium tin oxide) can be done with hydrochloric and sulphuric acid, although in general higher acid concentrations, higher temperatures and longer times are required than for the other oxides [88, 90-93].

The cheapest, and therefore most commonly used mineral acid, is sulphuric acid [94]. However, there are several advantages with chloride leaching, including; high reaction rates, high solubility of the formed chlorides, a large number of available valence states and easy separation by solvent extraction [88]. In solvent extraction chlorine as a ligand gives many extraction possibilities, both for neutral and anionic complexes [95].

2.10.3 Solvent extraction

Considerable work has been done on the extraction of copper, indium and gallium from various media with different extractants. Copper is most commonly extracted with phenolic oximes, such as LIX 84-I and LIX860, which give good separation of copper from other base metals [95]. It has also been shown that LIX 984 (a mixture of LIX 84-I and LIX860 at a volume ratio of 1:1) is suitable for extraction of copper from chloride media [96]. Although gallium is usually extracted from alkaline solutions with Kelex 100 (7-(4-ethyl-1-methyloctyl)-8-hydroxyquinoline) [41] extraction from chloride media with several different extractants has also been described [89, 97-104]. The extraction of indium has mainly been studied with acidic extractants, in particular di-(2-ethylhexyl) phosphoric acid (D2EHPA), from sulphate media [105]. However, extraction of indium with solvating extractants (e.g. tributylphosphate (TBP) and trioctyl phosphine oxide (TOPO)), chelating acidic extractants (e.g. oximes) and basic extractants (e.g. amines) has primarily been done from chloride media [105]. As a consequence, several studies on indium extraction from chloride media with different extractants have been presented [106-117].

Separation of copper, indium and gallium has been done by extraction of the elements from chloride media with solvating extractants. It has been shown that TBP can be used to separate indium and copper [118] and that gallium and indium can be separated using different chloride concentrations [119]. In a similar way, gallium and indium can be separated at different chloride concentrations using TOPO [120] and TPPO (triphenyl phosphine oxide) [121]. Gupta *et al.* have presented comprehensive studies on the extraction of both indium and gallium with Cyanex 923 (a mixture of four different trialkyl phosphine oxides) from different media [101, 110]. These studies showed that chloride media gave the best extraction of both indium and gallium, and that copper, indium and gallium could be separated by extraction at different chloride concentrations or by selective stripping after extraction. Another study, by Rafaeloff, showed that extraction with methyl butyl ketone (MEK) from a mixed chloride and sulphate media could be used to separate copper from indium and gallium [122].

Copper, indium and gallium separation has also been done by extraction with acidic extractants. Fortes *et al.* showed that indium could be separated from copper and gallium by extraction with D2EHPA from sulphate media by adjustment of the pH [123]. In addition, extraction with D2EHPA from chloride media has been shown to give relatively good separation of indium and gallium by varying the chloride concentration [124, 125]. Extraction with Cyanex 272 (di(2,4,4-trimethylpentyl)phosphinic acid) did not only give separation of indium and gallium at different hydrochloric acid concentrations, but also separation from several other elements, including copper [126]. Carboxylic acids can be used for extraction of indium and gallium from copper in chloride media with a pH of between 3 and 4 [127]. After stripping of the organic phase, separation of indium and gallium can then be done by extraction with TBP (indium) and iso-propyl ether (gallium).

Finally, there are some examples of amines and quaternary ammonium chloride (e.g. Aliquat 336) being used for separation of indium and gallium [128, 129]. Also in these cases, separation was achieved by varying the chloride concentration in the aqueous phase.

2.10.4 Electrodeposition

Both electrorefining and electrodeposition used for copper recovery from different ores are normally done in sulphate media [36, 37] and the techniques are constantly being developed [130]. It has been suggested, however, that chloride media could give a lower energy consumption during the electrolysis [131, 132] and a more effective leaching of some ores [96, 133, 134]. The electrodeposition of copper from chloride media has therefore been studied by several authors [132-136]. However, so far it has proven difficult to realize commercial processes due to technical difficulties [133].

Indium can be electrodeposited from several different media, including cyanide [137-139], sulphate [138-142] and chloride [38, 139, 140, 142-147]. For instance, the company Copper Pass in the United Kingdom has developed a process for the electrorefining of indium using chloride solutions, which results in high purity indium for the semiconductor industry [38].

Since gallium is most often produced from alkaline Bayer liquids most studies on electrodeposition of gallium have been done in alkaline solutions [65, 87, 148-153]. Nevertheless, there are also some examples of gallium electrodeposition from chloride solutions [65, 154-157]. One difficulty with the electrodeposition of gallium from aqueous solutions is that large overpotentials are required [150, 154, 158], which leads to low current efficiencies due to the simultaneous reduction of hydrogen [150]. It has been found for example that high hydrochloric acid concentrations completely inhibit electrodeposition of gallium [156]. Another challenge in electroplating gallium is the low melting point, which causes gallium droplets, rather than solid metal, to form if the solution is not cooled [159].

As described above (Section 2.2.1), it has been shown that copper can be electrochemically separated from indium after dissolution of CIS materials in nitric acid [21]. For the separation of indium and gallium it has been reported that electrodeposition of gallium from an aqueous solution containing both indium and gallium, using a controlled current, starts only after most of the indium has been removed from the solution [158]. In addition, it has been shown that indium and gallium can be separated by the electrodeposition of indium from solutions with high sulphuric acid concentrations [159].

3. Theory

3.1 High-temperature chlorination

A thermodynamic analysis was made using HSC Chemistry software for Windows version 5.1 [160], to predict if high-temperature chlorination could be used to separate copper, indium and gallium. The equilibrium composition as a function of temperature was calculated for systems containing CuO, In_2O_3 and Ga_2O_3, in addition to chlorine gas, chlorine gas and carbon, hydrogen chloride gas or ammonium chloride, respectively, as the chlorination agents. The calculations were done taking all copper, indium and gallium chlorides available in the HSC Chemistry Main database [160] into consideration as products. CuO and In_2O_3 were chosen as the starting materials since they were the most dominant copper and indium species identified in the selenium-depleted material, as can be seen in Section 6.1.1. The other oxides found in the starting material were not available in the database so Ga_2O_3 was chosen as a model compound for gallium. The input data for the calculations was based on the metal composition in the starting material and the amounts of chlorination agents used in the experiments. The results from the calculations for the system where chlorine gas was used as the chlorination agent are shown in Fig. 3.1.

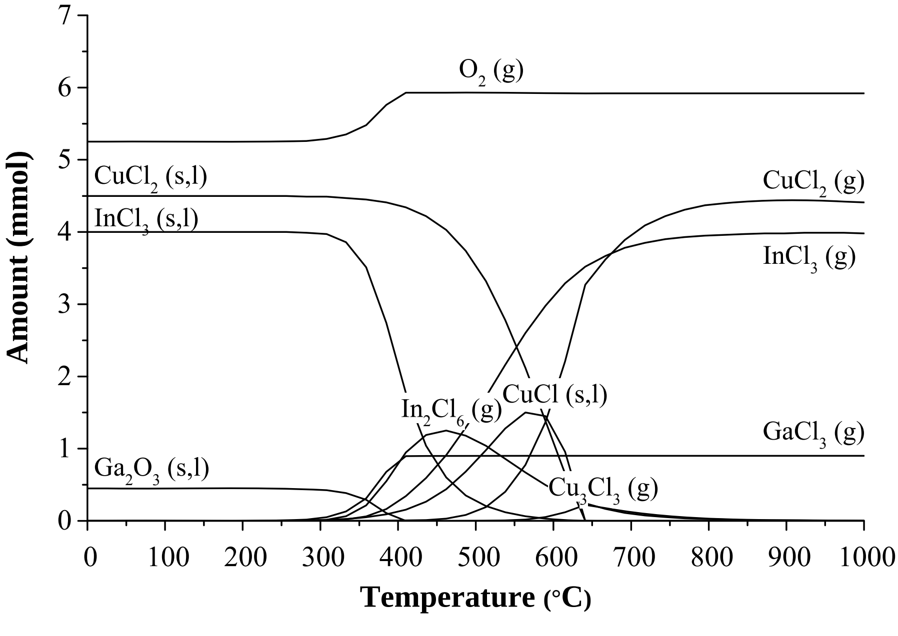

Fig. 3.1 Equilibrium composition, as a function of temperature, for the chlorination of CuO, In_2O_3 and Ga_2O_3 when using chlorine gas as the chlorination agent.

As can be seen in the figure, the thermodynamically stable compounds of copper and indium at low temperatures are $CuCl_2$ (s,l) and $InCl_3$ (s,l) while gallium remains in the form of gallium oxide. Gaseous chlorides of indium and gallium are formed above 300 °C and $CuCl_2$ (g) is formed above 450°C. This indicates that from a thermodynamic perspective the separation of indium and gallium will be difficult, whereas it may be possible to separate indium and gallium from copper.

As mentioned in Section 2.10.1, the reaction temperatures needed for chlorination reactions to take place when using chlorine gas as the chlorination agent can be lowered by carbochlorination. The role of carbon was originally suggested to be that of a reducing agent, since it reacts with oxygen to form carbon monoxide or carbon dioxide [81]. However, more recent studies have shown that carbon, in addition to having reducing properties, also functions as a catalyst for the formation of active chlorine species that work as chlorination agents [83, 84]. Adding carbon to the input data in the thermodynamic calculations gave the results presented in Fig. 3.2.

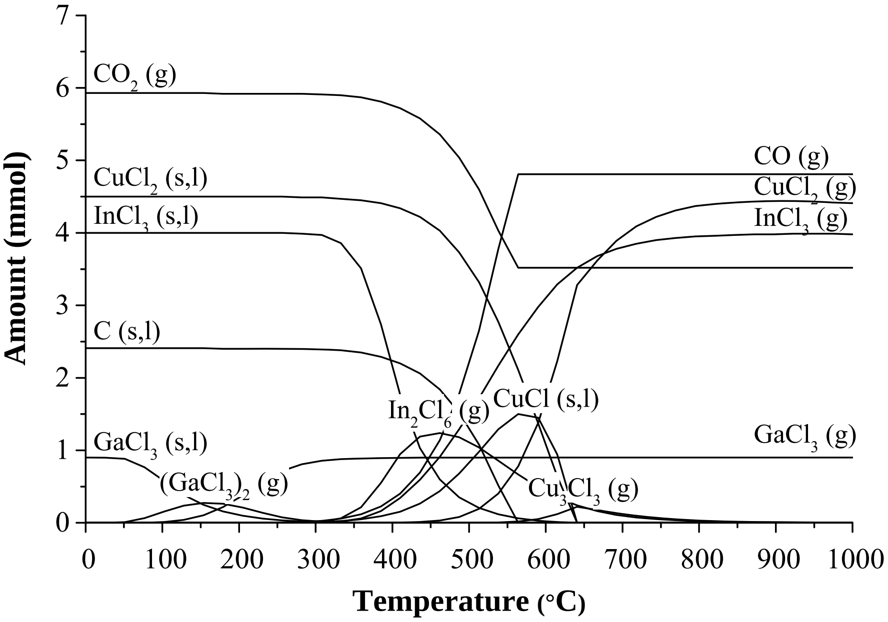

Fig. 3.2 Equilibrium composition, as a function of temperature, for the chlorination of CuO, In_2O_3 and Ga_2O_3 when using chlorine gas in the presence of carbon as the chlorination agent.

It is apparent that carbon greatly affects the gallium speciation and that gaseous gallium chlorides are thermodynamically stable at relatively low temperatures. Indium and copper chlorides in gas phase are stable above 350 and 450 °C, respectively. According to these results it should be possible to separate gallium from indium and copper. In addition, separation of indium from copper may also be feasible.

Changing the chlorination agent from chlorine gas to hydrogen chloride gas gave the equilibrium composition shown in Fig. 3.3.

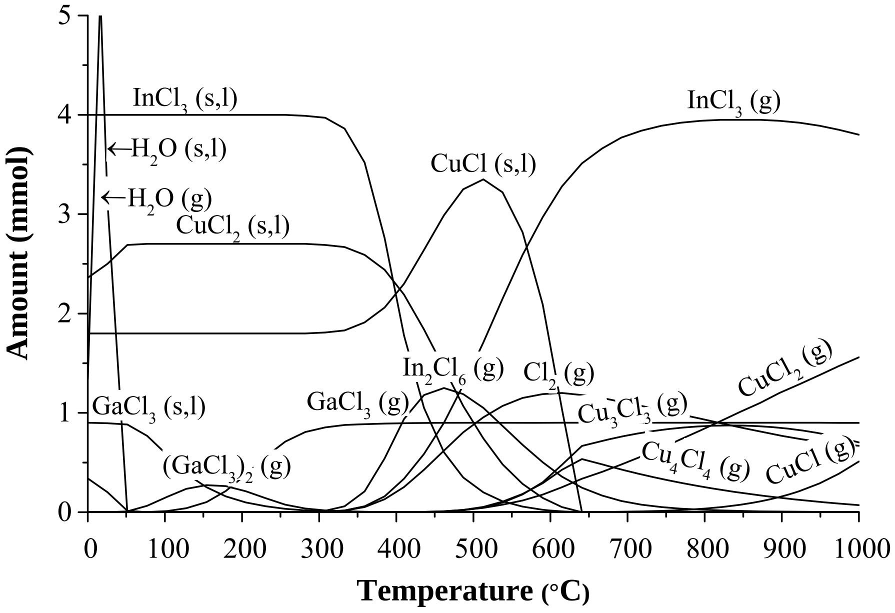

Fig. 3.3 Equilibrium composition, as a function of temperature, for the chlorination of CuO, In_2O_3 and Ga_2O_3 when using hydrogen chloride gas as the chlorination agent.

Similar to the results for the carbochlorination system calculations (Fig. 3.2), gaseous gallium chlorides are stable at low temperatures and gaseous indium chlorides are stable above 350 °C. On the other hand, higher temperatures are needed for copper chlorides to be stable in gas phase. The larger temperature differences between the onset of formation of the different chlorides indicates that hydrogen chloride could give an even better separation between the elements than carbochlorination.

Ammonium chloride sublimes at temperatures above 200 °C and after sublimation it decomposes completely to hydrogen chloride gas and ammonia, according to Reaction (3.1) [161].

$$NH_4Cl\ (g) \leftrightarrows NH_3\ (g) + HCl\ (g) \tag{3.1}$$

After decomposition the hydrogen chloride gas will act as the chlorination agent, presumably in the same way as when pure hydrogen chloride gas is used. However, the results from the equilibrium calculations for a system containing ammonium chloride (Fig. 3.4) were very different compared to the results from the hydrogen chloride gas calculations (Fig. 3.3).

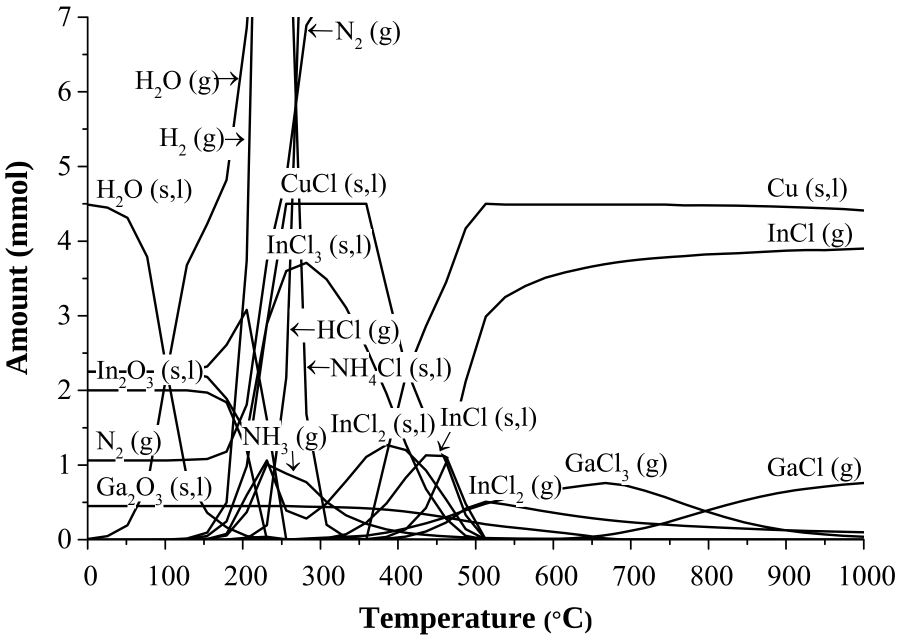

Fig. 3.4 Equilibrium composition, as a function of temperature, for the chlorination of CuO, In_2O_3 and Ga_2O_3 when using ammonium chloride as the chlorination agent.

As expected ammonium chloride decomposes to ammonia and hydrogen chloride, but the formed ammonia in turn decomposes to hydrogen gas and nitrogen gas. The reducing conditions cause copper metal to be the stable copper species instead of copper chloride in gas phase. Both indium and gallium chlorides are stable in gas phase above 300 °C. These results predict that ammonium chloride might not give separation between indium and gallium, but that indium and gallium could be separated from copper.

Here it is important to remember the shortcomings of this kind of modelling. If the data for some species is not included in the database it will not show up as a resulting species, even if it is identified in the product of the experiments. Uncertainties in the data present in the database might also have a significant effect on the speciation. Furthermore, if the products that are formed (in this case the chlorides in gas phase) are removed from the reaction site the chemical equilibrium reactions will promote the formation of more products. In the extreme this can lead to completion of the reaction. It is also worth pointing out that thermodynamic predictions give no information on the kinetics of a reaction.

Regarding the thermodynamics of reactions it has become clear that some erroneous use of thermodynamic entities are present in the literature. In order to predict whether a reaction is spontaneous or not the correct entity to use is Gibbs free energy (ΔG). In some cases [73-76, 83, 162, 163] the standard Gibbs free energy ($\Delta G°$) has been used. $\Delta G°$ is only an expression of the reaction constant and must be complemented with the actual state of the system in order to predict whether a reaction will occur or not, see Equation (3.2).

$$\Delta G = \Delta G° + RT\ln Q \tag{3.2}$$

where Q is the actual state of the system.

3.2 Dissolution of metal oxides in acid media

The dissolution of metal oxides in acid media can be described by Reaction (3.3) [164]

$$M_mO_n\ (s) + 2nH^+\ (aq) \rightarrow mM^{(2n/m)+} + nH_2O\ (l) \qquad (3.3)$$

Unlike the dissolution of metals, which are governed by differences in the electrochemical potential of the half reactions involved, the oxidation state of the elements does not change and the dissolution depends on the activities of the reactants and products. The degree of dissolution is therefore dependent on the concentrations in the solution (metal concentration, pH etc.), while the kinetics of the dissolution are governed by for example the temperature, particle size and stirring rate used [94].

After dissolution the metal ion forms different complexes with ions present in the solution, such as the counter ion from the acid (e.g. chloride in hydrochloric acid). The complexes formed depend on the stability constants of the complexes and on the counter ion concentration in the solution [165]. Since the further recovery of the metals, e.g. solvent extraction or electrodeposition, is influenced by factors such as pH and complexation the choice of acid media for the dissolution is of great importance.

3.3 Solvent extraction

In solvent extraction the distribution of a solute between two immiscible phases, usually an aqueous and an organic phase, is used for separation purposes [166].

$$A\ (aq) \rightleftarrows A\ (org) \qquad (3.4)$$

The organic phase always consists of a diluent and sometimes one or more extractants, while the aqueous phase contains the solute. Upon mixing of the phases the solute is transferred from the aqueous phase to the organic phase. This is usually facilitated by the extractant. The distribution of the solute between the phases is characterized by the distribution ratio (D-value) defined by Equation (3.5).

$$D = \frac{[A_{org}]}{[A_{aq}]} \qquad (3.5)$$

where $[A_{org}]$ and $[A_{aq}]$ are the concentration of metal A in the organic and aqueous phase, respectively. If the volume ratio (Equation (3.6)) deviates from unity

$$\theta = \frac{V_{org}}{V_{aq}} \qquad (3.6)$$

the distribution factor, according to Equation (3.7), can be used

$$P = \theta D \qquad (3.7)$$

If two different solutes (A and B) are present in the aqueous phase the separation factor (α) between the solutes is defined by Equation (3.8).

$$\alpha = \frac{D_A}{D_B} \tag{3.8}$$

where D_A is by definition larger than D_B. If the separation factor is high enough A and B can be separated.

The extractants used in solvent extraction can be divided into several different classes: solvating extractants, acidic extractants and basic or ion pair extractants [166]. The extraction mechanisms of each class are exemplified in Reaction (3.9)-(3.11).

$$MX_x{\cdot}mH_2O\ (aq) + nL\ (org) \rightleftarrows MX_xL_n\ (org) + mH_2O \tag{3.9}$$

$$M^{z+}\ (aq) + zHA\ (org) \rightleftarrows MA_z\ (org) + zH^+ \tag{3.10}$$

$$MX_x^{(z-x)-}\ (aq) + (z-x)R_3NH^+X^-\ (org) \rightleftarrows R_3NH_{(z-x)}MX_x\ (org) + (z-x)X^-\ (aq) \tag{3.11}$$

In addition, at high acid concentrations solvation extractants such as TBP and MIBK may become protonated and extract melanate anions, $MX_x^{(z-x)-}$ [95].

It is clear that the complexation of the metals in the aqueous phase is of importance if successful separation by solvent extraction is to be achieved. The complexation of copper, indium and gallium as a function of chloride concentrations was therefore determined using the stability constants for the chloride complexes given in [167-169], see Fig. 3.5.

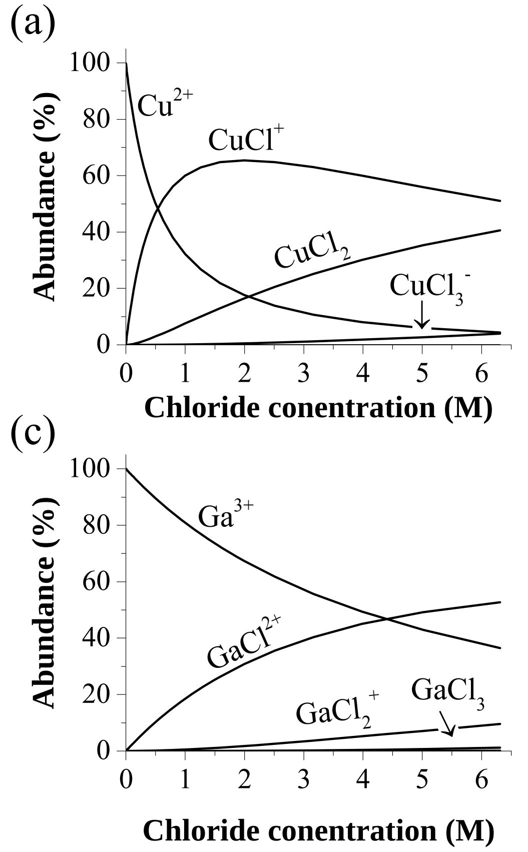

Fig. 3.5 Abundance of (a) copper(II) chloride, (b) indium(III) chloride and (c) gallium(III) chloride complexes in chloride media as a function of chloride concentration.

The difference in complexation of the elements dependant on the chloride concentration indicates that the elements can be separated by solvent extraction at different chloride concentrations.

A simple solvent extraction process usually contains two sub-processes; extraction and stripping (the back-extraction of an extracted solute into a new aqueous phase). Fig. 3.6 shows a process where both extraction and stripping is done in a cascade of counter-current steps. A counter-current process, where flows run in opposite directions, is used to reduce the volume of the process flows. One step is one extraction unit, or stripping unit, allowing contact between the phases. Addition of more than one step can be used to achieve metal fractions with higher purity.

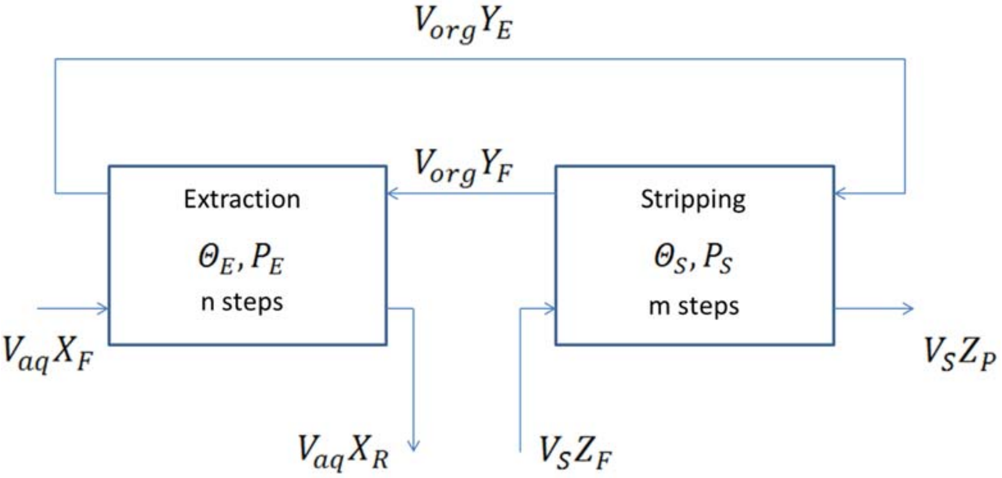

Fig. 3.6 Schematics of a solvent extraction process containing counter-current extraction and stripping steps. The notations include volume flow (V), aqueous fraction (X and Z) and organic fraction (Y). The indices denote feed (F), extraction (E), stripping (S) or raffinate (R and P).

For each metal, the mass balance for the extraction is expressed by Equation (3.12)

$$V_{org}Y_F + V_{aq}X_F = V_{org}Y_E + V_{aq}X_R \tag{3.12}$$

In the same way a mass balance can be done for the overall process with a cascade of extraction and stripping steps. Under the assumption that Y_Z is 0 and that the distribution ratio for the extraction and stripping steps are constant, the raffinate fraction (X_R) for n extraction steps can be expressed by Equation (3.13)

$$X_R = \frac{X_F - \theta Y_F \sum_0^{n-1} \prod_0^i P_i}{\sum_0^n \prod_0^i P_i} \tag{3.13}$$

where X_F and Y_F are the feed concentrations, θ is the volume ratio and P_i is the distribution factor in each step. The same equation can also be used for stripping with m steps. By coupling the mass balances of the extraction and stripping the overall separation system can be solved through numerical iteration.

3.4 Electrodeposition

During electrodeposition metal ions in solution are reduced to the metal by applying a current through the solution. The standard reduction potentials (E^0) for the reduction of copper(II), indium(III) and gallium(III) according to Reactions (3.14), (3.15) and (3.16) are reported to be 0.34, -0.338, and -0.529 V vs standard hydrogen electrode, respectively [170].

$$Cu^{2+} (aq) + 2e^- \rightarrow Cu (s) \qquad (3.14)$$

$$In^{3+} (aq) + 3e^- \rightarrow In (s) \qquad (3.15)$$

$$Ga^{3+} (aq) + 3e^- \rightarrow Ga (s) \qquad (3.16)$$

The differences in standard reduction potentials indicate that separation of copper from indium and gallium by electrodeposition should be possible. On the other hand, separation of indium from gallium could be more difficult, since the standard reduction potentials are relatively similar. However, the actual potential needed for reduction usually deviates from the standard potential due to several different factors. Firstly this depends on the deviation from the standard state, according to the Nernst equation (3.17) [171].

$$E=E^0+\frac{RT}{nF}\ln\frac{[O]}{[R]} \qquad (3.17)$$

Where [O] and [R] are bulk concentrations of the oxidized and reduced species, respectively, F is the Faraday constant and n is the number of electrons involved in the reaction. The actual potential also depends on possible complexation of the desired element in solution, which will affect the potential according to Equation (3.18) [172].

$$\ln K=\frac{nFE}{RT} \qquad (3.18)$$

The equilibrium constant, K, in this case is the same as the stability constant for the formed complex. In addition, an additional potential called the activation overpotential is needed to overcome the potential barrier at the interface between the electrode and the solution [173]. At the same time the resistance in the solution causes a potential drop, according to Ohm's law ($U=R \cdot I$), which also increases the potential needed for reduction [171]. The potential drop, however, affects all elements to the same extent and does not influence the separation of the elements.

For the reduction of copper in chloride solution Napp and co-workers have shown that copper(II) is reduced to copper(0) via the intermediate copper(I) in the chloride media [136]. The reaction mechanism has been suggested to be an anion-bridged (Cu-Cl-Cu) reaction [174] and the formation of CuCl on the electrode surface via Reaction (3.19) has been confirmed [175].

Cu^{2+} (aq) + Cl^- + e^- → CuCl (s) (3.19)

At more negative potentials copper(I) is further reduced to copper (0) according to Reaction (3.20) [175].

CuCl (s) + e^- → Cu (s) + Cl^- (3.20)

The reduction of copper(I) takes place in parallel with the direct reduction of copper(II) to copper(0) according to Reaction (3.14) [175, 176].

The current efficiency for electrodeposition can be calculated by comparing the charge (Q) used in the experiments, which can be calculated from Equation (3.21)

$$Q = \int_0^t I(t)dt \tag{3.21}$$

with the charge needed to produce the metal obtained calculated from Equation (3.22).

$$Q = FNz \tag{3.22}$$

where F is Faraday’s constant, N is the number of moles of metal formed and z is the number of electrons transferred per ion.

3.5 Uncertainties

Unless otherwise stated, the experiments in this study were done in triplicate to evaluate the uncertainty in the results and all uncertainties are expressed as one standard deviation. The standard deviation from three or more replicates of an experiment can be calculated using Equation (3.21)

$$\mathrm{s} = \sqrt{\frac{\sum(\mathrm{X}-\bar{\mathrm{X}})^2}{\mathrm{n}-1}} \tag{3.23}$$

where s is the standard deviation, $\bar{\mathrm{X}}$ is the mean value of all samples and n is the number of samples [177]. The uncertainty propagation for C=A+B and for C=AB is expressed by Equation (3.22) and (3.23), respectively.

$$s_C = \sqrt{\mathrm{s}_A^2 + \mathrm{s}_B^2} \tag{3.24}$$

$$s_C = \mathrm{C}\sqrt{\left(\frac{s_A}{A}\right)^2 + \left(\frac{s_B}{B}\right)^2} \tag{3.25}$$

4 Analytical techniques

A description of the analytical techniques, e.g. ICP-OES, XRD and NAA, used in this work can be found in Appendix B.

5. Experimental

5.1 Equipment

5.1.1 Furnaces

For the selenium distillation study and the chlorination study two different furnaces were used; a horizontal tube furnace and a fluidized bed furnace. The horizontal tube furnace is shown in Fig. 5.1. The starting material used in the respective studies was placed in a furnace crucible, which was placed in the middle of the quartz tube reactor in the furnace. The temperature in the furnace was measured with a thermocouple on the outside of the quartz tube. During the experiments gas was passed through the quartz reactor via a flow meter (Platon NG) and the product formed was sublimed in the quartz tube after the furnace. After the furnace the gas was passed through a condenser, cooled with 20 °C water, to trap the products that did not sublime in the quartz tube directly after the furnace. In the high-temperature study the gas was scrubbed using three Dreschel bottles containing 1 M sodium hydroxide.

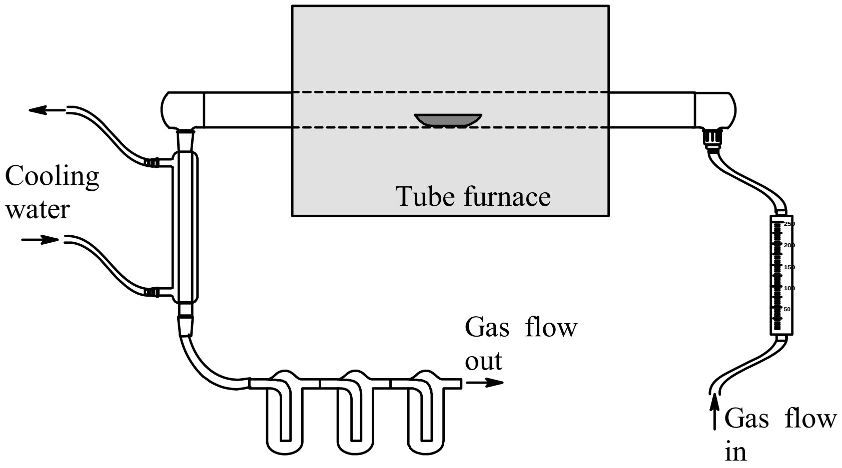

Fig. 5.1 Experimental setup for the tube furnace used in the in the selenium separation and high-temperature chlorination studies. The gas was passed (from right to left) through the quartz tube placed in the tube furnace. The starting material used for the respective studies was heated and the products that formed were sublimated outside the furnace (on the left).

The fluidized bed batch reactor, seen in Fig. 5.2, was made from a 480 mm long quartz tube with an inner diameter of 20 mm. The middle of the tube was fitted with a porous quartz plate on which the starting material was placed. The connections at each end of the tube held a thin quartz glass tube through which thermocouples were inserted into the reactor. The topmost thermocouple, measuring the temperature in the bed, was used to control the temperature in the reactor. The thermocouple below the bed was used as a reference. The gas used in the experiment was passed through the reactor from the bottom to allow reaction with the starting material. After the furnace, the gas was passed through a horizontal glass tube to allow the formed products to condense. Next a condenser, cooled with 20 °C water, was used to trap any remaining products. Finally, three Dreschel bottles containing 1 M sodium hydroxide were used in the high-temperature chlorination study to absorb all of the reaction gas that did not react.

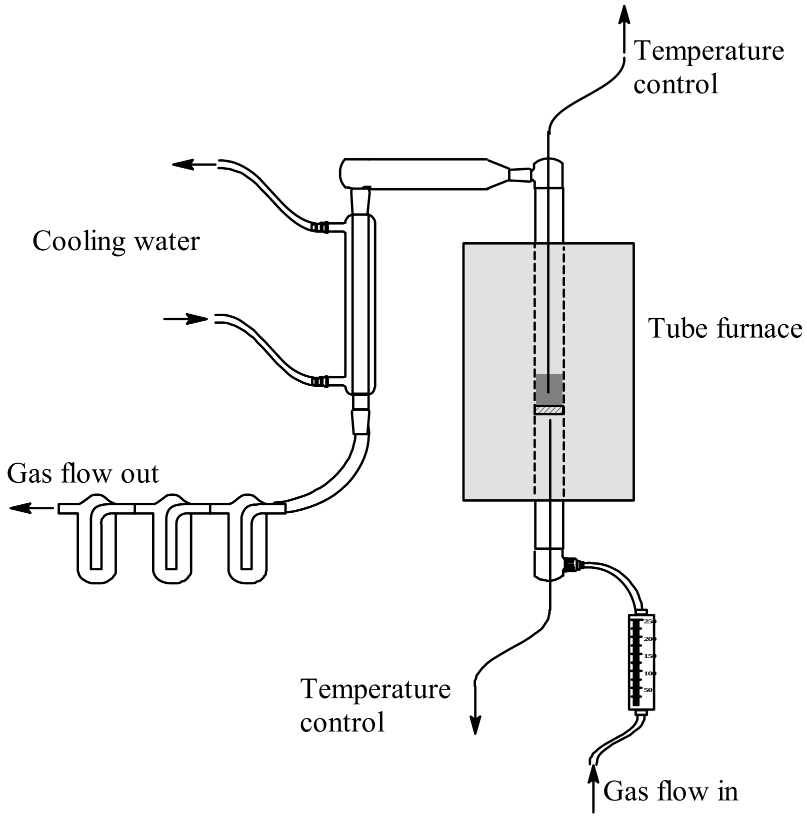

Fig. 5.2 Experimental setup for the fluidized bed reactor used in the selenium separation and high-temperature chlorination studies. The gas (oxygen, chlorine or hydrogen chloride) was passed from the bottom up through the fluidized bed reactor placed in the tube furnace. The starting material was placed on a porous plate in reactor and heated. The products formed were sublimated in the horizontal tube, after the furnace.

5.1.2 Solvent extraction equipment

All solvent extraction experiments were performed in a thermostatic shaking machine (IKA Vibrax VXR Basic).

5.1.3 Electrochemical cell

The electrochemical separation study was performed in a three electrode electrochemical cell connected to a galvanostat (VersaSTAT 3, Princeton Applied Research). For the cyclic voltammetry study the three electrodes used were a working electrode of glassy carbon (MF-2012, Basi), a platinum wire counter electrode (MW-1032, Basi) and a silver/silver chloride reference electrode (MF-2052, Basi). For the electrodeposition study the working electrode was changed to a glassy carbon rod (GC 20SS, Tokai Carbon Co.) with a diameter of 3 mm and the counter electrode was a thick (Ø 8 mm) glassy carbon rod. During the experiment the working electrode was submerged 10 mm into the solution.

5.2 Separation of selenium from CIGS materials

5.2.1 Feasibility of separating selenium by distillation of selenium dioxide

To study the feasibility of the separation of selenium in the form of selenium dioxide from CIGS by oxidation at elevated temperatures, a series of tests were performed in the tube furnace (Fig. 5.1). The starting material for the selenium separation study, in the form of spent sputtering targets containing CIGS, was supplied by Midsummer AB [178]. For the feasibility study a sample from one of the sputtering targets was crushed in an agate mortar and mixed carefully to homogeneity. The particle size distribution in the material was determined by sieving through a mesh 10 sieve, followed by a mesh 60 sieve, and finally a mesh 200 sieve (ASTM E-11, W.S Tyler). The material passing each sieve was weighed to give the particle size distribution of the starting material. The uncertainty of the particle size distribution in each sample was determined by the sieving of five different 13.5 g samples.

To determine the temperature dependence of the selenium separation, 13.5 g of starting material was treated at six different temperatures (500, 600, 700, 800, 900 and 1000 ± 10 °C). During the heating of the furnace the tube was rinsed with nitrogen to avoid any reaction. When the temperature reached the set temperature the gas was switched to oxygen gas (99 %, AGA) at 200 ml/min and the timer was started. The reaction was allowed to proceed for 24 h, after which the gas was again switched to nitrogen and the furnace was allowed to cool. When the furnace had reached room temperature the gas flow was turned off and the selenium dioxide crystals were collected.

To confirm that the selenium separation was mainly due to the formation of selenium dioxide and not to distillation of selenium a test was performed under a nitrogen atmosphere. 13.5 g of the starting material was placed in a furnace crucible in the tube furnace at 1000 °C for 24 h. The nitrogen flow through the tube was set to 200 ml/min during the whole experiment. The selenium formed during the experiment was collected and weighed.

The composition of the CIGS material, before and after the oxidation reactions and the distillation test, was determined using ICP-OES. The starting material was dissolved in nitric acid (puriss, 69 %, Sigma-Aldrich) and the residue was dissolved in hot aqua regia with an addition of hydrogen peroxide (30 %, Sigma-Aldrich). The aqua regia was prepared by mixing nitric acid (puriss, 69 %, Sigma-Aldrich) and hydrochloric acid (puriss, 37 %, Sigma-Aldrich) with a molar ratio of 1:3 respectively. Mass balance calculations over the aqua regia dissolution showed that total dissolution had been achieved. X-ray powder diffraction was used to identify crystalline compounds in the CIGS material, before and after the oxidation.

5.2.2 Optimization of the selenium separation

After the feasibility study the selenium separation step was optimized in order to extract more of the selenium from the CIGS material. Optimization tests were performed both in the fluidized bed reactor (Fig. 5.2) and in the tube furnace used for the feasibility study. The fluidized bed reactor was used to improve the contact between the gas and the CIGS material. For the optimization experiments CIGS from several different sputtering targets were combined to give a representative sample for the entire waste stream. The crushed material was sieved (Mini-sieve set, Bel-art products) and crushed again until the preferred particle size was attained.

To evaluate the optimization potential of the oxidation reaction a sample of 20.0 g of the starting material with a size of 125-180 µm was treated in the fluidized bed reactor at 900 ± 10 °C. Oxygen gas was passed through the reactor from the bottom at a flow rate high enough to cause fluidization of the particles. The gas flow was adjusted for each experiment depending on the particle size and temperature used. The experiment was allowed to proceed for 3, 6 and 12 h to determine the rate of selenium recovery yield. An additional experiment was performed on particles with a size of 90-125µm for 3 h to determine if smaller particles could give higher selenium recovery. The flow rate at which fluidization occurs was determined at room temperature for each particle size and was then calculated for the temperature used in the experiment. The flow rate correlates to the temperature in such a way that when the temperature is doubled the required flow rate is halved. During the heating and cooling of the furnace the reactor was purged with nitrogen gas to avoid any oxidation reaction.

As a complement to the optimization in the fluidized bed reactor a test was performed in the tube furnace using the fraction of the starting material with a particle size of less than 63 µm. Due to problems with entainment this fraction could not be treated in the fluidized bed and an alternative treatment method had to be tested. 13.5 g of the CIGS material was placed in a furnace boat and oxidized in the tube furnace. Tests were made at 900 ± 10 °C for 12, 6, 3 and 1 h to evaluate the selenium recovery rate. In addition, tests were also made at 800 and 700 ± 10 °C for 1 h. The same experimental setup and procedure was used as in the feasibility study.

5.2.3 Reduction of selenium dioxide

The selenium dioxide formed during the selenium separation step was reduced using two different reduction methods. First a Riley reaction (see Reaction 2.3), in which the organic reactant deoxybenzoin was used as a reducing agent was tested. The deoxybenzoin was at the same time oxidized to benzil, which is a diketone used in solvent extraction. 2.00 g (0.018 mol) selenium dioxide was dissolved in 7 ml glacial acetic acid (pro analysis, 100 %, Merck) and 3.54 g (0.018 mol) deoxybenzoin (98 %, Acros organics) was added. The mixture was heated to 126 ± 2 °C and refluxed for 3 h. The cooled solution was decanted and the elemental selenium was washed with dietylether (99+ %, Acros organics). The organic product was extracted with dietylether from the acetic acid phase. After the extraction the organic product was washed with ultrapure water, a saturated solution of sodium bicarbonate and then again with brine before it was dried with sodium sulphate and concentrated under reduced pressure. Both the selenium and the organic product were weighed, after drying, to determine the yield. The purity of the organic product was analysed with GC-MS. Before the analysis the product was dissolved and diluted to a concentration of 16 mg/l in acetone (pro analysis, Fischer Scientific). A solution prepared in the same way, containing a mixture of deoxybenzoin (99+ %, Acros Organics) and benzil (99+ %, Acros Organics), was analysed as a reference. The amount of selenium dioxide remaining in the reaction liquid after the reduction of selenium dioxide with sulphur dioxide was analysed with ICP-OES to determine the selenium content in the liquid.

The second reduction agent used was sulphur dioxide. For these experiments 1.00 g (0.009 mol) of selenium dioxide was placed in a Dreschel bottle and dissolved in 50 ml ultrapure water. The solution was heated to 80 ± 2 °C and stirred with a magnetic stirrer. Sulphur dioxide gas (99.8 %, AGA) was bubbled through the solution at a flow rate of 40 ml/min. Due to the heating of the solution during the experiment the red selenium formed from the reduction reaction was continuously transformed into black selenium within less than a minute. When the reaction was complete no more red selenium could be observed. From these observations the reaction time needed for complete reduction could be determined to be less than 15 min. Therefore, after 15 min the gas flow was stopped and the selenium was collected, decanted, washed with ultrapure water obtained from a Milli-Q® system (>18 MΩ·cm, Millipore Milli-Q Advantage A10) and allowed to dry before it was weighed to determine the yield.

The purity of the recycled selenium and selenium dioxide, with respect to scandium, titanium, vanadium, chromium, manganese, iron, nickel, copper, zinc, gallium and indium was determined using a combination of ICP-MS, ICP-OES and NAA (see Appendix B for a description of the analytical techniques). The concentrations of all the impurities except iron were analysed using ICP-MS on a solution containing 1000 µg/ml selenium using standard addition. The exact concentration of selenium in the selenium solution was determined with ICP-OES. To determine the iron content in the recycled selenium or selenium dioxide NAA was used. Samples containing 0, 0.1, 1, 10 and 100 ppm of iron were prepared and irradiated for a total of 123 hours and 23 minutes before the 1099 and 1291 keV gamma lines of ^{59}Fe were used to determine the concentration of iron in the materials. Due to limitations in the number of samples that could be sent to NAA, triplicate experiments could not be performed. The uncertainty of the results was therefore evaluated using the methods developed by the Eurachem organization [132]. The evaluation was performed with the software GUM workbench [133].

5.3 Separation of copper, indium and gallium from selenium-depleted CIGS material using high-temperature chlorination

5.3.1 Preparation of the starting material

The residue after selenium separation from CIGS material with a particle size of less than 63 µm at 800 ± 10 °C for 1 h was used as the starting material for the high-temperature chlorination study. Before the material was used the particle size was again reduced to less than 63 µm. To determine if the material had been completely oxidized during the selenium recovery step a mass balance was performed, using the data from the ICP-OES measurements. The amount of oxygen needed to completely oxidize the metals in the CIGS material was compared with the actual amount of oxygen in the oxidized material. A completely oxidized material would contain 1.5 moles of oxygen per mole of gallium or indium and 1 mole oxygen of per mole of copper. The calculations showed that the metals in the starting material were 96.4 ± 6.0 % oxidized.

5.3.2 Initial study on the chlorination treatment using chlorine gas and hydrogen chloride gas

First, the separation of copper, indium and gallium was tested using chlorine gas and hydrogen chloride gas in the fluidized bed furnace shown in Fig. 5.2. For each experiment 1.0 g of the starting material was placed in the reactor and the furnace was heated to the correct temperature before a flow of 50 ml/min of chlorine gas (99.8 %, AGA) or hydrogen chloride gas (99.8 %, AGA) was passed through the reactor. For the carbochlorination experiments 0.1 g of carbon nanopowder (99.95 %, Supelco Analytical) was thoroughly mixed with the starting material before it was placed in the reactor. Experiments were performed at temperatures between 200 and 750 ± 10 °C with chlorine gas and at 150 to 600 ± 10 °C with hydrogen chloride gas. Each experiment was allowed to proceed for 2 h before the furnace was turned off. During the heating and cooling of the furnace the reactor was purged with nitrogen gas (99 %, AGA) at 100 ml/min to avoid any reactions. The products were rinsed from the collection tube with Milli-Q® water and analysed with ICP-OES. The residues were scraped from the reactor and analysed with ICP-OES and XRD.

5.3.3 Initial study on the chlorination treatment using ammonium chloride

After the tests with chlorine gas and hydrogen chloride gas the separation of the elements was tested using ammonium chloride as the chlorination agent. The experiments were done in the horizontal tube furnace shown in Fig. 5.1. For these experiments the sample had to be introduced and removed from the reactor to control the reaction time and the vertical furnace could therefore not be used. The reason for this was that ammonium chloride is a solid that was mixed with the starting material and not a gas that could be turned on and off to control the reaction time. 1.0 g of the starting material was mixed with ammonium chloride (99.5 %, J.T

Baker) at a ratio of 40:60 (starting material:ammonium chloride). Experiments were performed at temperatures from 200 to 750 ± 10 °C and 200 ml/min of nitrogen gas (99 %, AGA) was used to transport volatile products from the reaction to the cold end of the furnace. This gas flow was chosen since it was the lowest gas flow that ensured transportation of all products to the correct side (left-hand side in Fig. 5.1) of the furnace at all reaction temperatures. The furnace crucible containing the reaction mixture was inserted into the furnace when the furnace had reached the desired temperature. The sample was kept in the furnace for 2 h before it was removed and the furnace was turned off. Following the experiments the products were collected by rinsing the quartz tube with Milli-Q® water. When the product was mixed with water the small fraction of selenium remaining in the selenium-depleted material precipitated and red selenium was formed. To dissolve the selenium before analysis the tube was rinsed with a few millilitres of sulphuric acid (puriss, 95-97 %, Sigma-Aldrich) and the acid was then added to the solution, which was analysed with ICP-OES. Residue remaining in the furnace crucible after each experiment was collected and analysed with ICP-OES and XRD.

5.3.4 Study of the overall kinetics of the recovery of copper, indium and gallium from oxidation residues using ammonium chloride as the chlorination agent

After the initial studies on the separation of the elements with high-temperature chlorination a more in-depth study using ammonium chloride as the chlorination agent was done. First, the kinetics of the recovery of copper, indium and gallium from the selenium-depleted material was investigated. The aim of the study was to find the optimum temperatures and treatment times for the separation of these three elements. The overall chlorination process consists of several steps, including:

(1) the decomposition rate of ammonium chloride to hydrogen chloride and ammonia in gas phase,
(2) the kinetics of the chlorination reactions,
(3) the evaporation kinetics of the chlorides that are formed,
(4) the diffusion of the gaseous reactants and products through the residual material.

Experiments were carried out at temperatures between 220 and 560 ± 10 °C and a gas flow of 200 ml/min. At each temperature samples were treated for 1, 2, 4 and 8 h. For each experiment 1.0 g of the starting material was thoroughly mixed with 1.5 g of ammonium chloride (99.5 %, J.T Baker) and placed in a crucible. The amount of ammonium chloride used corresponded to 3 moles of chloride per mole of metals in the starting material. The products were dissolved and analysed in the same way as in the initial ammonium chloride study.

5.3.5 Optimization of the chlorination with ammonium chloride using Ga_2O_3 as a model compound

After the kinetics study the optimum addition of ammonium chloride for chlorination of the selenium-depleted material was studied using Ga_2O_3 as a model compound. Ga_2O_3 was chosen since it was assumed to react in a similar way to the gallium and indium oxides present in the starting material ($CuInGaO_4$, In_2O_3 and $Cu_2In_2O_5$). The temperature and gas flow used were 260 ± 10 °C and 200 ml/min, respectively, and the samples were treated for 1, 2 and 4 h. Each sample contained 0.07 g of Ga_2O_3 (99.99 %, Alfa Aesar), corresponding approximately to the amount of gallium present in the 1.0 g of selenium-depleted material. All samples were mixed with 0.15, 0.30 or 0.45 g of ammonium chloride (99.5 %, J.T Baker), which corresponded to 3, 6 or 9 moles of chloride per mole of gallium (see Table 5.1).

Table 5.1 Summary of the test parameters used in the chlorination optimization study.

	Temp. (°C)	**Recovery time (h)**	**NH_4Cl addition (moles/mole gallium)**	**Al_2O_3 addition (g)**	**Gas flow (ml/min)**	**Note**
Test 1	260	1, 2 and 4	3	0	200	
Test 2	260	1, 2 and 4	6	0	200	
Test 3	260	1, 2 and 4	9	0	200	
Test 4	260	1, 2 and 4	3	0.4	200	
Test 5	260	1, 2 and 4	3	0.9	200	
Test 6	260	1, 2 and 4	6	0.9	200	
Test 7	260	1, 2 and 4	9	0.9	200	
Test 8	260	1, 2 and 4	3	0.4	200	Pellet
Test 9	260	1, 2 and 4	6	0.4	200	Pellet
Test 10	260	1, 2 and 4	3	0.9	200	Covered

To more accurately simulate the diffusion of the formed gallium chlorides in the real material some tests (4-9) were made with a filler material added to the gallium oxide. Aluminium oxide was chosen as the filler material since it is an inert material under the conditions tested and would not interfere with the chlorination reaction. The amount of aluminium oxide (99.5 %, Alfa Aesar) used was either 0.4 or 0.9 g. To investigate if an increased contact between the gallium oxide and the ammonium chloride would increase the gallium recovery pellets were made and tested (8-9). Gallium oxide, aluminium oxide and ammonium chloride were mixed and made into pellets with a diameter of 13 mm using a pressure of 7 bar. A final test (10) was made where gallium oxide was mixed with 0.15 g of ammonium chloride, placed in the furnace boat and covered by a layer of aluminium oxide (0.9 g).

After each experiment the product was rinsed from the quartz tube with Milli-Q® water and analysed with ICP-OES. X-ray powder diffraction was used to determine if the gallium remaining in the residues was gallium oxide or gallium chloride.

5.3.6 Separation of gallium from indium and copper

The results from the kinetics study and the optimization study were used to decide on the parameters to be used for separation of the elements from the selenium-depleted CIGS material. Firstly gallium separation (GS) was tested at 260 ± 10 °C in two test sets, see Table 5.2.

Table 5.2 Summary of the test parameters used in the gallium separation (GS) study.

	Temp. (°C)	**Recovery time (h)**	**NH_4Cl addition (moles/mole metals)**			**Gas flow (ml/min)**
			1st	2nd	3rd	
GS 1:1	260	4	9	-	-	200
GS 1:2	260	8	9	-	-	200
GS 1:3	260	8	9	-	-	400
GS 2:1	260	3*2	3	0	0	200
GS 2:2	260	3*2	3	3	3	200
GS 2:3	260	3*2	3	0 (mixing)	3	200
GS 2:4	260	3*2	3	1	1	200
GS 2:5	260	3*2	3	1	1	100
GS 2:6	260	3*2	3	1	1	400

In the first set (GS 1:1-1:3) a large addition of ammonium chloride was made: 1.0 g of starting material mixed with 4.5 of ammonium chloride (corresponding to 9 moles of chloride per mole of metals) was treated for 4 or 8 h. In the second set of tests (GS 2:1-2:6) 1.0 g of starting material was mixed with three smaller batches of ammonium chloride and treated for a total of 6 h. The first batch (1.5 g) was mixed with the staring material (1.0 g) before treatment in the furnace and the second and third batches were added after 2 and 4 h, respectively. The product formed was collected after each treatment. The second and third batch of ammonium chloride additions were either 0.5 g or 1.5 g, which corresponded to 1 or 3 moles of chloride per mole of metals. One test (GS 2:3) was also made where, after 2 h, the material was mixed but no ammonium chloride was added, in order to determine if the mixing increased the gallium recovery. In addition, the effects of different nitrogen gas flows were tested for both sets of tests.

5.3.7 Separation of indium and copper

After the gallium separation tests, the separation of indium from copper was tested at 340 ± 10 °C. The indium separation tests are summarized in Table 5.3.

Table 5.3 Summary of the test parameters used in the indium separation (IS) study.

	Treated material	**Temp. (°C)**	**Recovery time (h)**	**NH_4Cl addition (moles/mole metals)**			**Gas flow (ml/min)**
				1st	2nd	3rd	
IS 1:1	Residue GS 1:3	340	4	0	-	-	200
IS 1:2	Residue GS 1:3	340	8	0	-	-	200
IS 1:3	Residue GS 1:3	340	8	13.5	-	-	200
IS 1:4	Residue GS 1:3	340	8	13.5	-	-	400
IS 2:1	Residue GS 2:4	340	3*2	0	1.1	1.1	200
IS 2:2	Residue GS 2:4	340	3*2	3.4	0 (mixing)	3.4	200
IS 2:3	Residue GS 2:4	340	3*2	3.4	3.4	3.4	200
IS 2:4	Residue GS 2:4	340	3*2	3.4	3.4	3.4	400
IS 2:5	Residue GS 2:6	340	3*2	3.4	3.4	3.4	400

The residue from GS 1:3 was either treated directly or mixed with 6 g ammonium chloride (equivalent to 13.5 moles of chloride per mole metals remaining in the material after gallium separation) before being introduced into the furnace again and heated for 4 or 8 h (IS 1:1-1:4). Residues (GS 2:4 or GS 2:6) from the second set of gallium separation tests were either treated directly or mixed with 1.5 g of ammonium chloride (corresponding to 3.4 moles of chloride per mole of metals remaining in the material after gallium separation) before they were treated in the furnace for 2 h. Two more batches of 0.5 or 1.5 g ammonium chloride (corresponding to 1.1 or 3.4 moles of chloride per mole of metals remaining in the material after gallium separation) were added to the material after 2 and 4 h. In IS 2:2 the material was mixed after 2 h, but no ammonium chloride was added, in order to determine if mixing increased the indium recovery. The gas flow used in the tests was either 200 or 400 ml/min.

5.4 Dissolution of the selenium-depleted CIGS material

To allow for hydrometallurgical separation methods to be used on the elements in the selenium-depleted material the material first had to be dissolved. Two different dissolution methods were tested: (1) direct dissolution of the material in mineral acids and (2) complete chlorination of the material using ammonium chloride followed by dissolution in mineral acids. Also in this study the selenium-depleted material was reduced to a particle size of less than 63µm before it was used.

5.4.1 Direct dissolution in mineral acids

First, the selenium-depleted material (0.5 g) was leached in 6 M solutions of sulphuric acid, hydrochloric acid and nitric acid for 8 h at room temperature. After the screening tests, leaching of the material in different concentrations (1, 3 and 6 M) of hydrochloric acid was tested over 100 h. Next, the dissolution using 1, 3 and 6 M hydrochloric acid was tested at 75 ± 5 °C for 8

h. For all of the experiments 25 ml of acid was used and the solution was stirred at 500 rpm. Samples of 0.1 ml for ICP-OES analysis were taken regularly during the experiments.

5.4.2 Dissolution of pre-chlorinated material

To increase the solubility of the selenium-depleted material it was mixed with ammonium chloride at a weight ratio of 1:1.5 (oxidized material:ammonium chloride) and treated in the horizontal tube furnace at 650 ± 10 °C for 1 h. The product formed was collected and 1.5 g was dissolved in water, sulphuric acid (0.1 M), hydrochloric acid (0.1 and 1 M) or nitric acid (0.1 M) for 8 h. Again, 25 ml of solution was used in each test, the stirring rate was 500 rpm and 0.1 ml samples were taken for ICP-OES analysis.

5.5 Separation of copper, indium and gallium using solvent extraction

5.5.1 Screening of different extractants

A study to determine suitable extractant(s) for the separation of copper, indium and gallium from solutions of dissolved selenium-depleted CIGS material (Section 5.4) was performed. Organic phases containing kerosene (Solvent 70, Statoil) and 0.2 M TOPO (90 %, Sigma Aldrich), Cyanex 923 (93 %, Cytec Canada), TBP (97 %, Aldrich Chemicals), D2EHPA (97 %, Aldrich Chemicals), Cyanex 272 (80 %, Cytec Canada) or LIX 984 were prepared. LIX 984 was made by mixing LIX 860N-I (97 %, Corgnis Ireland) and LIX 84-I (95 %, Corgnis Ireland) at a volume ratio of 1:1. Kerosene was chosen since it is a solvent which is commonly used in industrial solvent extraction applications. The chosen extractants had previously been shown to give separation of the elements (see Section 2.10.3). Aqueous phases with a total metal content of 4 mM were prepared by diluting a solution from the direct dissolution of selenium-depleted material in 0.01, 0.1, 1, 3 and 6 M hydrochloric acid. The metal composition in the solutions was 45 mol% copper, 13 mol% gallium and 42 mol% indium. In the extraction experiments 1.5 ml of each phase was mixed at 25 °C for 2 h at 1500 rpm. This was determined to allow for equilibrium to be reached. Before sampling the phases were allowed to separate for 5 min. The samples were diluted and analysed with ICP-OES.

5.5.2 Investigation of extraction kinetics using TOPO and Cyanex 923

A kinetic study was done to determine the mixing time needed to reach equilibrium when using TOPO and Cyanex 923. The experimental procedure was the same as for the screening study, but the mixing time varied between 5 and 120 min. The aqueous phase used was the 3 M hydrochloric acid solution with 4 mM total metal content and the organic phases were 0.2 M of the extractants in kerosene.

5.5.2 Selective stripping of extracted metals

Selective stripping of the metals extracted with Cyanex 923 and TOPO was tested using several different stripping phases. The solutions and extraction procedure were the same as for the kinetics study, however, the phases were mixed for 20 min. The organic phase was then mixed with an equal volume of stripping phase for 1 h at 1500 rpm. The stripping phases used were Milli-Q® water, 0.1, 0.8 and 3 M hydrochloric acid, and 0.2 M EDTA. The EDTA (99.999 %, Sigma-Aldrich) was dissolved in Milli-Q® water by drop wise addition of 5 M sodium hydroxide. Sampling after stripping was done in the same way as described above.

5.5.2 Modelling of a possible solvent extraction separation process

A process based on the results from the solvent extraction studies was suggested and a simulation of the process was made. Each process step was set up to be counter current, to increase the efficiency of the process, and the simulation was made using mass balances based on Equation (3.13). For simplicity all phase ratios (θ) were set to 1. The aqueous feed was assumed to be provided from the dissolution of the selenium-depleted CIGS material and the metal content in the aqueous feed was set to match the concentrations in the solvent extraction experiments. In the simulation the following assumptions were made:

(1) The phases are immiscible so that the volumetric flows are constant.
(2) The D-values for each step are constant.
(3) In each step dynamic equilibrium is obtained.
(4) The aqueous stripping feeds are assumed to contain no metals.

Each flow was calculated by numerical iterations.

5.6 Electrochemical separation of copper, indium and gallium

5.6.1 Cyclic voltammetry

To determine the potentials needed for reduction of copper(II), indium(III) and gallium(III) to the respective metals the redox behaviour of the elements in chloride solutions was studied with cyclic voltammetry. The experiments were performed using the electrochemical cell described in Section 5.1.3, at a scan rate of 100 mV/s. The analysed solutions, containing 0.05 M copper(II), indium(III) or gallium(III), were prepared by dissolving copper(II) chloride (99.999 %, Sigma-Aldrich), indium(III) chloride (99.999 %, Sigma-Aldrich) or gallium(III) chloride (99.999 %, Sigma-Aldrich) in 1 M hydrochloric acid. The electrolyte, 1 M hydrochloric acid, was prepared by dilution of hydrochloric acid (puriss, 37 %, Sigma-Aldrich) in Milli-Q® water. The electrolyte was also analysed to determine the background signal and solutions containing 0.05 M of indium and gallium, or all three elements, were tested to investigate if the redox behaviours of the elements were influenced by each other.

5.6.2 Electrochemical separation of copper, indium and gallium

To determine if electrochemical separation can be used to separate copper, indium and gallium the separation was first investigated using a synthetic solution containing 0.25 M of copper(II), indium(III) and gallium(III) in 1 M hydrochloric acid (Solution 1). The solution was prepared from the metal chlorides in the same way as the solutions used for the cyclic voltammetry study. For each experiment 50 ml of solution was used and the solution was stirred at 500 rpm to facilitate a homogeneous concentration of the metals. Firstly copper was separated from the solutions by applying a constant potential of -0.5 V vs. the reference electrode to the working electrode over 8 h. During the experiments the current was recorded and samples (10 µl) were taken from the solution after 0.25, 1, 2, 4, 6 and 8 h and were analysed with ICP-OES. After the copper separation indium was separated from the solutions using a constant potential of -0.9 V vs. the reference electrode over 8 h. The current was recorded and samples of the solution were taken and analysed in the same way as for the copper separation. The formed copper and indium deposits were weighed before they were dissolved in concentrated nitric acid (puriss, 69 %, Sigma-Aldrich) and analysed with ICP-OES.

After the experiments on the synthetic solution the same separation procedure was tested on solutions of dissolved selenium-depleted CIGS waste material to determine if the separation method could be used for the recycling of copper, indium and gallium. Two solutions were prepared from the selenium-depleted CIGS material using the different dissolution methods in Section 5.4. However, the amount of dissolved material was increased to give solutions containing higher concentrations of metal.

5.6.2.1 Dissolution of selenium-depleted CIGS material in 3 M hydrochloric acid and hydrogen peroxide

The first solution containing real CIGS waste material (Solution 2) was prepared by dissolving 1.5 g of the residue from the selenium separation in 46 ml of 3 M hydrochloric acid at 75 ± 5 °C. To improve the dissolution of the material 1 ml/h of hydrogen peroxide (30 %, Sigma-Aldrich) was added over 4 h. The solution was stirred at 500 rpm during the dissolution. After the dissolution the leachate was diluted with Milli-Q® water to 50 ml. ICP-OES analysis showed that the metal concentrations in the resulting solution were 0.24 ± 0.01 M copper, 0.21 ± 0.01 M indium, 0.061 ± 0.002 M gallium and 0.005 ± 0.001 M selenium.

5.6.2.2 Dissolution of chlorinated, selenium-depleted CIGS material in 1 M HCl

The second solution of dissolved CIGS waste material (Solution 3) was prepared by dissolving 8 g of chlorinated product (described in Section 5.4.2) in 50 ml 1 M hydrochloric acid. The solution was filtered prior to ICP-OES to remove small amounts of precipitated selenium residues. The metal concentrations in the solution were 0.24 ± 0.01 M copper, 0.22 ± 0.01 M indium and 0.066 ± 0.001 M gallium. The selenium concentration was below the detection limit of the ICP-OES.

6. Results and discussion

6.1 Separation of selenium from CIGS materials

6.1.1 Feasibility of separating selenium by distillation of selenium dioxide

Before the selenium separation the particle size distribution and the chemical composition of the starting material was examined. The results of the examination of the particle size distribution are presented in Paper I, Table 1. It could be concluded that most of the particles had a size between 0.25 to 2.0 mm. ICP-OES analysis of the starting material showed that it contained 17.1 ± 0.5 wt% copper, 30.3 ± 1.4 wt% indium, 5.2 ± 0.16 wt% gallium and 47.4 ± 1.3 wt% selenium.

The results from the selenium separation study showed that the selenium content in the residues after oxidation decreased with increasing temperature. As can be seen in Fig. 6.1 the selenium separation starts at 500 °C, but at this temperature very little of the selenium present is extracted. After oxidation at 1000 °C, however, only 1.5 ± 2.5 % of the original amount of selenium remains in the residue. These temperatures are higher than the temperature at which selenium dioxide is formed from pure selenium. This is probably due to the higher melting temperature of CIGS, at around 1000 °C, compared to that of selenium at 217 °C.

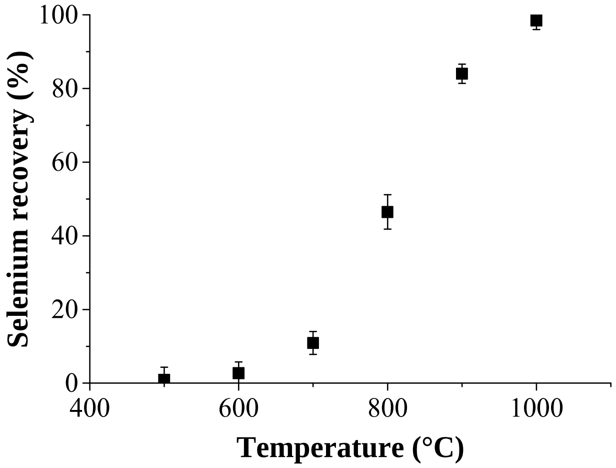

Fig. 6.1 Selenium recovery after the oxidation of CIGS as a function of temperature. The selenium recovery is stated as a percentage by weight of the selenium content in the residues compared to the selenium content in the starting material.

The mass balance for the experiments was used to calculate the selenium yield. Independent of the oxidation temperature approximately 85 % of the selenium removed from the CIGS was collected as selenium dioxide. The yield could probably be increased by rinsing out the selenium dioxide instead of collecting the crystals.

The crystalline composition, given by XRD analyses, of the starting material and the residues after treatment at 800 and 1000 °C are shown in Fig. 6.2.

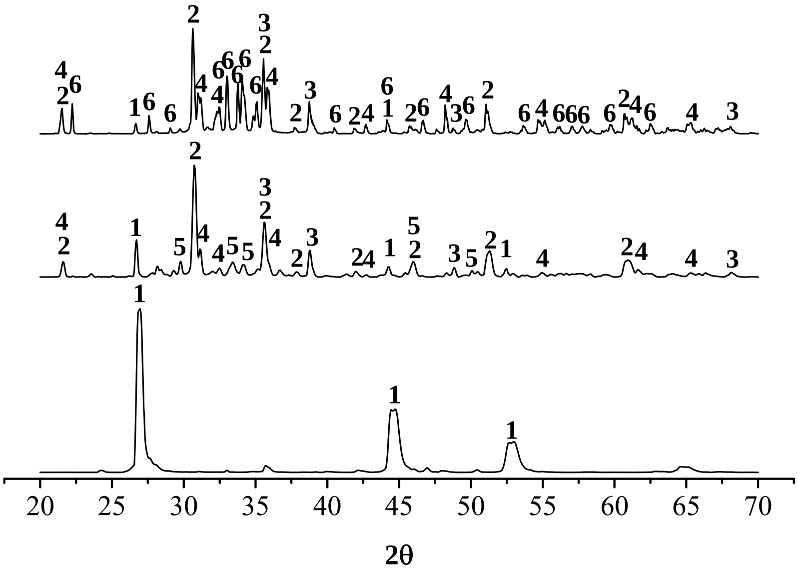

Fig. 6.2 XRD patterns for the starting material (bottom), residue after oxidation at 800°C (middle) and residue after oxidation at 1000°C (top). 1) Cu(In,Ga)Se_2, 2) In_2O_3, 3) CuO, 4) $CuGaInO_4$, 5) $SeCu_2$, 6) $Cu_2In_2O_5$.

The characteristic peaks of Cu(In,Ga)Se_2 (1) decrease after oxidation at 800 °C and indium oxide (2), copper oxide (3) and copper indium gallium oxide (4) are formed. There also seems to be some copper selenide (5) formed. After oxidation at 1000 °C additional peaks, identified as indium copper oxide (6), can be seen. It is apparent that some recrystallization occurs and new compounds are formed at different temperatures. This can be important in the further treatment of the residue since the chemical properties differ between different species.

When the residues from the oxidation tests were inspected it was noticed that they contained two different layers, a porous grey and blue top layer and a more compact yellow bottom layer. This was more pronounced at high temperatures. To explore the differences between these two layers, a sample from each layer was taken from the 1000 °C test for analysis. The analysis showed that all the remaining selenium in the residue was concentrated to the bottom layer. This might be due to insufficient contact between the gas and the solid material in the bottom of the crucible, indicating that mixing during the oxidation step could improve the selenium separation. It was also seen that the copper concentration was higher in the top layer and that almost all of the gallium had been concentrated to the bottom layer. This is most probably due to differences in the densities of the compounds (In_2O_3, CuO, $CuGaInO_4$ and $Cu_2In_2O_5$) formed during the oxidation.

Heating the CIGS starting material in an inert atmosphere did not result in any selenium separation at relatively low temperatures. When the temperature reached 960 °C a thin layer of selenium could be seen on the inside of the quartz tube on the far side of the furnace. The analysis of the residue from the distillation showed that only approximately 10 % of the selenium was recovered after treatment at 1000 °C for 24 h. This means that the majority of the selenium recovery in the previous experiments is due to the formation of selenium dioxide and not to the distillation of selenium.

6.1.2 Optimization of the selenium separation

The particle size distribution of the material prepared for the optimization study is presented in Table 6.1. Just below 50 wt% of the material was of the preferred particle size of 125-180 µm and more than 20 wt% was smaller than 63 µm and so could not be used in the fluidized bed due to entrainment of the particles in the gas flow. Since there will always be a fraction of small particles (<63 µm) formed when the CIGS material is crushed it was obvious that these particles would have to be treated in some other way. Therefore a series of experiments on this fraction were done in the tube furnace and the results were compared to the results from the tests in the fluidized bed reactor.

Table 6.1 Particle size distribution of the starting material for the optimization study.

Particle size (µm)	**Proportion of material with the given particle size (wt%)**
125-180	48
90-125	22
63-90	8
<63	22

The chemical composition of the starting material was determined to be 17.7 ± 0.38 wt% copper, 30.5 ± 0.69 wt% indium, 5.11 ± 0.1 wt% gallium and 46.45 ± 0.44 wt% selenium. The chemical composition for each particle size fraction was also analysed to demine if there were any deviations between the fractions. From this analysis it could be concluded that the composition of the different fractions differed very little, but still the values for each fraction were used when the selenium recovery from the different experiments was calculated.

Before the experiments in the fluidized bed reactor the fluidization gas flow for the different particle size fractions was determined at 22 ± 2 °C. These results were then used to calculate the fluidization flow at higher temperatures. At 900 °C a gas flow of 450 ml/min was used for particles with a size of 125-180 µm and for particles 90-125 µm in size the flow was set to 300 ml/min. The results from the tests in the fluidized bed reactor showed that, compared to the feasibility tests, the selenium recovery increased. After oxidation of particles with a size of 125-180 µm at 900 °C for 12 h the selenium recovery was 95 ± 1.5 %, compared to 84 ± 3 % after 24 h in the tube furnace. The selenium recovery increased with increasing reaction time, as can be seen in Fig. 6.3, which indicates that a relatively long reaction time was needed to remove the majority of the selenium. This experiment was not performed at a 1000 °C due to the risk of the bed melting at temperatures close to the melting temperature of CIGS.

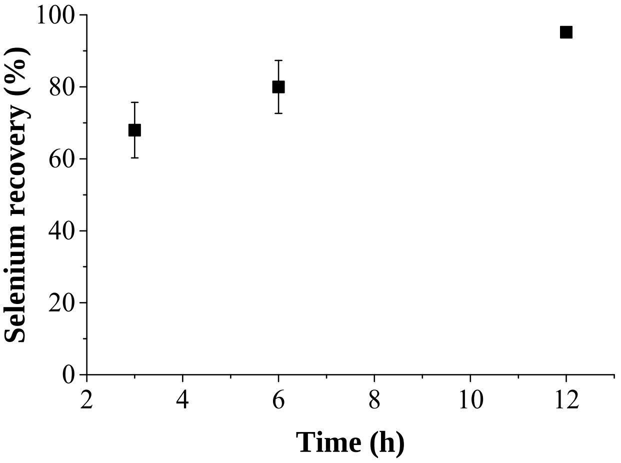

Fig. 6.3 Selenium recovery after 3, 6 and 12 h of oxidation of CIGS with a particle size of 125-180 µm at 900 °C and a gas flow of 450 ml/min in the fluidized bed.

The major drawback discovered while performing these experiments was that during the oxidation the particles agglomerated and sintered. This meant that the residue was difficult to remove from the reactor and that the expected benefit of better contact between the CIGS particles and the oxygen gas was not achieved. During some tests a core of CIGS material that had not reacted formed in the middle of the bed. This is the reason for the relatively large standard deviations seen in Fig. 6.3. A smaller particle size of 90-125 µm was also tested to determine if the selenium separation could be increased. It was found, however, that the selenium recovery only increased marginally from 68 ± 8 % to 71 ± 17 %. Here the standard deviation was even larger, also due to a core of material that had not reacted forming in some residues. This is a problem because it makes the process unpredictable and difficult to control.

The oxidation of particles with a size of less than <63 µm in the tube furnace gave a much better result than the oxidation in the fluidized bed. After oxidation at 900 °C for 12 h less than 1 % of the selenium remained in the residue. When shorter times were tested the results were the same, even for an oxidation time of only 1 h. This means that all of the selenium was recovered in less than 1 h. To optimize the process even further, lower temperatures were tested. The results of these tests can be seen in Fig. 6.4. After oxidation at 800 °C approximately 99 % of the selenium was recovered from the CIGS material, while at 700 °C only 50 % was recovered. These results imply that the oxidation temperature could be lowered to 800 °C and still give a high selenium recovery. It can also be seen that the standard deviation is much lower for these tests than for those performed in the fluidized bed reactor, which means that the process is more predictable and reproducible.

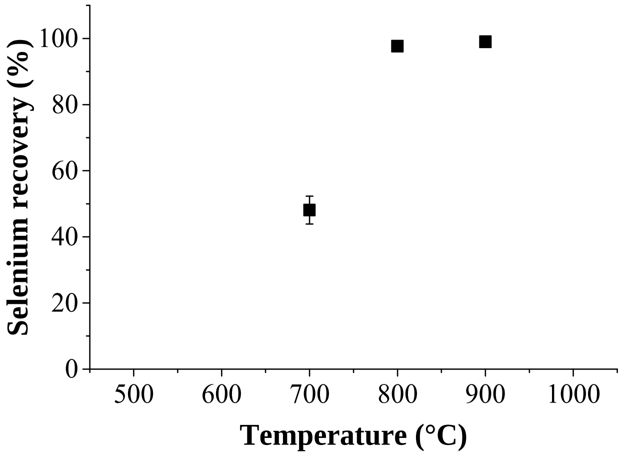

Fig. 6.4 Selenium recovery after oxidation of CIGS particles with a size of less than 63 µm for 1 h at 700, 800 and 900 °C in the tube furnace.

As mentioned above, the small particles (<63µm) used in the tube furnace are always produced when the CIGS material is crushed and it is therefore easier to crush the material to that particle size than to try to get the certain particle sizes needed for the fluidized bed. This is also an advantage when it comes to the development of an industrial process.

6.1.3 Reduction of selenium dioxide

After the oxidation reaction the selenium dioxide was reduced using the Riley reaction. The reaction resulted in 1.19 g of selenium, corresponding to a yield of 90.7 ± 0.6 %. The purity of the organic product is shown in Fig. 5 in Paper I. Weighing of the organic product gave 3.1 g and the yield was determined to be 96.6 ± 0.3 %.

The sulphur dioxide reduction reaction was first performed at room temperature and red selenium was formed. Due to the ability of the red selenium particles to stick to the surfaces of the reaction vials the selenium was very difficult to collect. However, upon heating to 80 °C the red selenium was observed to gradually transform into black selenium. The black selenium did not stick to surfaces and was therefore more easily collected. An additional advantage of this transformation was that the formation of new red selenium could be distinguished. The time needed for complete reduction could thereby easily be determined. It was concluded that 10 minutes was a sufficient time for a complete reaction. The reaction resulted in 0.67 g of selenium, corresponding to a yield of 93.8 ± 1.0 %. Analysis of the liquid from the reaction showed that less than 1.4 ± 0.5 % of the selenium was not reduced. This means that the selenium dioxide reduction was almost complete and that improvements in the collection of the selenium could result in higher yields.

6.1.4 Analysis of the purity of the recycled selenium

The purity of selenium from both reduction experiments was analysed along with the purity of the selenium dioxide from the oxidation test at 1000 °C (the same selenium dioxide that was used in the reduction experiments). The selenium dioxide was analysed to examine possible differences in the purity before and after the reduction. Difference in purity correlating to the reduction method used was also of interest. Scandium, titanium, vanadium, chromium, manganese, iron, cobalt, nickel and zinc were analysed, since these pose a potential problem in solar cell production by decreasing the efficiency of the solar cells. Copper, indium and gallium are not viewed as a problem, but they were also analysed since it was of interest to know if there were any residues in the selenium. The results from the ICP-MS measurements were analysed and the concentrations of all elements, except iron, in the selenium were calculated. The concentration of iron in the selenium was determined from the neutron activation analysis. The results from both of these analyses are presented in Table 6.2.

Table 6.2 Concentrations of the analysed impurities in the recycled selenium.

Elements	**Selenium dioxide (ppm)**	**Selenium – Riley reaction (ppm)**	**Selenium - Sulphur dioxide reaction (ppm)**
Sc	0.19 ± 0.33	0.19 ± 0.32	<0.1
Ti	0.13 ± 0.24	1.09 ± 1.05	0.49 ± 0.43
V	0.16 ± 0.05	0.13 ± 0.11	0.1 ± 0.08
Cr	0.17 ± 0.08	0.79 ± 0.33	0.23 ± 0.13
Mn	<0.1	<0.1	<0.1
Fe	0.95 ± 0.30	4.03 ± 0.88	3.36 ± 0.12
Co	<0.1	<0.1	<0.1
Ni	0.26 ± 0.13	0.51 ± 0.22	0.34 ± 0.19
Zn	0.30 ± 0.14	0.43 ± 0.21	0.18 ± 0.14
Cu	5.49 ± 0.45	13.5 ± 2.86	5.58 ± 0.46
Ga	0.35 ± 0.12	3.45 ± 0.26	0.29 ± 0.11
In	3.57 ± 0.22	6.55 ± 1.88	2.04 ± 0.95

The concentration of scandium, titanium, vanadium, chromium, manganese, cobalt, nickel and zinc in the selenium was determined to be low in both the selenium dioxide and in the reduced selenium from both reduction reactions. The iron concentration was higher for the reduced selenium than for the selenium dioxide, which shows that the contamination was introduced during the reduction step. The concentrations of copper, indium and gallium were determined to be higher than for the other elements, but the separation was still very good. Using the concentrations of the analyzed impurities the purity of the recycled selenium was calculated and can be seen in Table 6.3. The purity with respect to the critical elements, scandium, titanium, vanadium, chromium, manganese, iron, cobalt, nickel and zinc, was higher than 99.999 wt% for all three analyzed materials. The concentration of copper, indium and gallium in the recycled selenium was higher than the concentration of the critical elements, but the overall purity was still higher than 99.99 wt%. A comparison between the two different reduction methods showed that the Riley reaction resulted in a somewhat lower purity.

Table 6.3 Purity of the selenium dioxide from the oxidation and for the recycled selenium with respect to *Sc, Ti, V, Cr, Mn, Fe, Co, Ni and Zn, ** Sc, Ti, V, Cr, Mn, Fe, Co, Ni, Zn, Cu, Ga and In.

	Selenium dioxide (wt%)	**Selenium - Riley reaction (wt%)**	**Selenium - Sulphur dioxide reaction (wt%)**
Purity*	99.9998 ± 5.53E-05	99.9993 ± 1.52E-05	99.9995 ± 5.31E-05
Purity**	99.9988 ± 7.57E-05	99.9969 ± 3.76E-04	99.9987 ± 1.19E-04

6.2 Separation of copper, indium and gallium from selenium-depleted CIGS material using high-temperature chlorination

6.2.1 Initial study on the chlorination treatment using chlorine gas, hydrogen chloride gas and ammonium chloride

The first chlorination agent to be evaluated was chlorine gas. Fig. 6.5 shows the effect of temperature on the recovery of copper, indium and gallium when using chlorine gas.

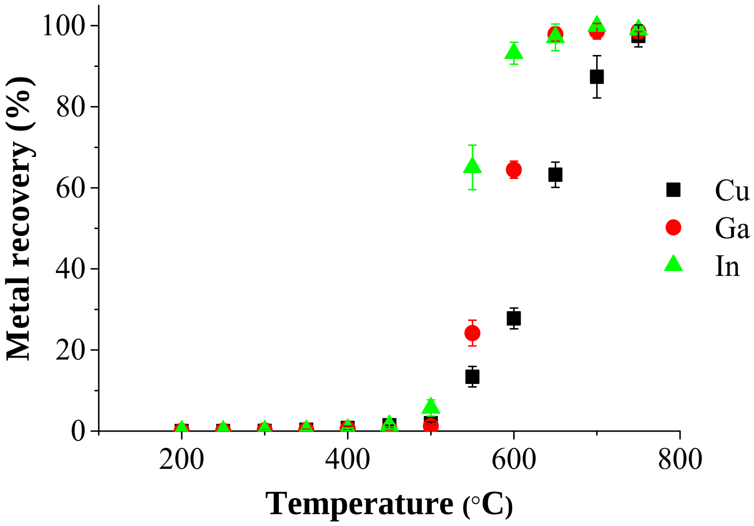

Fig. 6.5 Effects of temperature on the recovery of copper, indium and gallium from the starting material when using chlorine gas as the chlorination agent.

As can be seen, all three elements were recovered between 500 and 700 °C. This meant that no separation of the elements could be achieved during the chlorination. The result corresponded well with the result from the thermodynamic calculations (Fig. 3.1), which predicted that separation of the elements would be difficult when chloride gas was used as the chlorination agent due to $CuCl_2$ (s,l) and $InCl_3$ (s,l) being the stable species at low temperatures. However, XRD analysis of the residue after treatment at 500 °C showed the same XRD pattern as the starting material. In other words, the material had not been chlorinated and it was concluded that the lack of separation between the elements was due to the high temperature needed for the chlorination reactions to start. The reason for the deviation is probably that even if the chlorinated species are thermodynamically stable at low temperatures the kinetics of the chlorination reaction is slow. The high recovery yields (nearly 100 % for all three elements) at higher temperatures indicate complete chlorination of the starting material. This complete chlorination shows that it may still be possible to achieve separation of the elements by treating the chlorinated product in a subsequent separation step, as described by Ohwa *et al.* [66].

As mentioned above, the reaction temperature needed for chlorination could possibly be lowered for some or all of the elements in the starting material by carbochlorination and, according to the thermodynamic calculations (Fig. 3.2), the separation of the elements could therefore potentially be improved. The results from the carbochlorination tests, shown in Fig. 6.6, show that indium and gallium were recovered at significantly lower temperatures while the effect on copper was not as pronounced.

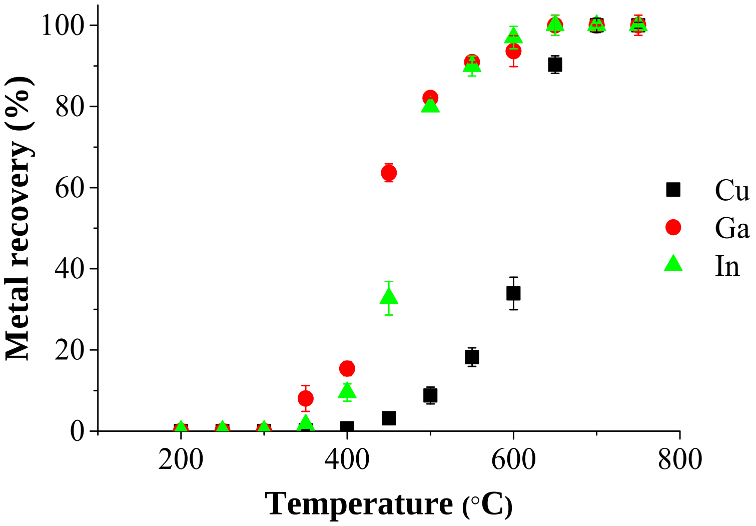

Fig. 6.6 Effects of temperature on the recovery of copper, indium and gallium when using chlorine gas as the chlorination agent and adding 0.1 g of carbon to the staring material.

At 500 °C, 80 % of the indium and gallium were recovered while only 10 % of the copper was recovered. This meant that, while no separation at all was achieved between indium and gallium, a relatively good separation could be achieved between copper and these elements. The result for gallium did not agree with the equilibrium calculation results, which suggested that gallium could be recovered at lower temperatures. Again, the deviation was attributed to the slow kinetics of the chlorination reaction at low temperatures.

The second chlorination agent to be evaluated was hydrogen chloride gas and the recovery of the respective elements as a function of chlorination temperature can be seen in Fig. 6.7.

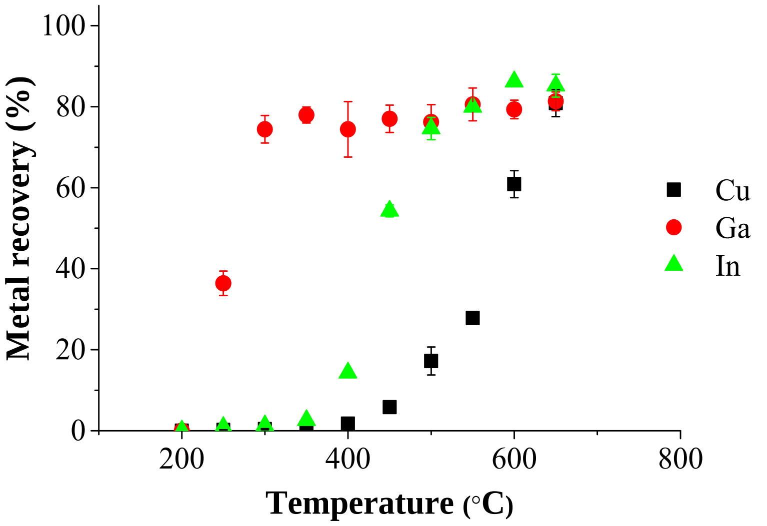

Fig. 6.7 Effects of temperature on the recovery of copper, indium and gallium when using hydrogen chloride gas as the chlorination agent.

As predicted by the thermodynamic calculations, chlorination with hydrogen chloride gas gave good separation between the elements, especially for gallium, which was recovered at temperatures below 300 °C while indium and copper were recovered above 350 and 400 °C, respectively. However, only around 80 % of the gallium and the indium was recovered at 600 °C, indicating that the starting material was not completely chlorinated. This was further proven by XRD analysis (Fig. 6.8), which showed that the residues after chlorination still contained oxides of copper, indium and gallium.

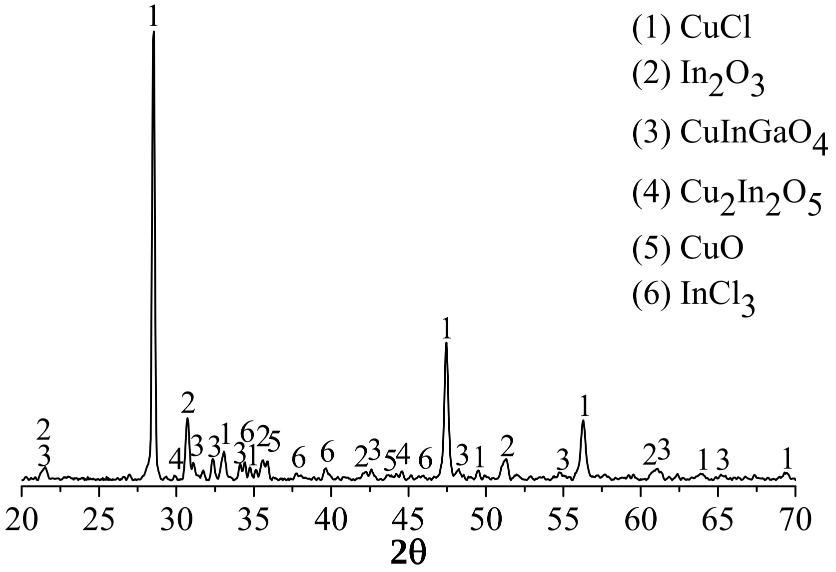

Fig. 6.8 XRD pattern for the residue after chlorination with hydrogen chloride gas at 600 °C.

An explanation for the incomplete chlorination could be that the water formed during chlorination with hydrogen chloride gas (see Fig. 3.3 above) causes agglomeration of the starting material. The agglomerates found in the material were relatively hard, indicating that the particles had also been sintered to some extent. The agglomeration and sintering may subsequently lead to incomplete chlorination due to insufficient contact between the starting material and the hydrogen chloride gas.

The final chlorination agent to be tested was ammonium chloride. The effect of temperature on the extraction of the elements is shown in Fig. 6.9.

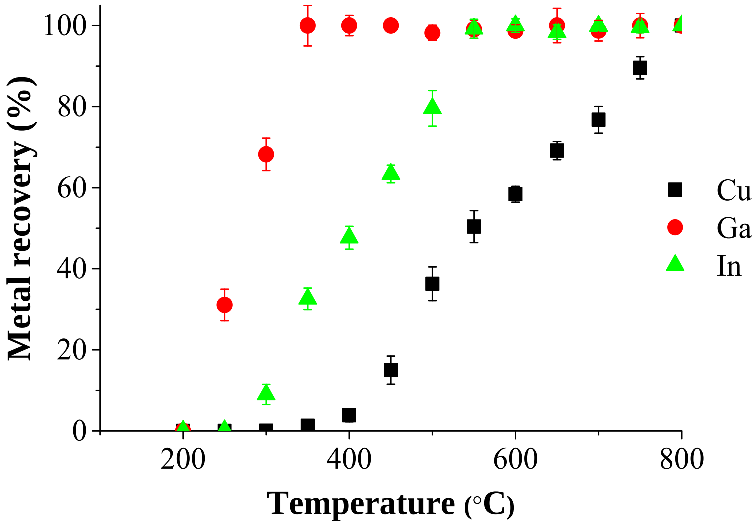

Fig. 6.9 Effects of temperature on the recovery of copper, indium and gallium when using ammonium chloride as the chlorination agent.

As can be seen in the figure, all of the gallium was recovered at 350 °C and since the copper recovery started at 400 °C it could be concluded that complete separation of gallium and copper could easily be achieved. Indium recovery started at 300 °C and a pure gallium fraction, corresponding to 35 % of the gallium, was recovered at 250 °C. This indicates that if the material is completely chlorinated at 250 °C complete recovery of the entire gallium content should be possible if the volatilization of the gallium chloride is allowed to proceed for a longer time. The same is true for the separation of indium from copper at 350 °C. It is clear that these results deviate from those predicted by the thermodynamic calculations (Fig. 3.4). The separation of indium and gallium was better than predicted. This deviation can be explained by the formation of species other than those that are included in the HSC database. One example is the compounds containing ammonium e.g $(NH_4)_2InCl_5{\cdot}H_2O$ found by XRD analysis of the material from the chlorination experiments (see below). It was also clear that the conditions in the reactor were not as reducing as predicted and that copper chlorides in gas phase could be formed. One explanation could be that the formation of ammonium containing compounds reduces the amount of free ammonium, and consequently the amount of hydrogen gas, in the atmosphere. To determine if the chlorination of the starting material was complete at low temperatures the residue after chlorination at 250 °C was analysed with XRD. The XRD pattern seen in Fig. 6.10 indicates that the residue contained the indium chlorides In_3InCl_6 and $(NH_4)_2InCl_5{\cdot}H_2O$, along with the copper chlorides CuCl and $CuCl_2$. The XRD pattern also suggests the presence of $CuInO_2$, which indicates that some of the starting material was not chlorinated at 250 °C.

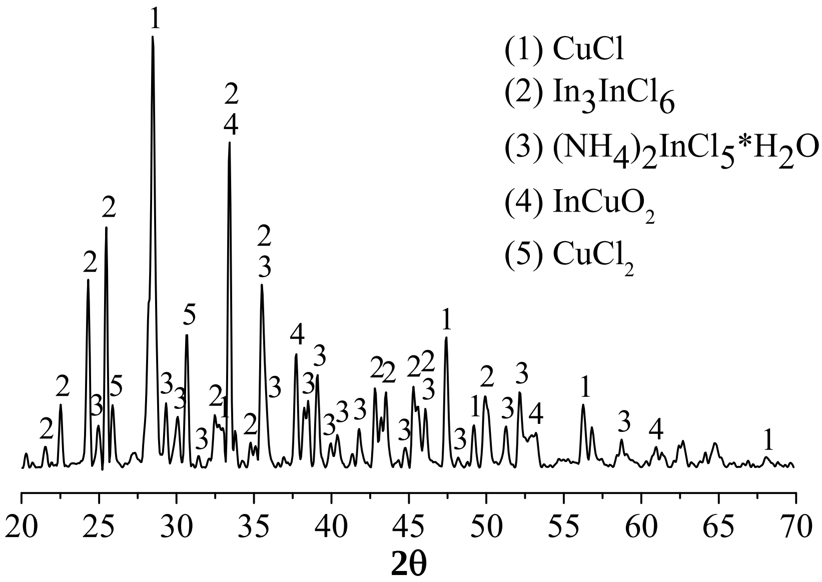

Fig. 6.10 XRD pattern for the residue after chlorination with ammonium chloride at 250 °C.

$CuInO_2$ was not present in the starting material before chlorination, but it might have formed from one of the oxides as a result of a change in crystal structure. The absence of compounds containing gallium in the residue was probably due to the concentration being below the detection limit of the XRD. Therefore the presence of gallium compounds that had not been chlorinated could not be ruled out. At the same time Fig. 6.9 shows that gallium, indium and copper were completely recovered at 350, 550 and 800 °C, respectively. This means that the materials containing the different elements were completely chlorinated at these temperatures. Compared to hydrogen chloride gas, ammonium chloride gave a higher reaction yield, even though hydrogen chloride works as the chlorination agent in both cases. The reason is most likely that the ammonium chloride was mixed with the starting material, thus giving a good contact between reactants.

The results for the three different chlorination agents were evaluated and ammonium chloride was determined to be the most promising for further process development. Hydrogen chloride gas gave the most efficient separation between the elements, but due to a metal recovery of less than 100 % of the starting material, hydrogen chloride gas was considered less suitable for further process development in comparison to the other reagents. One way to solve the problem of incomplete chlorination could be to reprocess the material with the next batch of starting material; however this was not investigated. Of the two remaining chlorination agents, ammonium chloride gave a better separation of the elements compared to chlorine gas.

In addition, ammonium chloride is less expensive and easier to handle than both of the gases, which are very corrosive.

6.2.2 Study of the overall kinetics of the recovery of copper, indium and gallium from oxidation residues using ammonium chloride as the chlorination agent

The recovery of gallium, indium and copper from the starting material, i.e. selenium-depleted CIGS waste material, as a function of time and at different temperatures is shown in Figs. 6.11, 6.12 and 6.13, respectively.

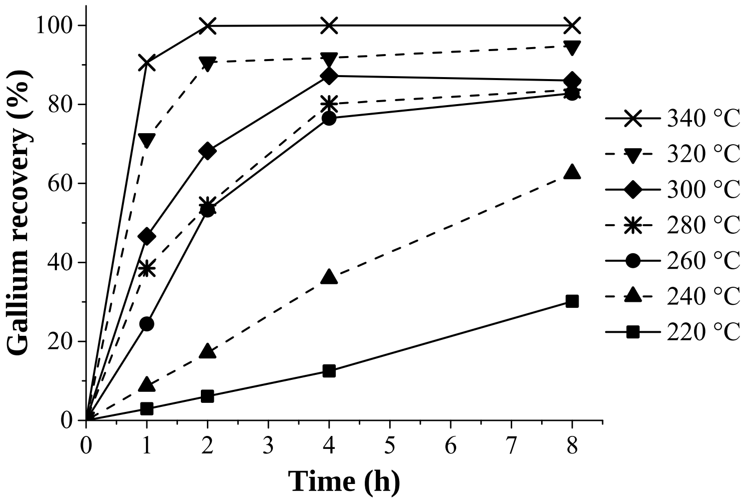

Fig. 6.11 Recovery of gallium as a function of time at temperatures between 220 and 340 °C.

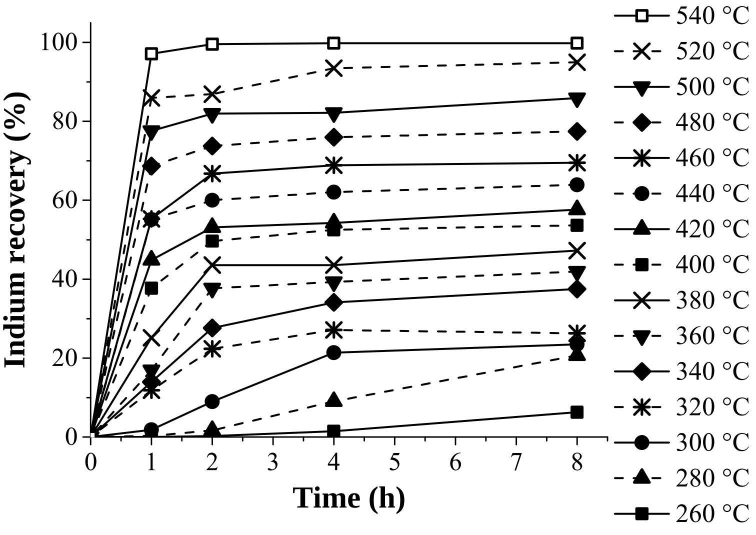

Fig. 6.12 Recovery of indium as a function of time at temperatures between 260 and 540 °C.

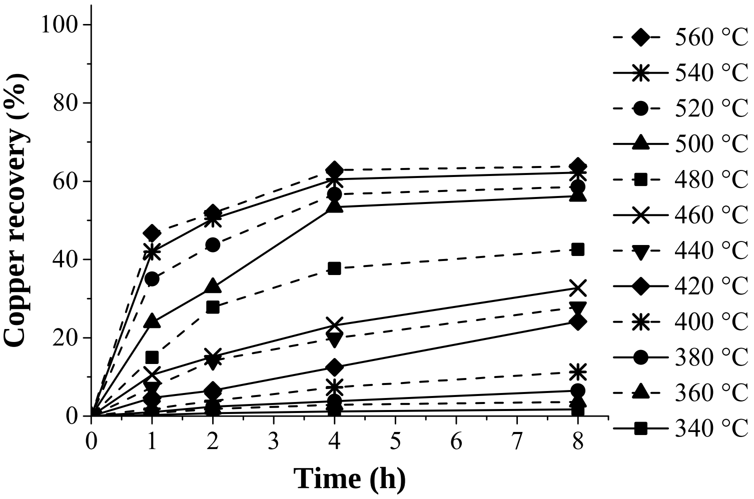

Fig. 6.13 Recovery of copper as a function of time at temperatures between 340 and 560 °C.

The evaporation of the gallium chlorination product (see Fig. 6.11) started at 220 °C and gallium was completely recovered after 2 h at 340 °C. The recovery of indium (Fig. 6.12), on the other hand, started at 260 °C, while evaporation of copper chloride (Fig. 6.13) was obtained at temperatures above 340 °C. Indium was completely recovered after 2h at 540 °C and the study was therefore stopped at 560 °C. It can be seen for all three elements that the recovery increased with temperature. At low temperatures the evaporation of chlorides increased linearly with time, as could be expected, but above a certain temperature the recovery did not increase with time. This indicates that either:

(1) the chlorination of the starting material was incomplete, or

(2) the diffusion of the formed chlorides was hindered by some change in the solid material, or

(3) the atmosphere in the reactor had been saturated with the chlorides.

Due to the gas flow through the reactor the latter explanation was considered unlikely to completely stop the recovery. In addition, higher temperatures give a higher gas flow rate in the reactor and this means that the higher the temperature the lower the likelihood of saturation should be. Since the ammonium chloride is liquid at temperatures above approximately 300 °C it is also unlikely that limited diffusion would stop the metal recovery completely. Since the XRD analysis of the residue after chlorination at 250 °C (Fig. 6.10) suggested that the material contained oxides, incomplete chlorination of the material was considered to be the most likely cause of the problem. In addition, XRD analysis showed that the products from the different experiments contained relatively high amounts of ammonium chloride. Since ammonium chloride is reformed when ammonium gas and hydrogen chlorine gas is cooled in the cold part of the reactor this suggested that part of the hydrogen chlorine chlorination agent had been removed from the reactor before it had time to react. The increasing recovery at higher temperatures indicates that the chlorination reactions are faster at higher temperatures, allowing more of the chlorination agent to react before it is removed. It was therefore concluded that the chlorination of the starting material needed to be optimized to give complete chlorination at low temperatures. If the chlorination is complete at low temperatures it should be possible to separate gallium at 260 °C, since the indium recovery at that temperature is less than 1.5 wt% after 4 h. In the same way, a good indium separation should be possible at 340 °C, since the copper recovery at that temperature is less than 2 % after 8 h. However, good separation requires that the time needed for complete recovery of gallium and indium, respectively, is relatively short.

6.2.3 Optimization of chlorination with ammonium chloride using Ga_2O_3 as a model compound

The recovery of gallium from Ga_2O_3 at 260 °C as a function of time and ammonium chloride addition is shown in Fig. 6.14.

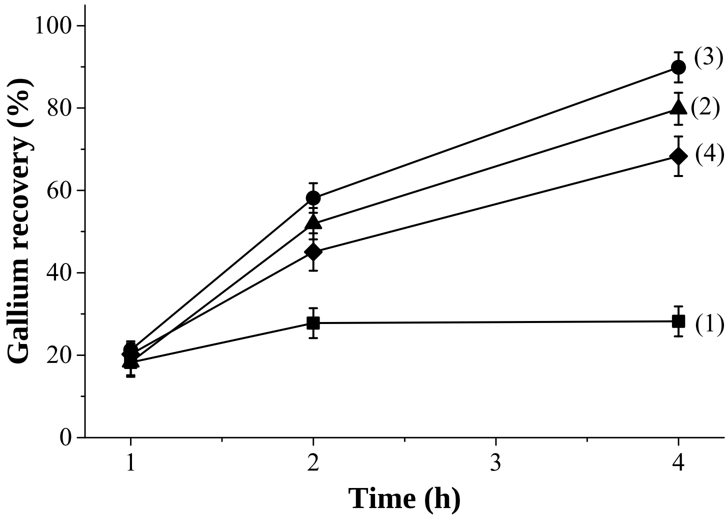

Fig. 6.14 Gallium recovery as a function of time at 260 °C after addition of (1) 3, (2) 6, or (3) 9 moles of NH_4Cl per mole of gallium to 0.07 g of Ga_2O_3 according to Test 1, 2 and 3 (described in Table 5.1). The results were compared to the gallium recovery from the starting material at 260 °C (4) taken from the kinetics study.

The results showed that a larger addition of ammonium chloride resulted in a higher recovery of gallium, and with addition of 9 moles of chloride per mole of gallium (Fig. 6.14, curve (3)) the recovery was almost 90 %. XRD analysis of the residues after the tests showed that the remaining gallium was in the form of gallium oxide, and not gallium chloride, and that no ammonium chloride remained in the residues. This confirmed that the incomplete gallium recovery was due to incomplete chlorination and not to slow evaporation of the chloride that was formed. However, since the treatment of the starting material (Fig. 6.14, curve (4)) resulted in higher gallium recovery than treatment of gallium oxide with the same gallium to ammonium chloride ratio (Fig. 6.14, curve (1)), experiments were also performed with an addition of aluminium oxide to the gallium oxide, to simulate the diffusion in the starting material. The results from those experiments are presented in Fig. 6.15.

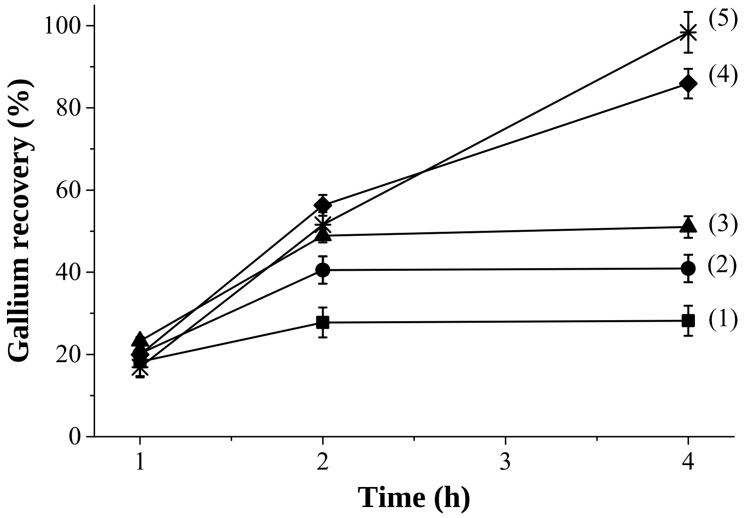

Fig. 6.15 Gallium recovery as a function of time at 260 °C from 0.07 g of Ga_2O_3 mixed with (1) 3 moles of NH_4Cl per mole of gallium (Table 5.1, Test 1), (2) 3 moles of NH_4Cl per mole of gallium and 0.4 g Al_2O_3 (Table 5.1, Test 4), (3) 3 moles of NH_4Cl per mole of gallium and 0.9 g Al_2O_3 (Table 5.1, Test 5), (4) 6 moles of NH_4Cl per mole of gallium and 0.9 g Al_2O_3 (Table 5.1, Test 6) and (5) 9 moles of NH_4Cl per mole of gallium and 0.9 g Al_2O_3 (Table 5.1, Test 7).

As can be seen, an addition of 0.4 or 0.9 g of aluminium oxide to the gallium oxide (Fig. 6.15, curve (2) and (3), respectively) increased the gallium recovery compared to the result in experiments with only gallium oxide (Fig. 6.15, curve (1)). This indicates that the aluminium oxide delays the removal of the hydrogen chlorine gas, allowing it to react for a longer time. The higher aluminium oxide addition gave a better simulation of the diffusion in the starting material than the lower addition. The higher amount of aluminium oxide was therefore used to study the effect of addition of different amounts of ammonium chloride. Also in this case a higher ammonium chloride addition gave a higher gallium recovery, and 9 moles of ammonium chloride per mole gallium, together with 0.9 g of aluminium oxide, resulted in 100 % gallium recovery. The gallium recovery was not improved by mixing gallium oxide, aluminium oxide and ammonium chloride and pelletizing the material, or by using the aluminium oxide as a cover. The results from Tests 8-10 in Table 5.1 can be seen in Fig. 7 and Fig. 8 in Paper III.

From the optimization study it was clear that a larger addition of ammonium chloride gave a higher gallium recovery. A large enough addition of ammonium chloride to samples similar to the real starting material gave almost complete gallium recovery. Increasing the sample height, by addition of an inert material also improved the gallium recovery. A more compact sample only marginally improved the result, since the pellets were ruptured by the gas evolution.

6.2.4 Separation of gallium from indium and copper

The temperature chosen for the separation of gallium from the starting material was 260 °C. Gallium separation using a large addition of ammonium chloride was tested first, see Table 6.4.

Table 6.4 Separation of gallium at 260 °C using one large addition of ammonium chloride.

	Temp. (°C)	**Recovery time (h)**	**NH_4Cl addition (moles/mole metals)**	**Gas flow (ml/min)**	**Metal recovery (wt%)**		
					Ga	**In**	**Cu**
GS 1:1	260	4	9	200	47.3 ± 4.1	0.2 ± 0.1	n.d
GS 1:2	260	8	9	200	75.9 ± 2.9	1.0 ± 0.1	n.d
GS 1:3	260	8	9	400	85.4 ± 1.9	1.3 ± 0.3	n.d

In the kinetics study (Fig. 6.11) approximately 76 % of the gallium was recovered after 4 h at 260 °C. By adding more ammonium chloride to the staring material, in accordance with the result from the optimization study, the recovery was expected to increase. However, when the separation was tested using 9 moles of ammonium chloride per mole of metals instead of 3 moles (see GS 1:1 in Table 6.4) only 47 % of the gallium was recovered. With the higher ammonium chloride addition a treatment time of 8 h (GS 1:2) was needed to achieve the same gallium recovery. It is obvious that the larger amount of ammonium chloride gave a slower gallium recovery. In addition, a higher gas flow through the reactor (GS 1:3) increased the gallium recovery to 85 %. This indicates that the lower gallium recovery is most likely due to saturation of the atmosphere in the reactor impeding the evaporation of the chlorides. GS 1:3 gave a gallium fraction containing 90.5 ± 3.7 wt% gallium and 9.5 ± 2.0 wt% indium. The copper recovery was below the detection limit of the ICP-OES.

To obtain a complete chlorination of the starting material and at the same time have a reasonable recovery time, three smaller additions of ammonium chloride to the starting material, at 2 h intervals, was tested. The results can be seen in Fig. 6.16. When the results for GS 2:1 (Fig. 6.16, curve (1)), where no extra ammonium chloride was added, were compared with the results for GS 2:2 (Fig. 6.16, curve (2)) and GS 2:4 (Fig. 6.16, curve (3)) it was seen that additions of 3 moles of chloride per mole of metals after 2 and 4 h lowered the gallium recovery, while addition of 1 mole of chloride per mole of metals increased the gallium recovery. As an explanation it was suggested that the larger ammonium chloride additions, despite the gas flow through the reactor, saturated the atmosphere in the reactor and thus hindered the evaporation of the metal chlorides. Smaller additions, however, gave the desired effect of increased chlorination in the reactor without impeding the chloride evaporation.

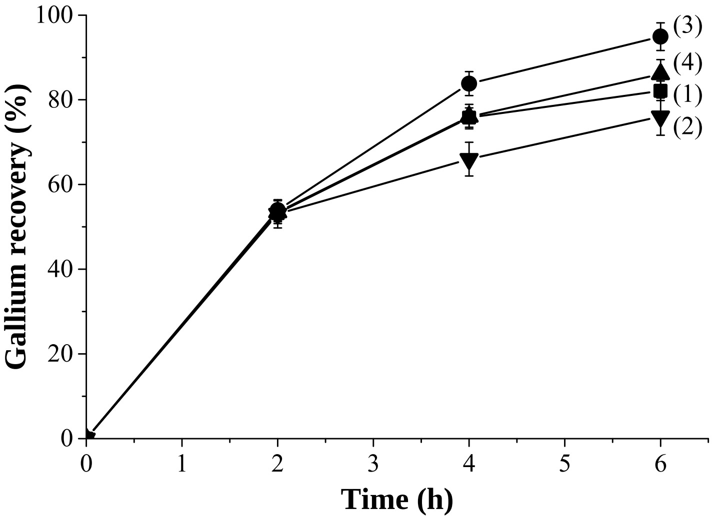

Fig. 6.16 Gallium recovery as a function of time at 260 °C and a gas flow of 200 ml/min when adding (1) 3; 0; 0, (2) 3; 3; 3, (3) 3; 1; 1 or (4) 3; 0; 3 moles of chloride per mole of metals after 0, 2 and 4 h, respectively, according to GS 2:1, GS 2:2, GS 2:4 and GS 2:3 as described in Table 5.2.

In GS 2:3 (Fig. 6.16, curve (4)) mixing the material after 2 h, without adding ammonium chloride, did not increase the gallium recovery compared to GS 2:1 (Fig. 6.16, curve (1)) where the material was not mixed. This indicates that the gallium recovery is not controlled by entrapment of gaseous species in the material. The results from tests with different carrier gas flows showed that a higher gas flow did increase the gallium recovery (Fig 6.17).

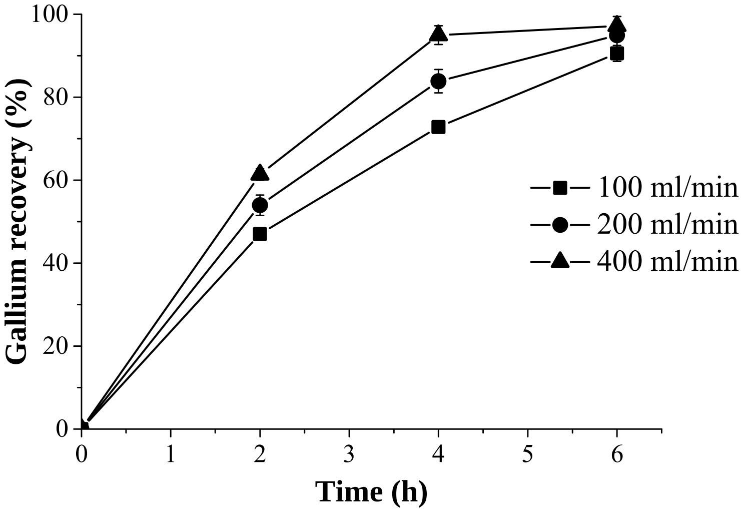

Fig. 6.17 Gallium recovery as a function of time and gas flow through the reactor at 260 °C. The ammonium chloride addition corresponded to 3, 1 and 1 moles of chloride per mole of metals after 0, 2 and 4 h, respectively (see GS 2:4-2:6 in Table 5.2).

A gas flow of 400 ml/min gave a gallium recovery of 95 % after 4 h and greater than 97 % after 6 h.

6.2.5 Separation of indium and copper

After removing the gallium from the starting material, indium separation was performed at 340 °C. Indium separation from the residue from the gallium separation using one large addition of ammonium chloride (GS 1:3) was tested first. The results are presented in Table 6.5.

Table 6.5 Separation of indium at 340 °C from the gallium separation residue (GS 1:3) using a large addition of ammonium chloride.

	Temp. (°C)	**Recovery time (h)**	**NH_4Cl addition (moles/mole metals)**	**Gas flow (ml/min)**	**Metal recovery (wt%)**	
					In	**Cu**
IS 1:1	340	4	0	200	52.1 ± 2.5	1.4 ± 0.3
IS 1:2	340	8	0	200	52.6 ± 1.9	2.2 ± 0.3
IS 1:3	340	8	13.5	200	75.6 ± 2.8	2.7 ± 0.4
IS 1:4	340	8	13.5	400	81.6 ± 2.4	3.1 ± 0.7

The first indium separation test (IS 1:1) was made without adding any additional ammonium chloride to the material. After 4 h just over 50 % of the indium in the starting material was recovered. In the kinetics study (Fig. 6.12) only 34 % of the indium was recovered after 4 h at 340 °C. The increase in indium recovery is probably due to increased chlorination of the indium achieved during the previous optimized gallium separation step. Increasing the recovery time to 8 h (IS 1:2) did not improve the indium recovery. This indicated that the indium had not been completely chlorinated after treatment at 260 °C for 8 h. Addition of 13.5 moles of ammonium chloride per mole of metals (indium and copper) to the gallium separation residue before the indium separation gave a higher indium recovery, and a higher gas flow improved the recovery further. By treating the material for 8 h at 340 °C, after addition of 13.5 moles of ammonium chloride per mole of metals and using a gas flow of 400 ml/min, around 81 % of the indium could be recovered. At the same time 3 % of the copper was recovered and the gallium remaining in the residue was also recovered. The resulting indium fraction contained 96.2 ± 4.4 wt% indium, 2.3 ± 0.5 wt% copper and 1.4 ± 0.3 wt% gallium, and the remaining copper fraction contained 76.4 ± 0.6 wt% copper and 23.6 ± 0.4 wt% indium.

Indium was next separated from the second set of gallium separation residues where several smaller additions of ammonium chloride after 0, 2 and 4 h and a gas flow of 200 ml/min had been used. Different ammonium chloride additions were tested in order to determine the effect on the indium separation, see Fig. 6.18. It can be seen that in all cases the indium recovery increased compared to the indium recovery from the kinetics study. Again this was attributed to the increased chlorination of the indium during the previous gallium separation. The figure also shows that larger ammonium chloride additions gave a higher indium recovery and that only mixing the material after 2 h (Fig. 6.18, curve (2)), without adding ammonium chloride, did not result in any additional indium recovery during the subsequent 2 h treatment.

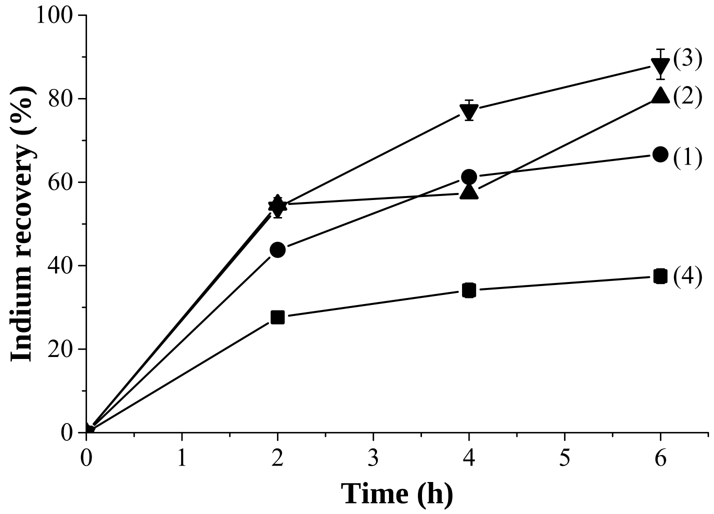

Fig. 6.18 Indium recovery from the gallium separation residue (GS 2:4) as a function of time at 340 °C and a gas flow of 200 ml/min when adding (1) 0; 1.1; 1.1, (2) 3.4; 0 (mixing); 3.4 or (3) 3.4; 3.4; 3.4 moles of chloride per mole of metals remaining in the residue from the gallium separation after 0, 2 and 4 h, respectively (see IS 2:1-2:3 in Table 5.3). (4) The indium recovery from the kinetics study where the starting material was mixed with 3 moles of chloride per mole of metals and treated directly at 340 °C with a gas flow of 200 ml/min.

The effect of the gas flow on the indium recovery was also investigated. The results are shown in Fig. 6.19.

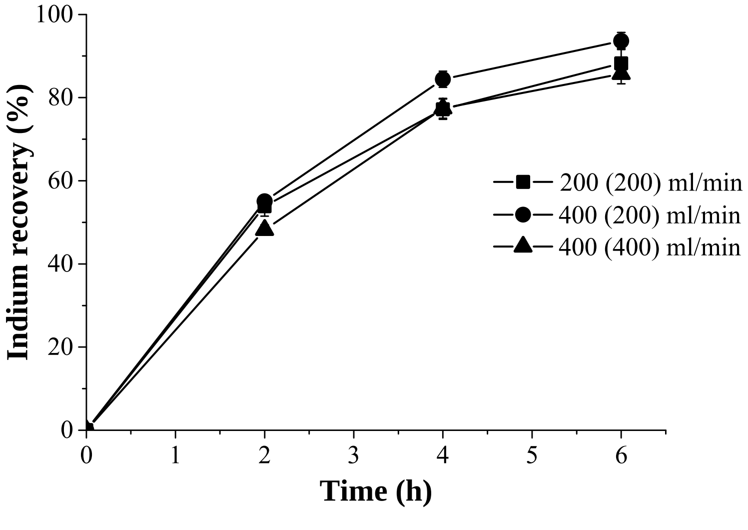

Fig. 6.19 Indium recovery as a function of time and gas flow through the reactor at 340 °C. The residue from the gallium separation was mixed with ammonium chloride, corresponding to 3.4 moles of chloride per mole of metals, after 0, 2 and 4 h (see IS 2:3-2:5 in Table 5.3). The number in brackets is the gas flow used during the previous gallium separation step.

From the results it was clear that a higher gas flow increased the indium recovery and that a higher gas flow during the preceding gallium separation gave a lower indium recovery. The highest indium recovery (93.6 ± 2.1 %) was achieved when a gas flow of 200 ml/min was used for the gallium separation and a gas flow of 400 ml/min was used for the indium separation. Other tests revealed that other factors, e.g. the amount of ammonium chloride added during the gallium separation, also affected the indium recovery. In the development of a process, the fact that the settings used for the gallium separation affect the indium separation needs to be taken into account.

6.2.6 Analysis of the composition of the separated metal fractions

The goal in this study was to achieve metal fractions containing less than 1 wt% of each of the other elements [179]. The compositions of the separated gallium and indium fractions were determined for GS 2:4 and IS 2:4, which gave the highest gallium and indium yields. The composition of the recovered gallium fraction was 90.6 ± 3.7 wt% gallium and 9.4 ± 2.7 wt% indium. The copper content was below the detection limit for the ICP-OES. The small amount of selenium remaining in the starting material after the selenium separation was separated together with the gallium. This was not seen as a problem, since the selenium can easily be removed by precipitation, followed by filtration. The remaining gallium in the residue after GS 2:4 and a small fraction of the copper was recovered together with the indium in IS 2:4. The resulting indium fraction contained 97.7 ± 9.1 wt% indium, 2.2 ± 0.2 wt% copper and 0.1 ± 0.01 wt % gallium. The copper fraction remaining after separation of gallium and indium contained 90.0 ± 0.7 wt% copper and 10.0 ± 0.6 wt% indium. The gallium content was below the detection limit of the ICP-OES.

These results show that good separation between gallium and copper can easily be achieved and that, due to the almost complete recovery of gallium, the gallium content in the recovered indium was well below the target of 1 wt%. The indium content in the gallium and copper fractions, and the copper content in the indium fraction was, however, higher than the target value. It can also be seen that the more complete recovery of gallium and indium resulted in better separation of the elements than GS 1:3 (see Section 6.2.4) and IS 1:4 (see Section 6.2.5), which gave the best recoveries of the elements in the first set of separation tests.

6.2.7 Process development considerations

It is clear that a relatively large amount of ammonium chloride is needed to achieve complete chlorination of the selenium-depleted CIGS starting material and obtain a good recovery of the metals. In an industrial process the amount of ammonium chloride needed could be lowered by recycling the ammonium chloride-rich products from the different separation steps back into the system. Adding all of the ammonium chloride at once gave a slow recovery of both gallium and indium, due to saturation of the atmosphere in the reactor. Increasing the gas flow through the reactor increased the recovery rate of the metals, but faster and almost complete recovery could only be achieved when the ammonium chloride was added in several smaller batches. In this study the time the material was heated between the ammonium chloride additions was relatively long (2 h). Perhaps the recovery time needed could be shortened by adding the ammonium chloride at more frequent intervals. The amount of ammonium chloride added in each batch also affected the metal recovery and an optimum amount will have to be found if an industrial process is to be developed. Another important finding was that the parameters used in the gallium separation step (gas flow, ammonium chloride addition etc.) affected the indium separation. Therefore first optimizing the gallium separation and then the indium separation might not give the optimum result for both metals. Almost complete recovery of gallium and indium from the selenium-depleted CIGS material was achieved in the separation study, but the gallium and copper fractions contained approximately 10 wt% indium and the indium fraction contained 2 wt% copper. To further separate the elements in an industrial process the metal factions could be distilled again.

It is apparent that the tube furnace design used in this study is unsuitable for further process development. For scaling up a larger furnace in which more material can be treated at once is needed. Easy collection of the separated metal fractions and the possibility to add ammonium chloride during the heating is required. In addition, easy recycling of the products is needed to lower the ammonium chloride consumption and to achieve better separation of the elements.

6.4 Dissolution of the selenium-depleted CIGS material

6.4.1 Direct dissolution in mineral acids

The dissolution of the selenium-depleted CIGS material in hydrochloric, nitric or sulphuric acid is presented in Fig. 6.20. As can be seen, hydrochloric acid is the most efficient followed by sulphuric acid. It is also clear that the copper oxides in the material are more easily dissolved than the gallium and indium oxides, which is in accordance with the literature values discussed in Section 2.10.2. Based on these results further studies were performed to examine dissolution in hydrochloric acid at different concentrations and over a longer period of time, see Fig. 6.21. From the tests it was obvious that dissolution at room temperature was slow even in 6 M hydrochloric acid and that complete dissolution could only be achieved after 96 h in 6 M hydrochloric acid. To increase the dissolution rate the temperature was increased to 75 °C, see 6.22. As expected the temperature increase greatly improved the dissolution and complete dissolution could be achieved after 2 h in 3 M hydrochloric acid. In 1 M hydrochloric acid almost complete dissolution was achieved for copper and gallium while only 92 % of the indium was dissolved. The small amount of selenium still present in the selenium-depleted material was precipitated as black selenium during the dissolution and could easily be separated by filtration.

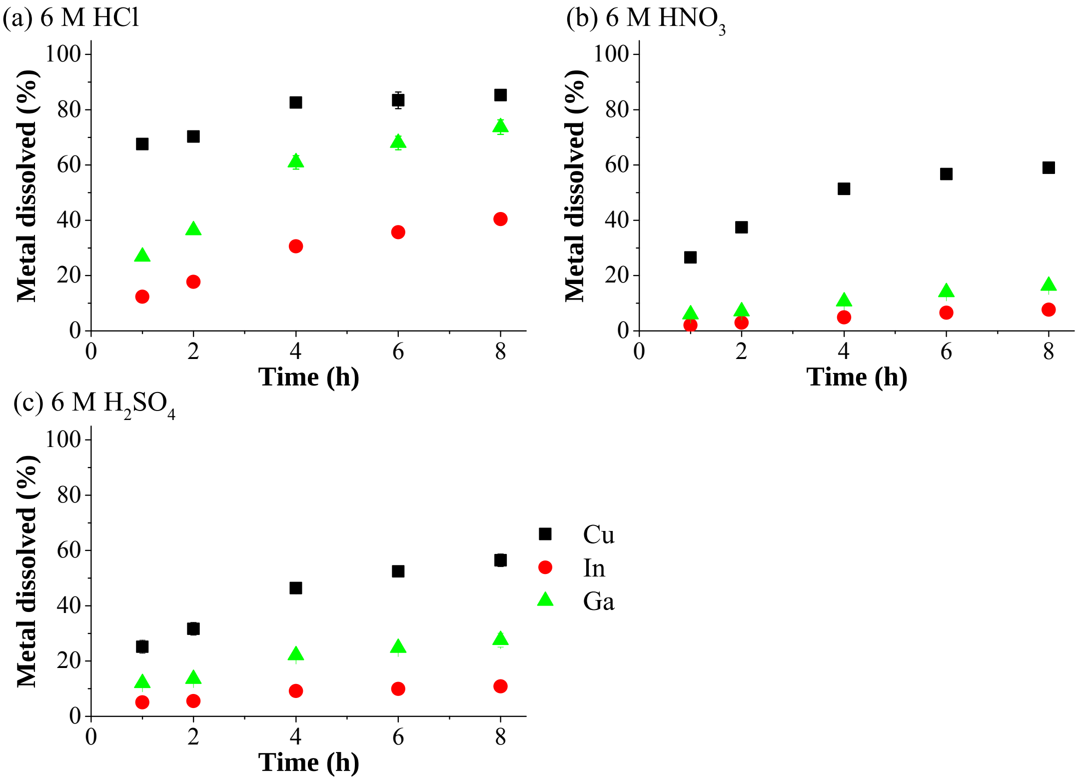

Fig. 6.20 Dissolution of copper, indium and gallium from selenium-depleted CIGS material in 6 M (a) hydrochloric, (b) nitric or (c) sulphuric acid as a function of time.

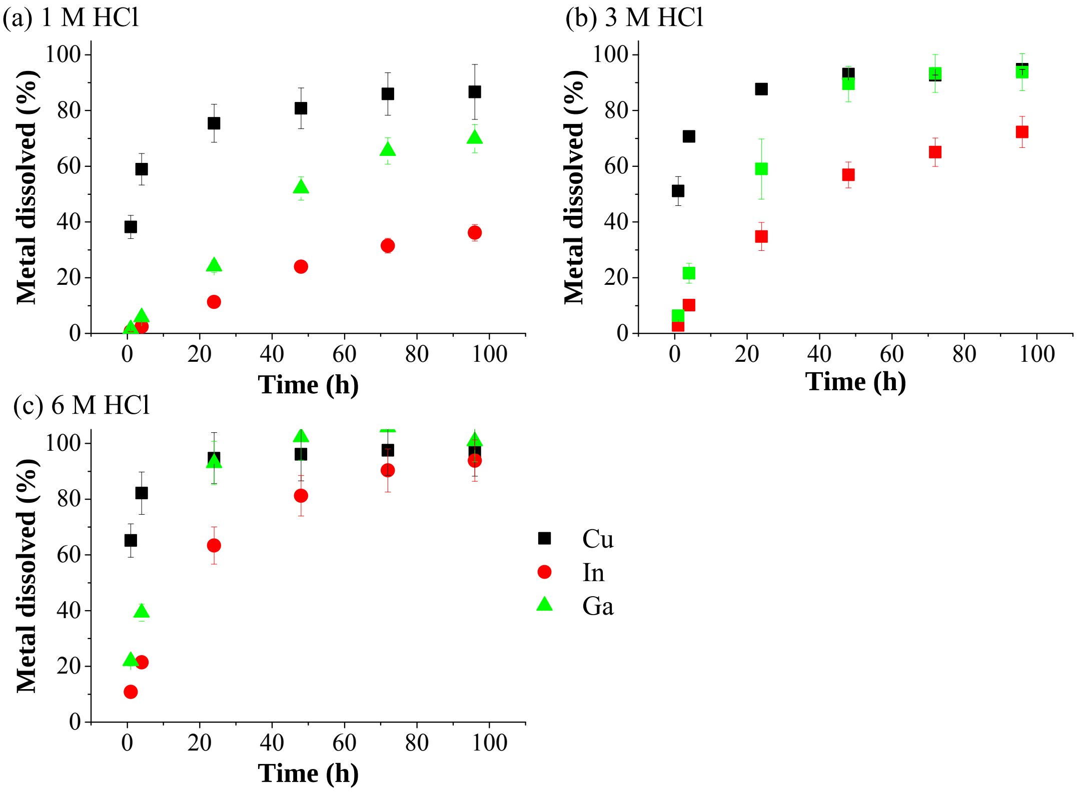

Fig. 6.21 Dissolution of copper, indium and gallium from selenium-depleted CIGS material in (a) 1 M, (b) 3 M and (c) 6 M hydrochloric acid as a function of time.

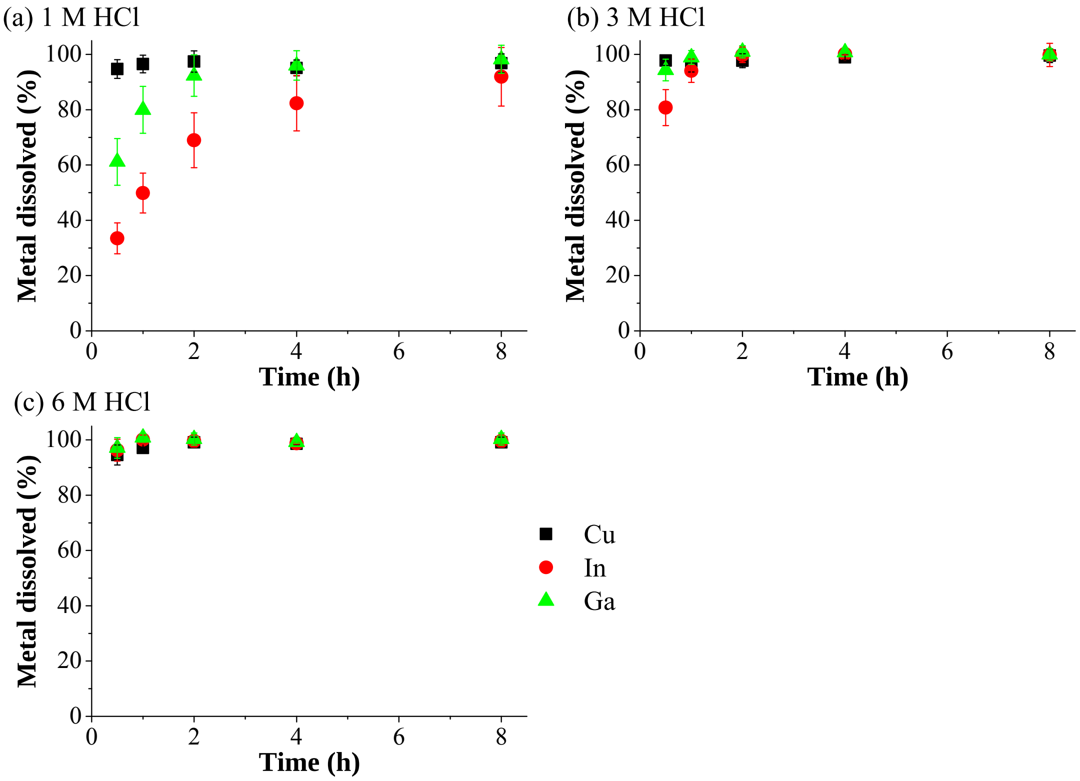

Fig. 6.22 Dissolution of copper, indium and gallium from selenium-depleted CIGS material in (a) 1 M, (b) 3 M and (c) 6 M hydrochloric acid at 75 °C as a function of time.

6.4.2 Dissolution of pre-chlorinated material

Dissolution of the pre-chlorinated material was tested in water, 0.1 M hydrochloric acid, 0.1 M sulphuric acid, 0.1 M nitric acid and 1 M hydrochloric acid, see Fig. 6.23. As can be seen in the figure, the material completely dissolved in all of the tested solutions within 30 min. In water, however, the gallium concentration decreased drastically after 4 h and at the same time a precipitate (probably GaO(OH), which starts forming above pH 6 [39]) could be seen in the solution. It was therefore concluded that all of the tested media, except water, could be used for dissolution. Also in this case the selenium precipitated and could be separated from the solutions by filtration.

(a) Water (b) 0.1 M HCl

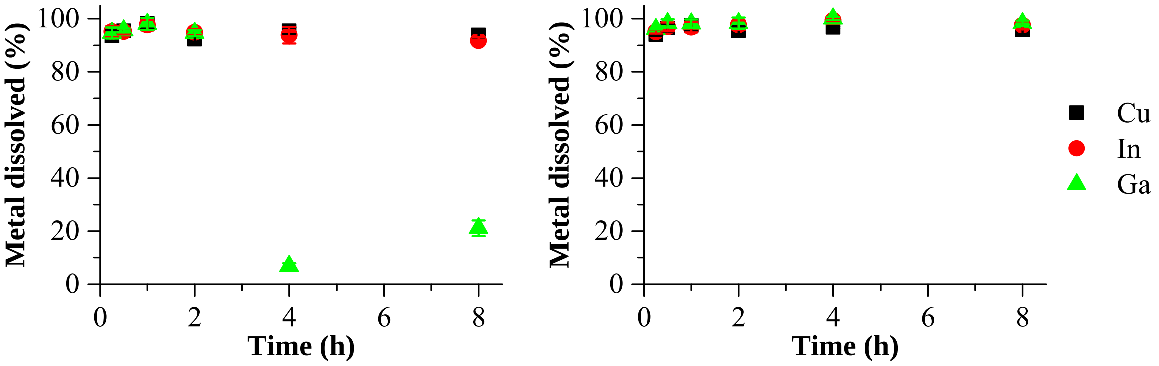

(c) 0.1 M H_2SO_4 (d) 0.1 M HNO_3

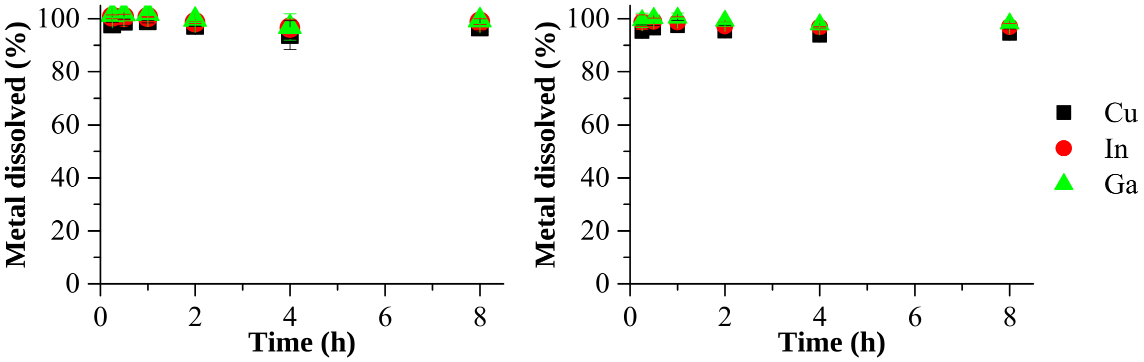

(e) 1 M HCl

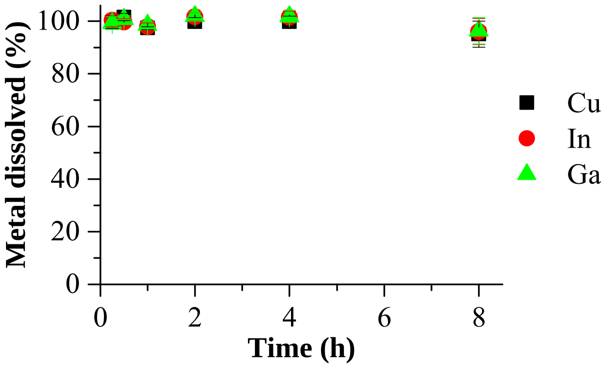

Fig. 6.23 Dissolution of copper, indium and gallium from pre-chlorinated, selenium-depleted CIGS material in (a) water, (b) 0.1 M hydrochloric acid, (c) 0.1 M sulphuric acid (d) 0.1 M nitric acid or (e) 1 M hydrochloric acid as a function of time.

6.4.3 Process development considerations

In industrial processes it is beneficial to treat process flows that have a high metal content. In the future it will therefore be necessary to test if the different dissolution methods can be used to produce concentrated metal solutions. The choice of dissolution method will also be dependent on the subsequent separation method used (e.g. solvent extraction or electrodeposition), since the separation method might work better for one solution than another. An iterative optimization of the dissolution and separation processes will therefore probably be necessary to achieve the best metal separation. Since both dissolution methods require heating the energy consumption of the overall process also needs to be compared to demine which is the most energy efficient.

6.5 Separation of copper, indium and gallium using solvent extraction

6.5.1 Screening of different extractants

The results from the screening study are presented in Fig. 6.24.

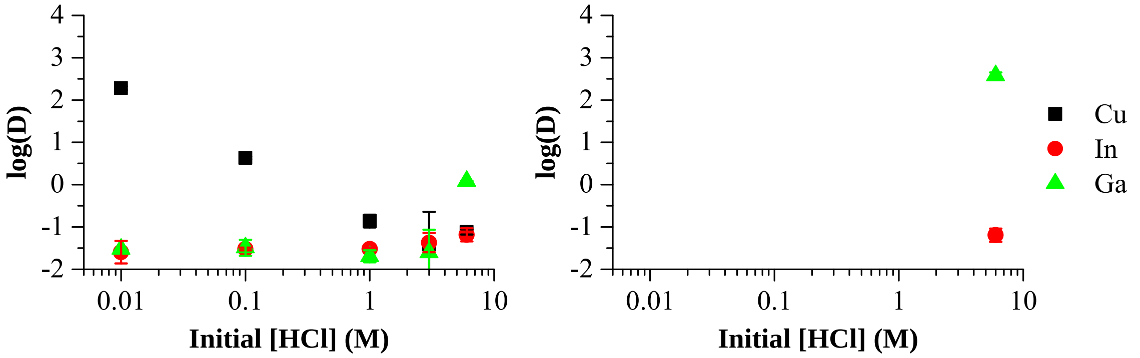
(a) LIX 984 (b) TBP

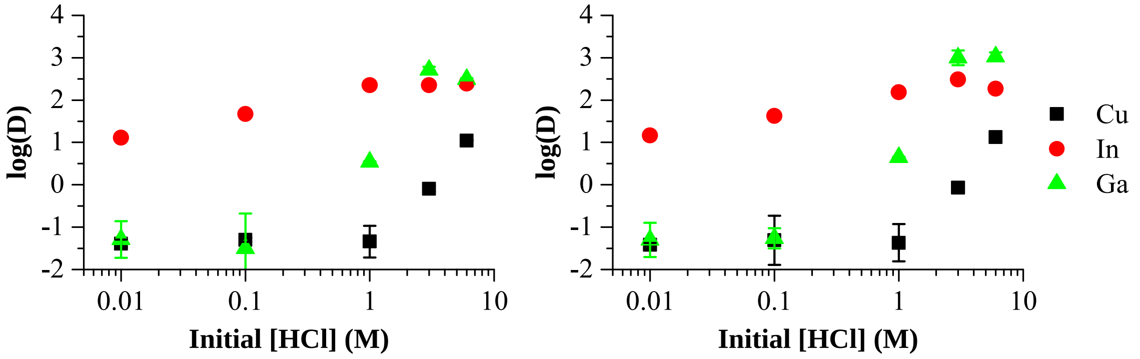
(c) TOPO (d) Cyanex 923

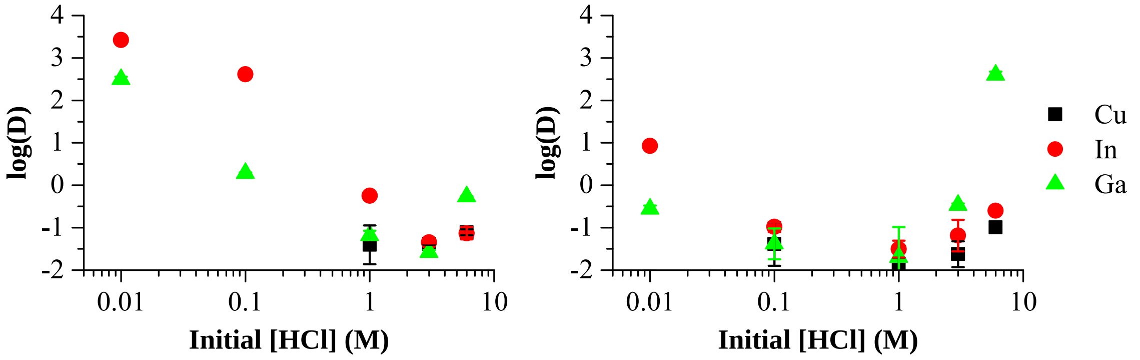
(e) D2EHPA (f) Cyanex 272

Fig. 6.24 Distribution ratio of copper, indium and gallium (4 mM) after extraction with 0.2 M of (a) LIX984, (b) TBP, (c) TOPO, (d) Cyanex 923, (e) D2EHPA or (f) Cyanex 272 in kerosene, as a function of hydrochloric acid concentration in the aqueous phase.

One parameter which was not examined in this study was the extraction of acid from the aqueous phase into the organic phase. The acid extraction is of great importance in an industrial process since it lowers the extraction efficiency and affects e.g. the phase ratio and the pH of the aqueous solution. Several of the tests did not result in any detectable extraction and these points have been omitted from the figure. One such example is extraction with TBP which only resulted in extraction of indium and gallium from a 6 M chloride solution. The difference in D-value indicates that TBP could be used to separate gallium from indium and copper. LIX 984 extracts copper at low hydrochloric acid concentrations, while D2EHPA extracts indium and gallium. However, the most promising results were achieved with TOPO and Cyanex 923, which extract only indium at low hydrochloric acid concentrations, indium and gallium at 1 M and all three elements at 3 and 6 M. This extraction behaviour could be used to extract all elements from a high acid concentration solution and then separate the elements by selective stripping. Such an approach ensures that no manipulation of the solution used for dissolution is needed to achieve separation of the elements. Since extraction from the 6 M hydrochloric acid resulted in the formation of a third phase the 3 M solution was chosen for further studies.

6.5.2 Investigation of extraction kinetics using TOPO and Cyanex 923

The kinetics of the extraction of copper, indium and gallium from 3 M hydrochloric acid with TOPO and Cyanex 923 was explored. The results from the experiments showed that equilibrium was obtained within 5 min.

6.5.3 Selective stripping of extracted metals

Distribution ratios for the stripping of the metals extracted from the 3 M hydrochloric acid solution with TOPO or Cyanex 923 are show in Table 6.6.

Table 6.6 D-values for the stripping of copper, indium and gallium from 0.2 M solutions of TOPO or Cyanex 923 in kerosene with different stripping solutions.

Extractant	**Stripping solution**	$\mathbf{D_{Cu}}$	$\mathbf{D_{In}}$	$\mathbf{D_{Ga}}$
TOPO	Water	0.1 ± 0.05	12 ± 0.7	0.06 ± 0.05
Cyanex 923	Water	0.1 ± 0.05	10 ± 0.4	0.04 ± 0.01
TOPO	0.1 M HCl	0.05 ± 0.01	47 ± 2	0.03 ± 0.03
Cyanex 923	0.1 M HCl	0.05 ± 0.04	42 ± 1	0.05 ± 0.02
TOPO	0.8 M HCl	0.10 ± 0.01	163 ± 7	1.9 ± 0.1
Cyanex 923	0.8 M HCl	0.07 ± 0.05	143 ± 5	1.8 ± 0.1
TOPO	3 M HCl	0.8 ± 0.1	224 ± 38	516 ± 88
Cyanex 923	3 M HCl	0.85 ± 0.02	307 ± 80	996 ± 379
TOPO	0.2 M EDTA	0.25 ± 0.13	0.48 ± 0.05	0.01 ± 0.05
Cyanex 923	0.2 M EDTA	0.13 ± 0.11	0.17 ± 0.05	0.01 ± 0.05

In this study only a few stripping phases were tested, however, several other solutions would be of interest for future studies. As an example, stripping with sulphuric acid solutions would be beneficial for a subsequent electrodeposition step. Complexation with EDTA was tested for stripping of indium, since both TOPO and Cyanex 923 gave a distribution ratio above 10 when stripping with water.

6.5.4 Modelling of a possible separation method

The distribution ratios presented in Table 6.6 were used in a simulation of the suggested solvent extraction separation process in Fig. 6.25. Cyanex 923 was chosen for the simulation as it was determined to be the most suitable extractant for separation of the elements. The aqueous feed was assumed to be provided by the dissolution of the selenium-depleted CIGS material in a suitable hydrochloric acid media. In the first stripping step 3 M hydrochloric acid was used to strip copper. For gallium stripping (Strip 2) the simulation was run with both 0.1 and 0.8 M hydrochloric acid. The best separation of the elements was achieved with the 0.1 M solution. In the final stripping step 0.2 M EDTA was used to recover indium.

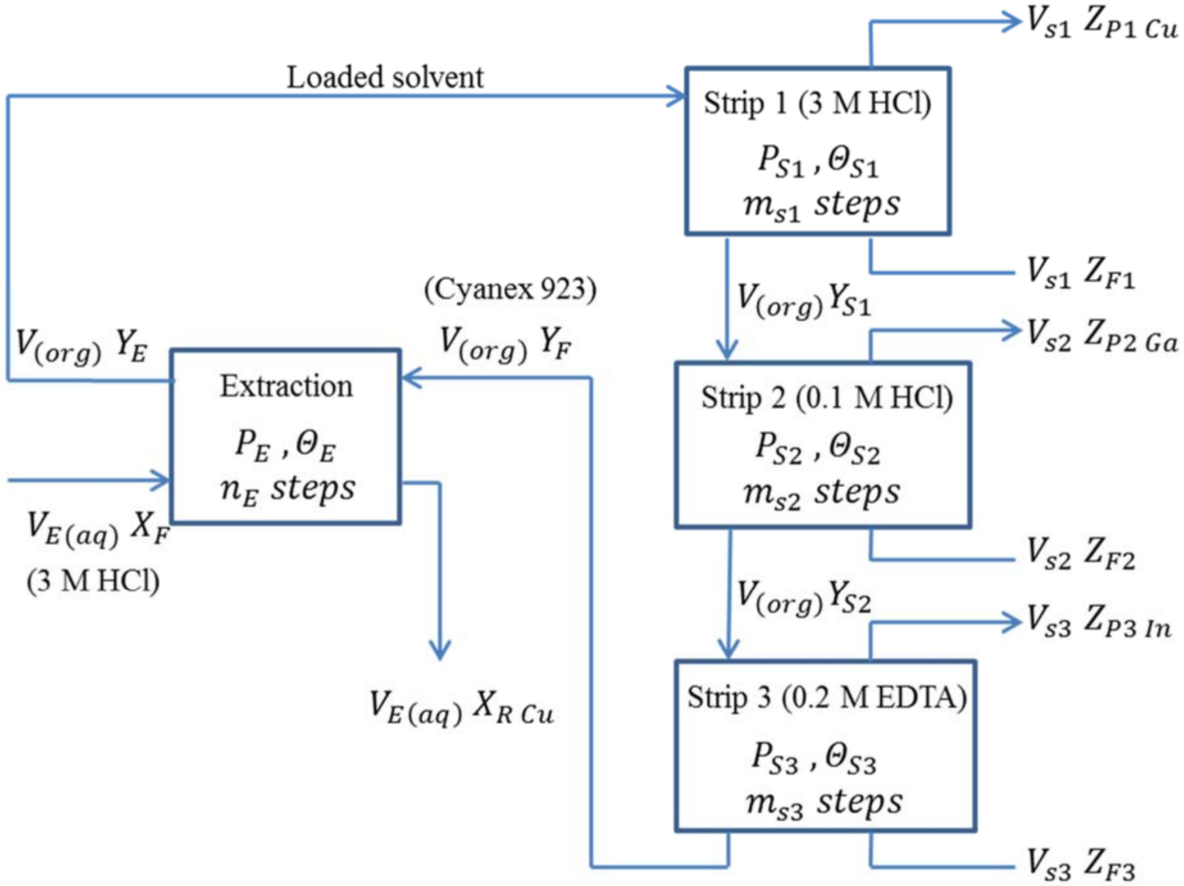

Fig. 6.25 Flowchart of the suggested process for the separation of copper, indium and gallium with solvent extraction using 0.2 M Cyanex 923 in kerosene as the organic phase and a 3 M hydrochloric acid solution containing the dissolved selenium-depleted material as the aqueous phase. The notations include volume flow (V), aqueous fraction (X and Z) and organic fraction (Y). The indices denotes feed (F), extract (E), strip (S) or raffinate (R and P_i).

The results from the simulation are presented in Table 6.7.

Table 6.7 Metal composition of the separated fractions after simulation of the suggested solvent extraction process.

n_E	m_{s1}	m_{s2}	m_{s3}	Process	Fraction	Cu (wt%)	In (wt%)	Ga (wt%)
1	1	1	1	Extraction	$X_{R\ Cu}$	98.8	1.1	0.1
				Strip 1	$Z_{P1\ Cu}$	97.5	2.4	0.1
				Strip 2	$Z_{P2\ Ga}$	39.8	8.4	51.8
				Strip 3	$Z_{P3\ In}$	0.5	98.7	0.8
1	2	2	1	Extraction	$X_{R\ Cu}$	98.8	1.1	0.1
				Strip 1	$Z_{1\ Cu}$	98.1	1.8	0.1
				Strip 2	$Z_{2\ Ga}$	28.7	9.7	61.6
				Strip 3	$Z_{3\ In}$	0.0	99.9	0.1
1	3	3	1	Extraction	$X_{R\ Cu}$	98.8	1.1	0.1
				Strip 1	$Z_{1\ Cu}$	98.3	1.6	0.1
				Strip 2	$Z_{2\ Ga}$	21.6	10.7	67.7
				Strip 3	$Z_{3\ In}$	0.0	100.0	0.0

The simulation shows that separation of copper, indium and gallium with the suggested solvent extraction process might be possible if the process parameters are optimized further. As can be seen, a pure indium fraction containing most of the indium can be achieved and the raffinate from the extraction step contains most of the copper, with only small contaminations of indium and gallium. To obtain a lower copper content in the gallium fraction the co-extraction of copper needs to be lowered or the scrubbing of copper in the first stripping step has to be improved. The indium content in the gallium fraction is also too high and needs to be lowered. To improve the separation of the elements the extractant and metal concentrations, along with the phase ratios in each step, could be varied. Other stripping phases, especially for the selective stripping of gallium, could also be investigated. Finally, experiments will have to be done on concentrated metal solutions from the dissolution of selenium-depleted CIGS material to ensure that the extraction process can be used on an industrial scale.

6.6 Electrochemical separation of copper, indium and gallium

6.6.1 Cyclic voltammetry

The results from the cyclic voltammetry experiments are presented in Fig. 6.26.

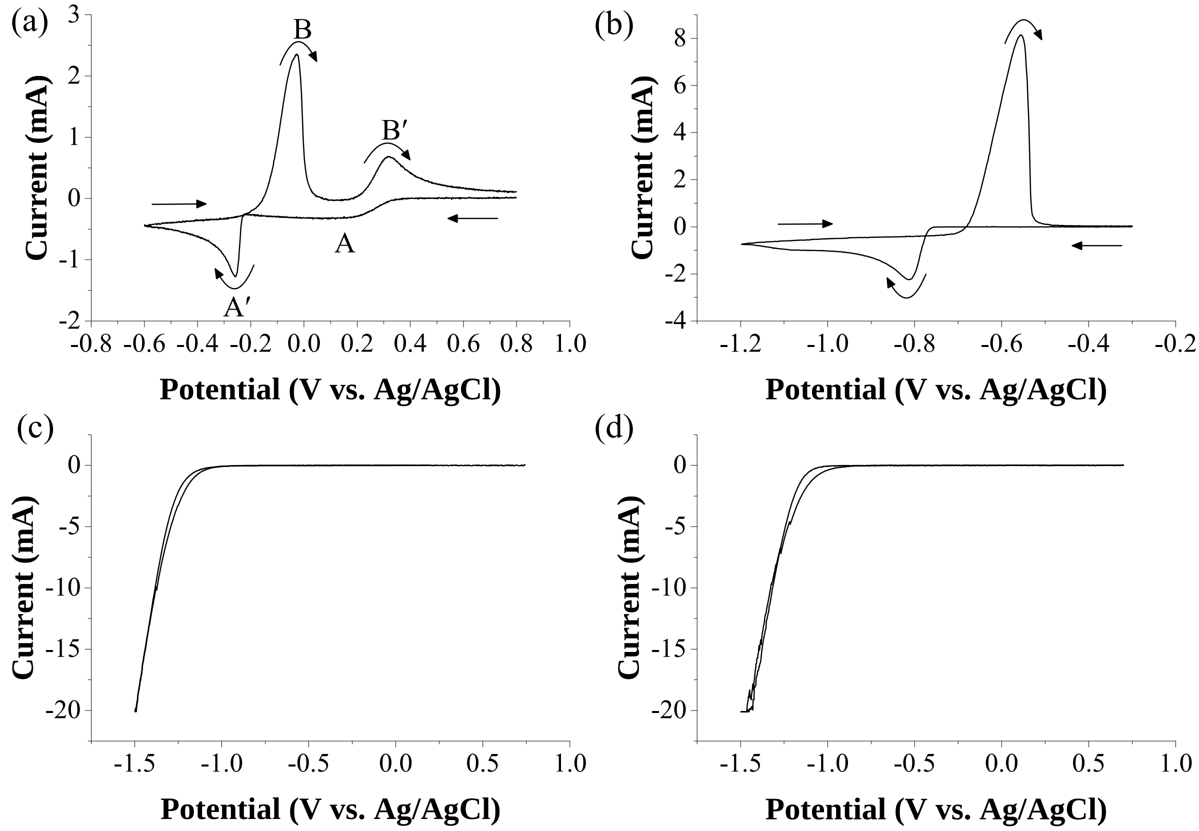

Fig. 6.26 Voltammogram for 0.05 M (a) copper(II), (b) indium(III) and (c) gallium(III) in an electrolyte of 1 M HCl (d). The solutions were analyzed using a scan rate of 100 mV/s.

The cyclic voltammogram recorded for copper is shown in Fig. 6.26a. In the figure two cathodic voltammetric waves (A and A') can be seen, at approximately 0.25 and -0.25 V. The reduction of copper (II) to copper (I), according to Reaction 3.19, explains the first reduction wave (A) in the cyclic voltammogram. The second larger reduction wave (A') is the combined result of the reduction of copper(I) and copper(II) to copper(0), according to Reaction 3.20 and 3.14, respectively. The shift in the potential needed for copper reduction to more negative values compared to the standard reduction potential is due to the factors discussed in the theory section. As an example, the complexes formed in chloride solution are more stable than the hydrated complexes in a pure water solution. In the reversed scan copper(0) on the electrode is oxidized, giving rise to the first metal stripping peak (B) at 0 V. Depending on the chloride concentration copper(0) is either oxidized to copper(I) or directly to copper (II) [180]. Above 1 M chloride copper(I) is the dominating species and this gives rise to the second metal stripping peak (B'), at 0.3 V, as copper(I) is oxidized to copper(II).

For indium(III) (Fig. 6.26b) the cathodic voltammetric wave at -0.8 V that was seen in the cathodic scan was attributed to the reduction of indium(III) by Reaction (3.15). In the reverse scan the oxidation of the formed indium metal gave one anodic wave at -0.6 V. The difference in potential between the reduction of copper(II) and indium(III) indicated that a separation of copper from indium could be achieved by electrodeposition of copper.

For gallium(III) (Fig. 6.26c) only reduction of water at potentials below -1 V was observed, even though the potential window was extended to -1.5 V. The result was the same as for the electrolyte without any metal species (Fig. 6.26d). It is clear that the actual reduction potential for gallium requires large overpotentials and that these results agree well with those reported by other authors cited in the theory section. This means that it is difficult, or even impossible, to electrowin gallium from this solution and that the separation of indium from gallium by electrodeposition should be easily achieved.

To investigate if the reduction potential of copper was influenced by indium and gallium a solution containing all three elements was analysed. The results presented in Fig. 6.27 show that the reduction potentials for copper(II) and indium(III) were the same in the solutions containing all three elements as in the solutions containing only copper or indium. In the reverse scan the indium oxidation wave was less pronounced and an additional wave could be seen before the anodic copper wave. The additional wave can be explained by the selective oxidation of indium from an alloy containing copper and indium [181]. This explanation was supported by the agreement between the decrease in area of the indium roxidation wave and the area of the additional wave. From Fig. 6.27 it could be concluded that a suitable potential for electrodeposition of copper was -0.5 V vs. the reference. To mimic a solution after copper separation a solution containing indium(III) and gallium(III) was analyzed. The result was the same as for a solution containing only indium(III) and a suitable reduction potential for indium was determined to be -0.9 V.

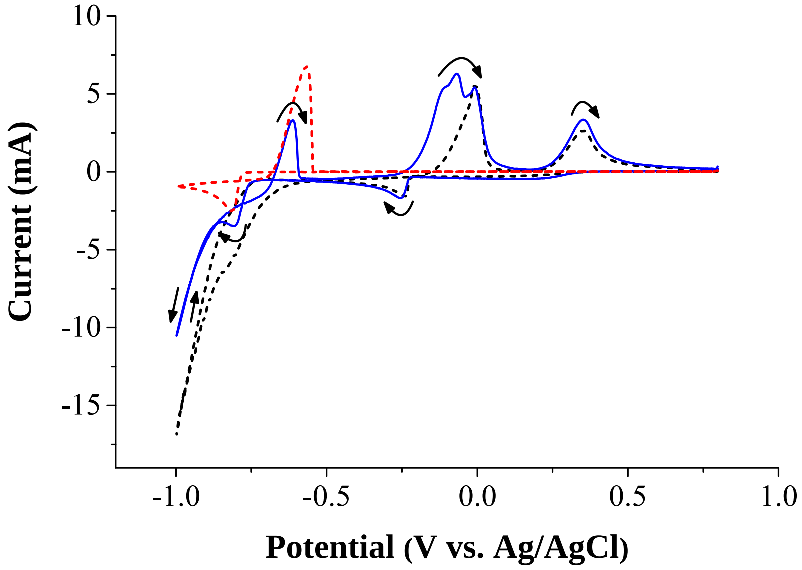

Fig. 6.27 Voltammogram of a solution containing copper(II), indium(III) and gallium(III) (blue) compared to a solution containing only copper(II) (black) or indium(III) (red) at a scan rate of 100 mV/s.

Before the separation tests, Solution 2 and 3 were tested with cyclic voltammetry to determine if the same copper reduction potential as for Solution 1 could be used. While the voltammogram for Solution 2 was slightly distorted, the voltammogram for Solution 3 was similar to that obtained for the synthetic solution. Both analyses showed that the same copper reduction potentials could be used. After the separation of copper the solutions were analysed again to determine if the indium reduction potential needed to be modified. The cyclic voltammogram had the same shape as that of the synthetic solution containing only indium (and gallium) and the same indium reduction potential could be used.

6.6.2 Electrochemical separation of copper, indium and gallium from a synthetic chloride solution

The copper deposition formed during 8 h of copper electrodeposition from the synthetic chloride solution (Solution 1) is shown in Fig. 6.28. The deposit had a highly dendritic and powdery morphology, which is typical for electrodeposition of copper from chloride solutions [132, 135].

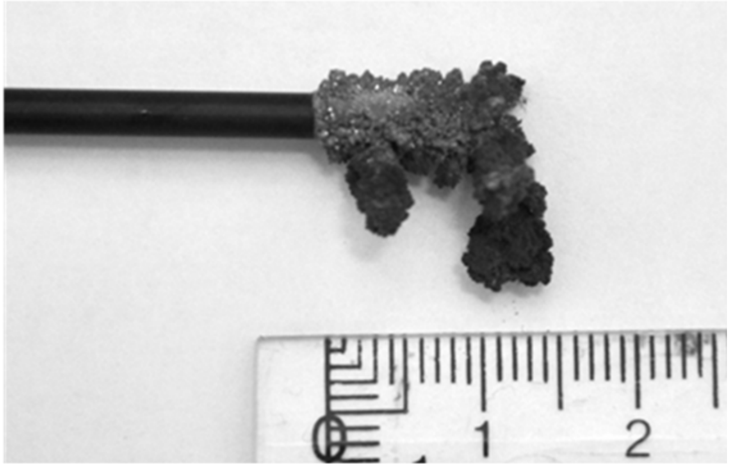

Fig. 6.28 Copper metal from electrodeposition from the synthetic solution (Solution 1), containing copper(II), indium(III) and gallium(III) in 1 M HCl, using a potential of -0.5 V.

The concentrations of metals in the solution and the current during the deposition are shown in Fig 6.29. The increase in cathodic current during the first 3 h is due to the increase in electrode surface due to the dendritic nature of the copper deposit. After approximately 5.5 h the solution lost its blue colour and ICP-OES analysis (Fig. 6.29a) after 6 h showed no significant traces of copper in the solution. The current (Fig. 6.29b) was basically 0 after 6 h. The copper yield was determined to be 99.8 ± 0.3 % and the indium and gallium concentrations in the copper deposit were below the detection limit of the ICP-OES. From the chronoamperogram (Fig. 6.29b) the charge passed during electrodeposition (Q) was determined by calculating the peak area using the trapezoidal rule. The current efficiency was determined by Equation 3.22 to be 46.3 ± 2.0 %.

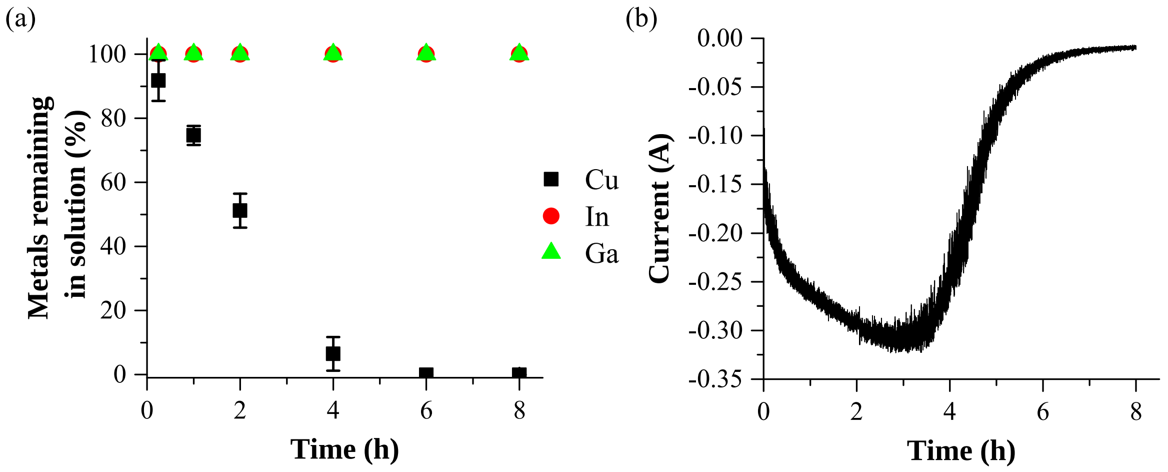

Fig. 6.29 Electrochemical separation of copper from Solution 1: (a) the metal concentration in the solution relative to the original concentration as a function of time, (b) the current passed through the circuit as a function of time.

Electrodeposition of indium from the copper-depleted synthetic solution for 8 h resulted in the indium deposit seen in Fig. 6.30.

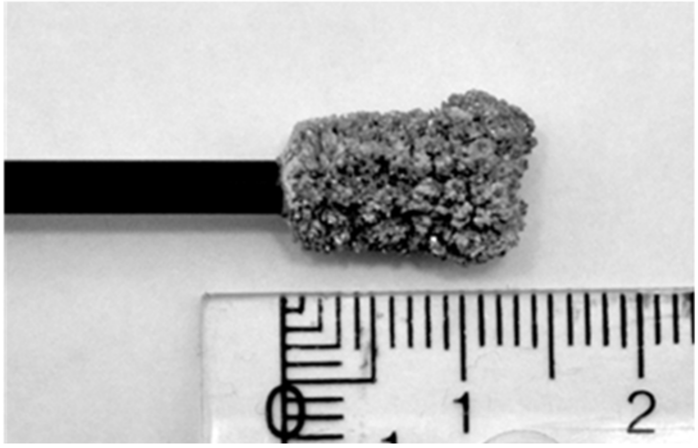

Fig. 6.30 Indium metal from electrodeposition from the copper-depleted synthetic solution after copper separation using a potential of -0.9 V.

Analysis of the metal concentrations in the solution during the experiment, presented in Fig. 6.31a, showed that no gallium was removed from the solution, while the indium concentration decreased steadily. After 8 h the indium concentration had decreased to 1.6 ± 0.2 % of the original concentration and the indium yield was determined to be 98.4 ± 0.2 %. ICP-OES analysis of the indium deposit showed no traces of copper or gallium and it was concluded that a pure indium fraction had been obtained. The current efficiency for the indium separation was calculated in the same way as for the copper separation (see above) and was determined to be 65.9 ± 7.2 %.

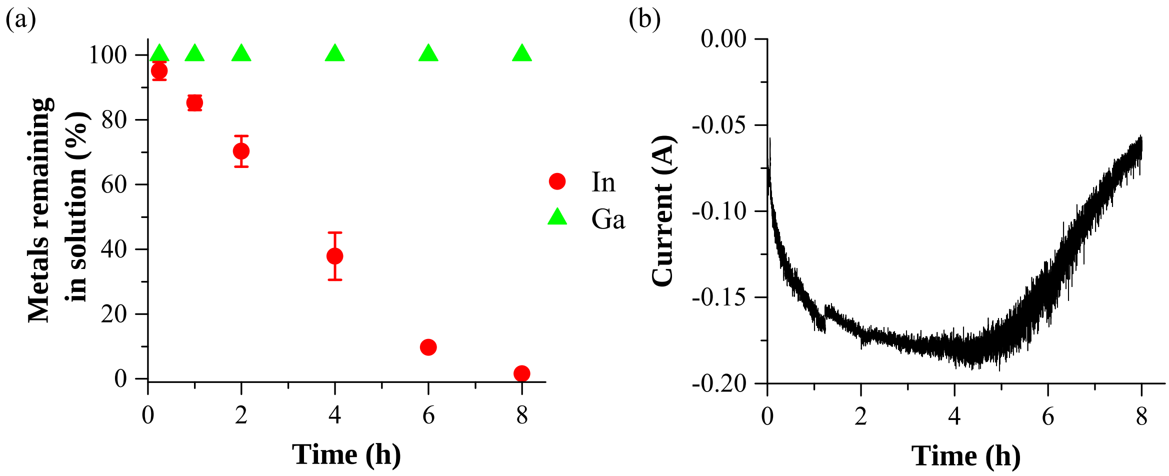

Fig. 6.31 Electrochemical separation of indium from the synthetic solution containing copper(II), indium(III) and gallium(III) in 1 M HCl (Solution 1): (a) the metal concentration in the solution relative to the original concentration as a function of time, (b) the current passed through the circuit as a function of time.

The study of the synthetic solution showed copper and indium separation could be achieved from chloride solutions. It was also clear that the current was higher during the electrodeposition of copper and the time needed for complete separation was therefore shorter for copper than for indium. The area of the copper deposit seems to be larger than the area of the indium deposit and this could be the reason for the higher rate of reduction. In addition, the electrodeposition of copper is catalysed by the presence of chloride ions in the solution [174, 175]. The reaction rate of the stepwise reduction of copper(II) via copper(I), described above, is higher than the direct reduction to copper(II). However, a similar catalysing effect has been indicated for indium [146]. Another reason could be that copper ions, due to a smaller ionic radius, diffuse faster towards the electrode than indium ions, but stirring of the solution should practically reduce this difference.

6.6.3 Electrochemical separation of copper, indium and gallium from a solution of selenium-depleted CIGS waste material dissolved in 3 M hydrochloric acid and hydrogen peroxide

After the successful separation of copper and indium from the synthetic solution, separation of copper was performed from Solution 2, which was prepared by dissolution of real waste CIGS material in 3 M hydrochloric acid with an addition of H_2O_2 at 75 °C. The results from the separation tests are shown in Fig. 6.32. Since the current was almost 0 A after 6 h it was determined that the experiment could be ended after 6 h. After the separation ICP-OES analysis showed no traces of copper in the solution, while the indium and gallium concentrations in the solution remained constant. The selenium content in the solution also remained constant, even though selenium should be co-deposited with copper [170, 182]. The lack of selenium reduction might be due to a high stability of the selenium chloride complexes in the solution. The copper yield was 100.0 ± 0.2 % and the concentrations of the other elements in the deposit were below the detection limit of ICP-OES. The current efficiency was determined to be 51.5 ± 3.3 %.

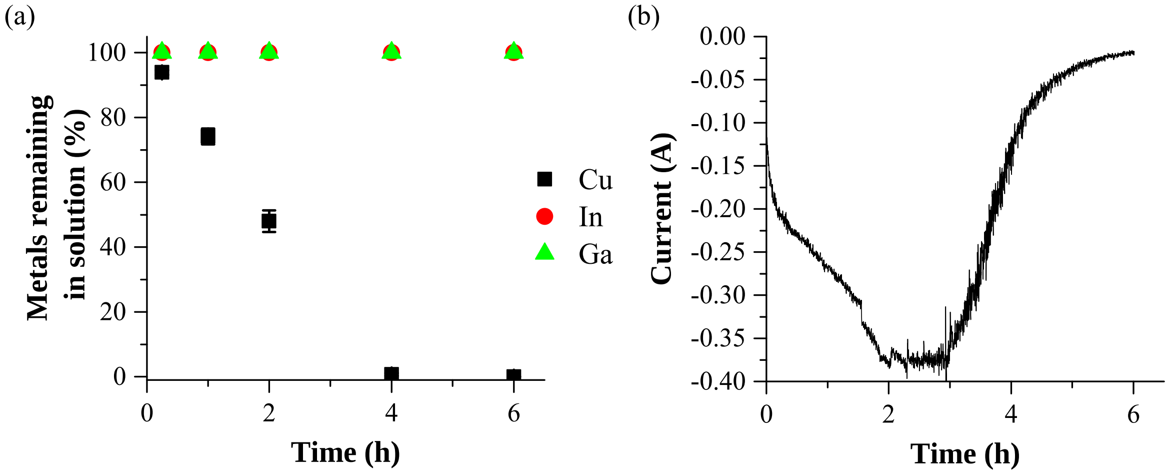

Fig. 6.32. Electrochemical separation of copper from a solution prepared by directly dissolving real waste material in 3 M HCl with an addition of H_2O_2 at 75 °C (Solution 2): (a) the metal concentration in the solution relative to the original concentration as a function of time, (b) the current passed through the circuit as a function of time.

Next, separation of indium was performed from the copper-depleted Solution 2. As can be seen in Fig. 6.33 the indium concentration decreased during the experiment, while the gallium concentration remained constant. However, 20.3 ± 2.2 % of the indium remained in the solution after 8 h and the indium yield was only 76.7 ± 4.7 %. It can also be seen that the indium concentration did not decrease linearly and that the current leveled out at approximately 110 mA after 6 h (see Fig. 6.33b). During the experiment an increase in gas production at the working electrode was observed. The incomplete indium separation and the gas production could be explained by an increase in proton reduction as the indium concentration decreases, which in turn leads to a lower indium reduction efficiency [139, 144]. Complete separation of indium from the solution might therefore be difficult even using longer time periods. The indium recovery from Solution 2 was lower compared to the indium recovery from Solution 1. The pH levels of the solutions were relatively similar and could not explain the difference. Solution 2 could however still contain hydrogen peroxide from the dissolution, which may influence the reduction of indium. The current efficiency for the indium separation was 68.9 ± 2.5 %.

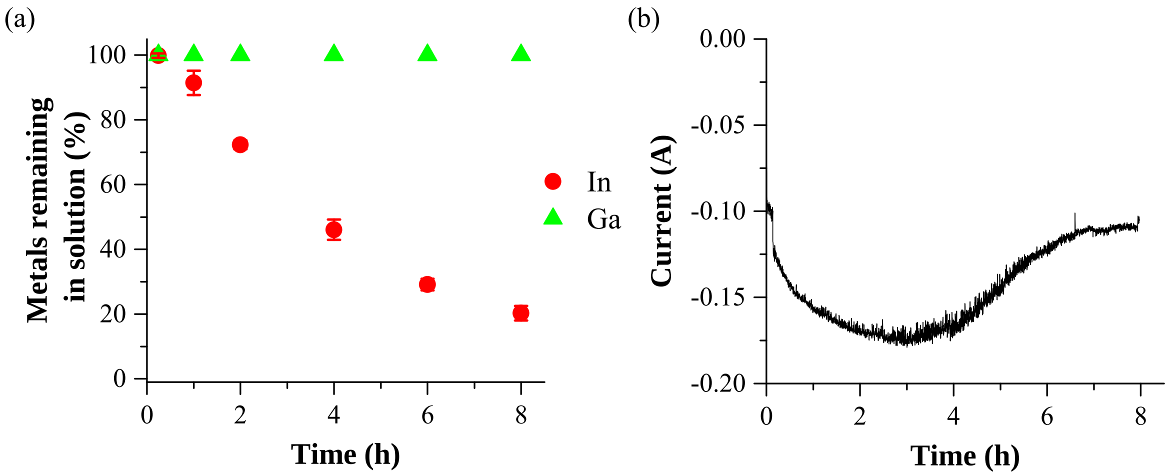

Fig. 6.33 Electrochemical separation of indium from a solution prepared by directly dissolving real waste material in 3 M HCl with an addition of H_2O_2 at 75 °C (Solution 2): (a) the metal concentration in the solution relative to the original concentration as a function of time, (b) the current passed through the circuit as a function of time.

6.6.4 Electrochemical separation of copper, indium and gallium from a solution of chlorinated, selenium-depleted CIGS waste material dissolved in 1 M hydrochloric acid

The results for the separation of copper from Solution 3 are shown in Fig. 6.34. Also in this case the indium and gallium concentrations in the solution remained constant, while the copper content decreased to below 0.5 % in 4 h. The copper yield after 6 h was 100.1 ± 0.5 %. The indium and gallium content in the deposit was below the detection limit for the ICP-OES and the current efficiency was 68.5 ± 2.5 %.

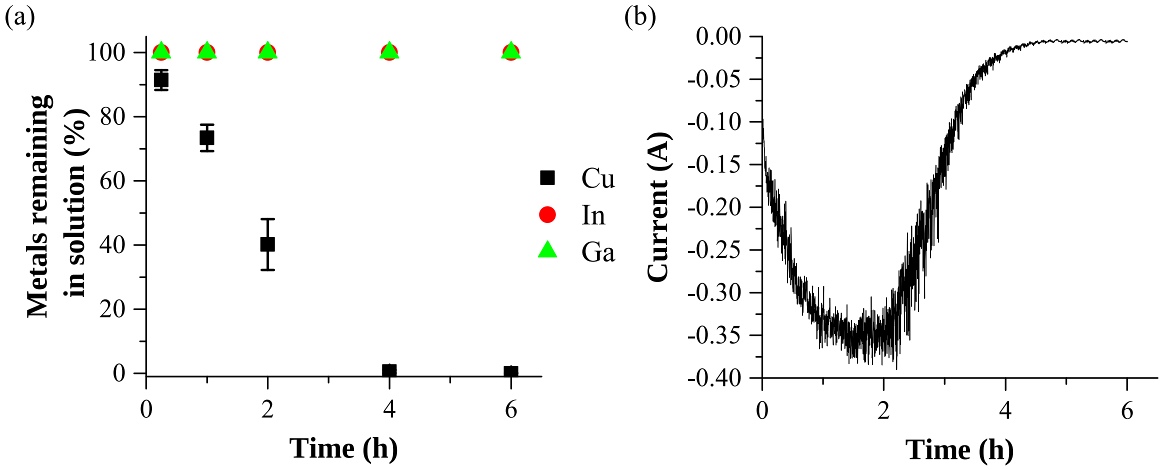

Fig. 6.34 Electrochemical separation of copper from a solution prepared by dissolving pre-chlorinated CIGS waste material in 1 M HCl (Solution 3): (a) the metal concentration in the solution relative to the original concentration as a function of time, (b) the current passed through the circuit as a function of time.

Finally, indium was separated from the copper-depleted Solution 3 (Fig. 6.35). Less than 1 % of the indium remained in the solution after 8 h of electrodeposition and the indium yield was 98.1 ± 2.5 %. The current efficiency for the indium separation was determined to be 61.2 ± 1.7 %. Similarly to the indium separation from Solution 2, the current levelled out after 6 h and an increase in hydrogen gas production at the working electrode could be seen as the indium concentration in the solution decreased. However, in this case the indium separation was still close to complete and the solution contained less than 1 % of the original amount of indium. It has been reported that ammonium chloride addition can be used to obtain chloride solutions with higher conductivity [183]. One explanation for the difference in indium separation could be that the conductivity of the ammonium chloride-containing solution (Solution 3) is higher than the conductivity of the hydrogen chloride solution (Solution 2), leading to a higher current and a higher indium reduction rate.

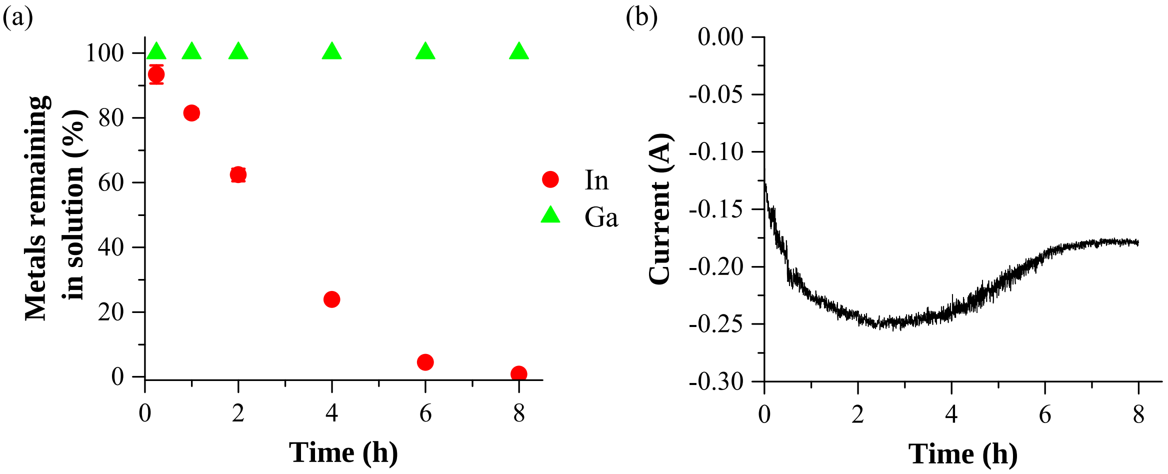

Fig. 6.35 Electrochemical separation of indium from a solution prepared by dissolving pre-chlorinated CIGS waste material in 1 M HCl (Solution 3): (a) the metal concentration in the solution relative to the original concentration as a function of time, (b) the current passed through the circuit as a function of time.

6.6.5 Comparison of the morphology of the deposits from electrodeposition of copper and indium from the different solutions

The morphology of the copper deposits from Solution 2 and 3 was slightly more powdery than the deposit from Solution 1. It has been shown that higher current densities give rough and powdery deposits [132, 135] and if Fig. 6.32 and 6.34 are compared with Fig. 6.29 it can be seen that the current was significantly higher during electrodeposition from Solution 2 and 3 than from Solution 1. The higher current might be due to a higher conductivity of the solutions. Kekesi *et al.* have also shown that the stirring rate, the copper and chloride concentrations in the electrolyte and the temperature influence the morphology of the deposit [135]. In order to get smooth and dense deposits low hydrochloric acid concentrations, high copper concentrations and relatively high temperatures (40-60 °C) should be used. However, if the hydrochloric acid concentration is too low [135] or the copper concentration too high [132] the copper deposit is contaminated with CuCl. The weight of the copper deposits formed during electrodeposition from all three solutions in the present study corresponded well with the amount of copper measured in solution with ICP-OES. Since no additional material was present in the deposit it is most likely that no CuCl contamination had been formed. In addition to optimum current density and concentrations of copper and chloride in the electrolyte, nitrogen sparging and additions of bone glue could be used to produce more dense and smooth deposits [132].

The deposits formed during the separation of indium from Solution 2 and 3 had similar dendritic structures to the one from the synthetic solution (see Fig. 6.30). To decrease the roughness of the deposits the current density, indium concentration and additives, such as glue, thiourea and sodium lignin sulphonate, must be carefully selected [147, 183].

6.6.6 Comparison of the current efficiencies for electrodeposition of copper and indium from the different solutions

According to Kekesi *et al.*, the current efficiency for copper electrodeposition from chloride solutions is influenced negatively by a high hydrochloric acid concentration, as the copper formed is partially re-dissolved. A high current density in a constant current experiment will, on the other hand, give a higher current efficiency as the re-dissolution is counteracted [135]. The high chloride concentrations in the three solutions tested in this study could explain the low current efficiencies (46.3 ± 2.0 % for Solution 1, 51.5 ± 3.3 % for Solution 2 and 68.5 ± 2.5 % for Solution 3). The current efficiencies were probably also lowered by particles released from the working electrode during the experiments. The majority of the particles seemed to be re-dissolved and no particles could be seen in the solution at the end of the experiment. The ammonium chloride-containing solution (Solution 3) gave the highest current efficiency for the copper separation and further optimization of the ammonium chloride and hydrochloric acid concentrations in the solution and the current density might lead to even higher efficiencies.

From experiments on gallium it has been concluded that a larger current density gives a higher metal reduction rate, but the current efficiency is affected negatively [151]. Since indium is similar to gallium this could also be the explanation for the lower current efficiency for the indium separation from Solution 3 (61.2 ± 1.7 %) compared to the other solutions (65.9 ± 7.2 % and 68.9 ± 2.5 %). According to Lee *et al.*, current efficiencies over 90 % can be achieved if the indium concentration is above 0.44 M (50 g/l) while concentrations below 0.26 M (30 g/l) give a decreased current efficiency due to proton reduction [144]. However, when the goal is to completely deplete the solution the indium concentration will inevitably be below those concentrations and other means (e.g. optimal current densities) must be used to increase the current efficiency.

6.6.7 Process development considerations

From the copper and indium separation studies it can be concluded that the ammonium chloride-containing solution (Solution 3) is the most promising for further development of an electrochemical recycling process for the selenium-depleted CIGS waste material. It gave the highest current efficiency for the copper separation, the highest copper reduction rate and the best indium separation. In this study the potential was kept constant in order to ensure good separation of the elements. In future studies, however, the current density should be kept constant and different current densities should be tested in order to optimize the current efficiencies and to produce smooth and dense deposits. The hydrochloric acid and ammonium chloride concentrations in the solution could also be modified and, if necessary, additives could be used for further improvements.

The difficulty in electrowining gallium from the tested chloride solutions also makes further development of the process necessary. Since electrodeposition of gallium is often done from alkaline solutions [65, 87, 148-151, 153, 184-186] one option could be to precipitate the gallium as gallium hydroxide and then proceed with the electrodeposition from the gallate ($Ga(OH)_4^-$) solution formed upon dissolution of the amphoteric precipitate [39].

During electrodeposition from the chloride solutions it was observed that chlorine gas was produced at the counter electrode. The chloride in the solution oxidizes to chlorine gas according to Reaction (6.1).

$$2Cl^- \rightarrow Cl_2\,(g) + 2e^- \qquad (6.1)$$

This is an unwanted reaction, both because the electrolyte is destroyed and because of the difficulties related to taking care of the gas produced. To avoid chlorine gas production a two compartment cell, where the anode is separated from the chloride solution by a membrane, could be used [147]. As another solution to the problem it has been suggested that the chlorine gas could be used to regenerate the electrolyte [134]. In our case the chlorine gas could be used instead of ammonium chloride to chlorinate the oxidized waste material. According to the high-temperature chlorination study, complete chlorination of the material with chlorine gas is possible at 750 °C. This would give a highly water-soluble material and solutions similar to the synthetic solution tested in this study.

7. Process suggestions

Based on the results from the studies presented in this thesis three different processes can be suggested, Fig. 7.1-7.3. All three suggestions start with separation of selenium as selenium dioxide, which has been shown to work well and should be relatively easy to develop on an industrial scale. After the selenium separation high-temperature chlorination could be used to recover gallium and indium from the selenium-depleted residue (Fig. 7.1).

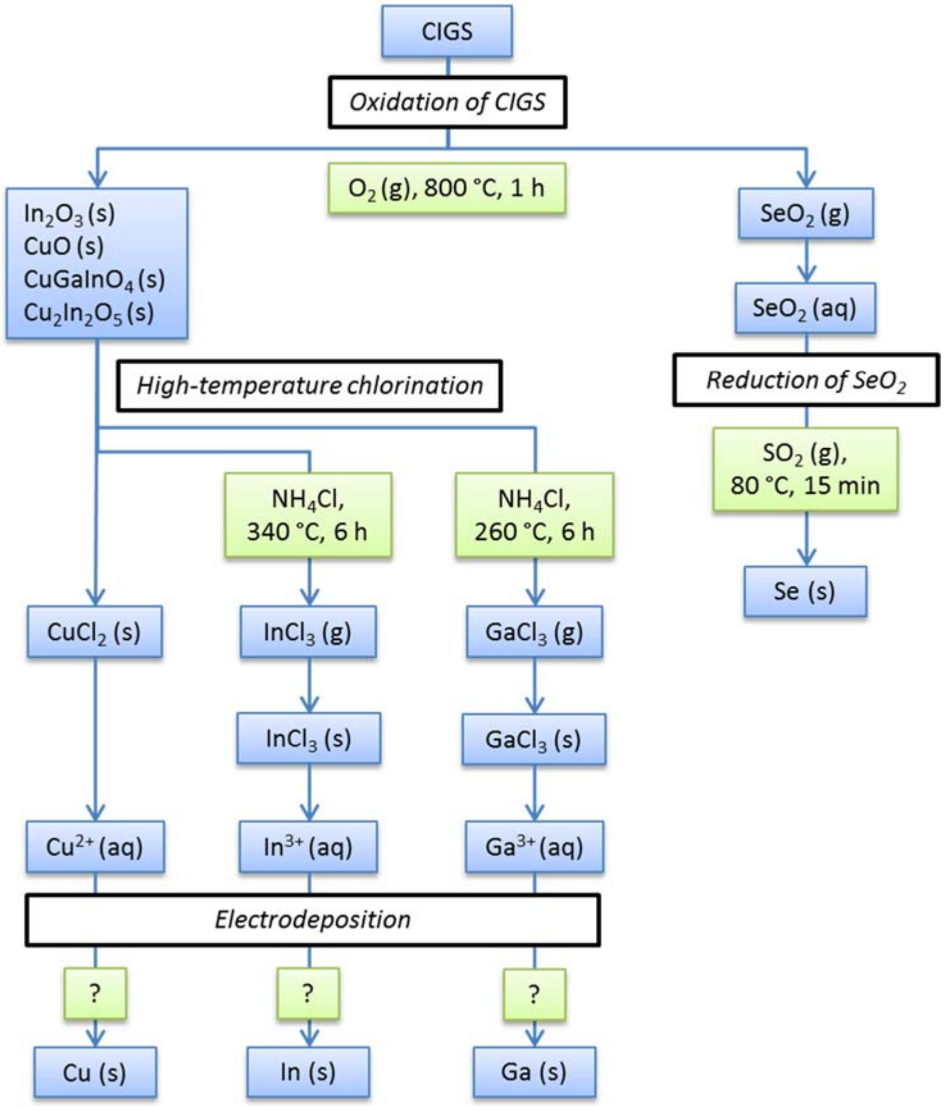

Fig. 7.1 Flowchart of a suggested separation process for CIGS waste material based on the separation of selenium as selenium dioxide followed by the separation of copper, indium and gallium from the residual material using high-temperature chlorination and finally electrodeposition for recovery of the metals.

As described above, the high-temperature chlorination is complex and to achieve complete separation of copper, indium and gallium the material might have to be processed more than once. The advantage is that the separation is done in gas phase, similar to the selenium separation, and could potentially result in high purity elements if the correct process parameters are used. However, the difference between this separation method and the selenium separation is that the impurities, such as iron, also form volatile chlorides, making the purification more complex. After the separation the sublimated chlorides need to be collected and treated to recover the elements as metals, unless a method is developed to produce new CIGS raw material directly from the chlorides. One recovery method that could be used is electrodeposition, which would be performed under different conditions depending on the media used for dissolution of the chlorides.

The separation of copper, indium and gallium could potentially also be achieved by solvent extraction followed by selective stripping (Fig. 7.2).

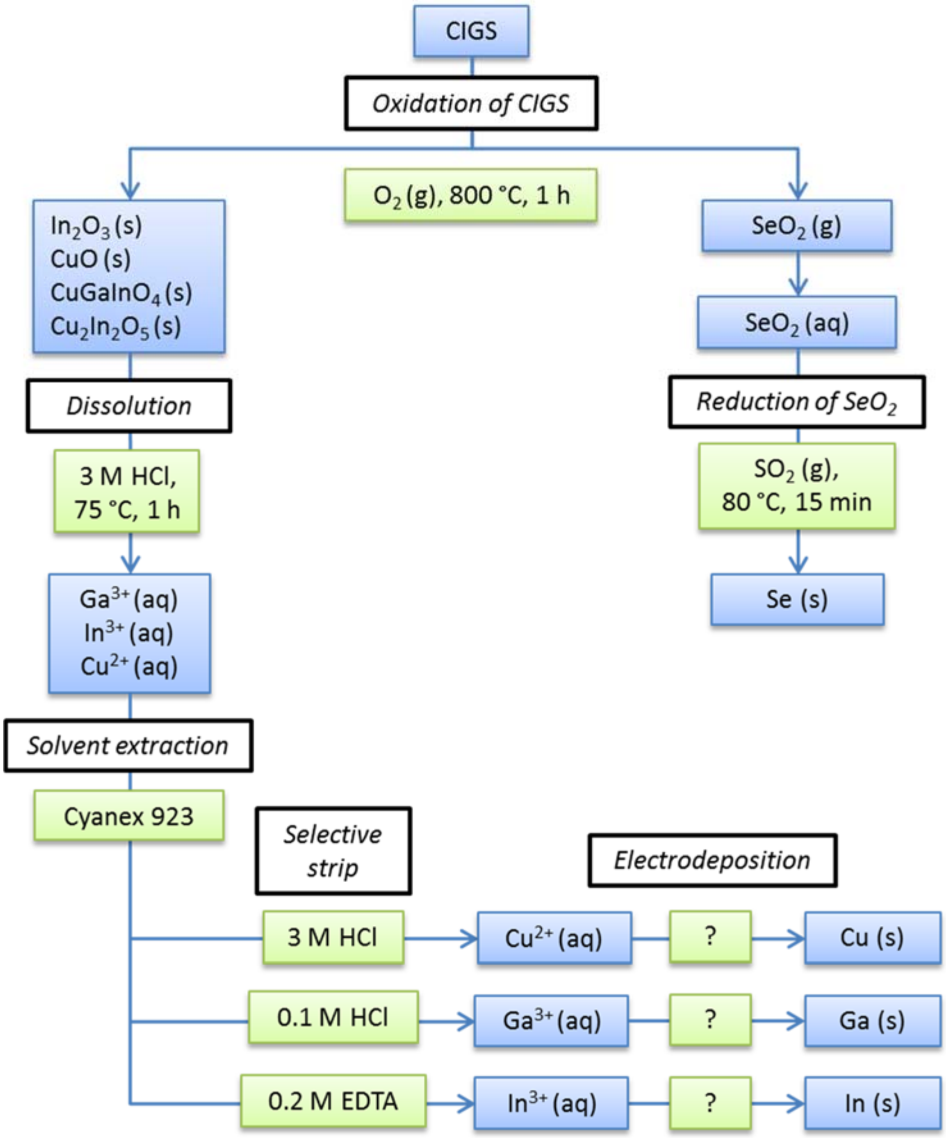

Fig. 7.2 Flowchart of a suggested separation process for CIGS waste material based on the separation of selenium as selenium dioxide, followed by the separation of copper, indium and gallium with solvent extraction and selective stripping.

This is a less complex separation method than high-temperature chlorination, but more work needs to be done to achieve complete separation of the elements. The possibility to recover the metals by electrodeposition will be greatly dependent on the media used for stripping and will have to be explored further.

Finally, it has been shown that separation of copper, indium and gallium can be achieved by direct electrodeposition of first copper and then indium after dissolution of the selenium-depleted material (Fig. 7.3). This separation method gave the best separation of the elements in only a few steps and is therefore considered the most promising for the development of an industrial process. However, work still remains to be done on the electrodeposition of gallium, which might require additional process steps. The purity of the recovered copper, indium and gallium fractions with respect to the critical elements listed in Section 2.3 will also have to be determined and optimized.

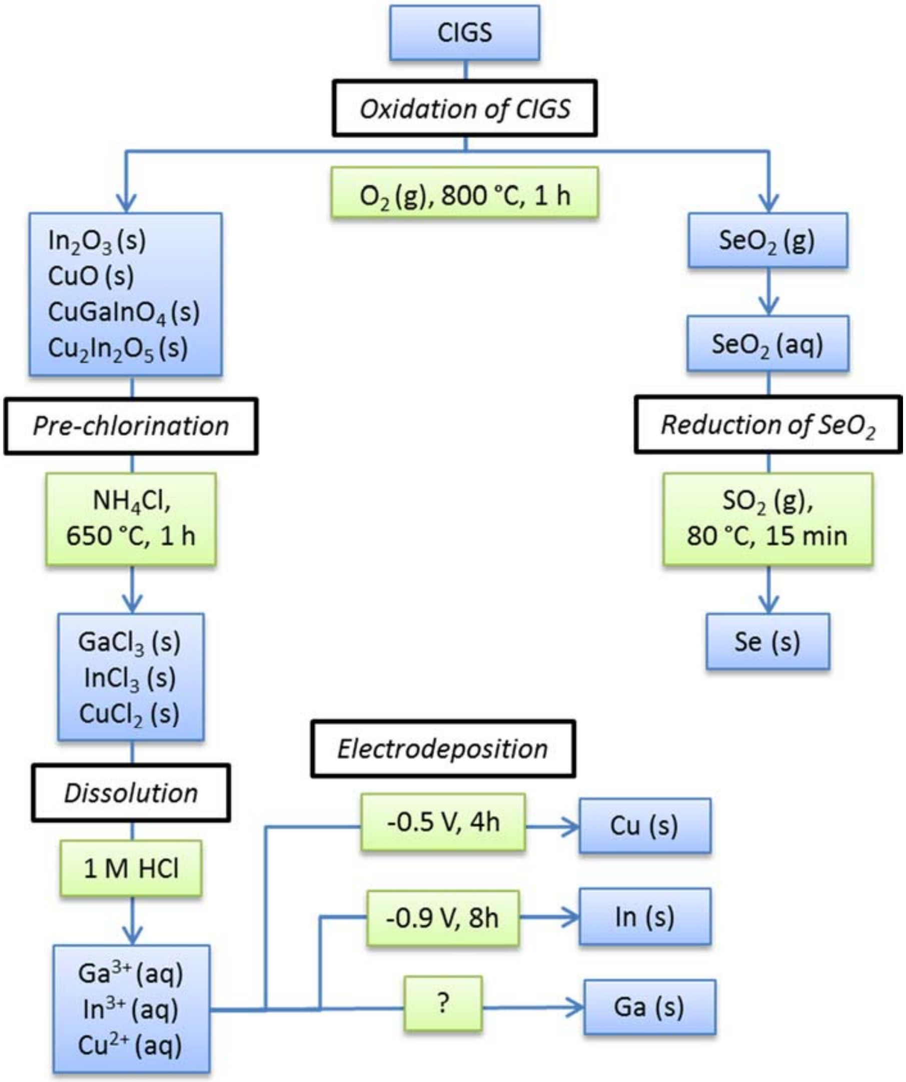

Fig. 7.3 Flowchart of a suggested separation process for CIGS waste material based on the separation of selenium as selenium dioxide followed by the separation of copper, indium and gallium by selective electrodeposition.

8. Conclusions

It has been shown that it is possible to separate selenium, as selenium dioxide, from CIGS materials through oxidation at elevated temperatures. The method gave a selenium recovery above 99 %. After reduction of the selenium dioxide selenium with a purity of 99.999 wt% with respect to scandium, titanium, vanadium, chromium, manganese, iron, cobalt, nickel and zinc (which are the elements that might decrease the solar cell efficiency) was obtained. This means that the purity of the selenium is high enough for the selenium to be used in new solar cells and that the separation method could be the first step in an industrial separation process.

The residue from the selenium separation was shown to contain oxides of indium, gallium and copper, which gave several possibilities for the further treatment of the residue. It was found that, after dissolution of the selenium-depleted material, electrochemical separation of copper, indium and gallium by electrodeposition of first copper and then indium could be done. No reduction of gallium could be detected in the examined potential window, making separation of indium and gallium easier than expected. Almost complete copper and indium recovery (above 99 % for copper and 98 % for indium) was achieved from a solution containing selenium-depleted CIGS material and the recovered metals contained no detectable contamination of the other elements.

Separation of copper, indium and gallium from the selenium-depleted CIGS material by high-temperature chlorination and solvent extraction was also tested. However, when comparing the different suggested processes it was clear that the electrochemical separation gave the best separation of the element and almost complete recovery of the metals in the least number of steps.

In the developed process new separation methods have been shown to give virtually complete separation and recovery of the elements. Furthermore, this is the first time a recycling process for CIGS materials has resulted in the direct recovery of any of the elements at high purity.

9. Future work

Electrochemical separation seems to be the most promising potential industrial separation process for copper, indium and gallium from the selenium-depleted CIGS material. To confirm this the purity of the metal fractions from the different suggested separation processes could be determined and compared. In addition, an estimation of the energy consumption and cost of the processes could be made.

Future work on electrochemical separation could be performed to optimize the energy consumption and the purity of the recycled metals. At the same time, the conditions used for the pre-chlorination and dissolution of the selenium-depleted CIGS material could be adapted to enable an effective metal separation process. To increase the current efficiencies and produce dense and smooth deposits further studies are needed in order to find the optimum current density and chloride concentration in the solution. Pre-chlorination of the selenium-depleted material using the chlorine gas produced at the counter electrode, instead of ammonium chloride, should also be tested and evaluated. In addition, recovery of gallium by electrodeposition, or any other method, needs to be developed.

After the development of the electrochemical separation the whole process, including the selenium separation, should be tested in pilot scale before the development of an industrial process.

Acknowledgements

I would like to thank:

my supervisors Christian Ekberg and Britt-Marie Steenari for invaluable feedback and help

my examiner Gunnar Skarnemark for always helping and supporting me

Eric, Sven and Jan at Midsummer AB for good collaboration and for supplying the raw materials

POWRES for arranging good courses, fun trips and much needed funds, as well as giving me the possibility to extend my network

Fredrik Björefors for giving me an understanding of electrochemistry and for reading and commenting

Henrik Ramebäck for help with uncertainty analysis and GUM workbench

all my colleagues at Industrial Materials Recycling and Nuclear chemistry. I have enjoyed working with you!

Stellan Holgersson for fixing broken equipment and answering questions

Elin, Hanna, Emma, Toni and Sravya for sharing the experience and being my friends

Toni and Filip for being the best of roommates. Good times!

Kristian Larsson for leading the way

all my friends outside of Chalmers. You are very important to me!

my family for believing in me and always supporting me. I would not be here without you. You mean everything to me!

Martin for being you and for being a part of us. I love you!

Ella for furry companionship and comfort when I needed it the most. Woff woff!

This work was funded by The Swedish Energy Agency and The Swedish Research Council FORMAS

References

1. Armaroli, N. and Balzani, V., *The Future of Energy Supply: Challenges and Opportunities.* Angewandte Chemie International Edition, 2007. **46**(1-2): p. 52-66.
2. Lewis, N.S. and Nocera, D.G., *Powering the planet: Chemical challenges in solar energy utilization.* Proceedings of the National Academy of Sciences, 2006. **103**(43): p. 15729-15735.
3. Becquerel, A.E., *Mémoire sur les effets électriques produits sous l'influence des rayons solaires.* Comptes rendus hebdomadaires des séances de l'Académie des Sciences, 1839. **9**: p. 561-567.
4. Fraas, L. and Partain, L.D., eds. *Solar Cells and Their Applications*. 2:nd ed. Wiley Series in Microwave and Optical Engineering, ed. K. Chang. 2010, John Wiley & Sons: Hobroken, New Jersey.
5. Miles, R.W., Hynes, K.M., and Forbes, I., *Photovoltaic solar cells: An overview of state-of-the-art cell development and environmental issues.* Progress in Crystal Growth and Characterization of Materials, 2005. **51**(1-3): p. 1-42.
6. Cotal, H., Fetzer, C., Boisvert, J., Kinsey, G., King, R., Hebert, P., Yoon, H., and Karam, N., *III-V multijunction solar cells for concentrating photovoltaics.* Energy Environ. Sci., 2009. **2**(2): p. 174-192.
7. Goetzberger, A., Hebling, C., and Schock, H.-W., *Photovoltaic materials, history, status and outlook.* Materials Science and Engineering: R: Reports, 2003. **40**(1): p. 1-46.
8. Goncalves, L.M., Bermudez, V.d.Z., Ribeiro, H.A., and Mendes, A.M., *Dye-sensitized solar cells: a safe bet for the future.* Energy Environ. Sci., 2008. **1**(6): p. 655-667.
9. Hoppe, H. and Sariciftci, N.S., *Organic solar cells: An overview.* Journal of materials research, 2004. **19**(7): p. 1924-1945.
10. Kippelen, B. and Bredas, J.-L., *Organic photovoltaics.* Energy Environ. Sci., 2009. **2**(3): p. 251-261.
11. Miles, R.W., *Photovoltaic solar cells: Choice of materials and production methods.* Vacuum, 2006. **80**(10): p. 1090-1097.
12. Mehta, S., *2009 Global PV cell and module production analysis*. 2010, GTM Research, Greentech media inc.
13. Green, M.A., *Thin-film solar cells: review of materials, technologies and commercial status.* J. Mater. Sci.: Mater. Electron., 2007. **18**(Suppl. 1): p. S15-S19.
14. Miles, R.W., Zoppi, G., and Forbes, I., *Inorganic photovoltaic cells.* Materials Today, 2007. **10**(11): p. 20-27.
15. Green, M.A., *Estimates of Te and In prices from direct mining of known ores.* Progress in Photovoltaics: Research and Applications, 2009. **17**(5): p. 347-359.
16. European Commission, *Critical raw materials for the EU - Report of the Ad-hoc Working Group on defining critical raw materials*. 2010, European Commission.
17. Of the European Parliament and of the Council, *Directive 2012/19/EU of the European Parliament and of the Council of 4 July 2012 on waste electrical and electronic equipment (WEEE)*. 2012.
18. Fthenakis, V., *Sustainability of photovoltaics: The case for thin-film solar cells.* Renewable and Sustainable Energy Reviews, 2009. **13**(9): p. 2746-2750.
19. Berger, W., Sapich, G., and Weimann, K., *RESOLVED (Recovery of Solar Valuable Materials, Enrichment and Decontamination), Technical Final Report LIFE04/ENV/D/00047*. 2008, Federal Institute for Materials Research and Testing: Berlin.

20. SENSE, *Sustainability EvaluatioN of Solar Energy systems - Recycling of Production Waste*. 2002, Zentrum fuer Sonnenenergie- und Wasserstoff-Forschung: Stuttgart.
21. Drinkard Jr, W.F., Long, M.O., and Goozner, R.E., *Recycling of CIS photovoltaic waste*. 1998.
22. Kushiya, K., Ohshita, M., and Tanaka, M. *Development of recycling and reuse technologies for large-area Cu(InGa)Se2-based thin-film modules*. in *Proceedings of the 3rd World Conference on Photovoltaic Energy Conversion*. 2003. Osaka, Japan.
23. Menezes, S., *Electrochemical solutions to some thin-film PV manufacturing issues.* Thin Solid Films, 2000. **361-362**: p. 278-282.
24. Palitzsch, W., *Method for recycling a thin layer solar module during simultaneous recovering of recyclable material, by loading photovoltaic cells to be processed so that the plastic portion is separated from remaining components of the module*. 2010.
25. Palitzsch, W. and Loser, U., *Systematic Photovoltaic Waste Recycling.* Green, 2013. **3**(1): p. 79.
26. Aberle, A.G., *Thin-film solar cells.* Thin Solid Films, 2009. **517**(17): p. 4706-4710.
27. Lundberg, O., Bodegård, M., Malmström, J., and Stolt, L., *Influence of the Cu(In,Ga)Se2 thickness and Ga grading on solar cell performance.* Progress in Photovoltaics: Research and Applications, 2003. **11**(2): p. 77-88.
28. Green, M.A., Emery, K., Hishikawa, Y., Warta, W., and Dunlop, E.D., *Solar cell efficiency tables (version 44).* Progress in Photovoltaics: Research and Applications, 2014. **22**(7): p. 701-710.
29. Patniak, P., *Handbook of Inorganic Chemistry*. 2003, New York: MacGraw-Hill.
30. Berger, W., Simon, F.G., Weimann, K., and Alsema, E.A., *A novel approach for the recycling of thin film photovoltaic modules.* Resources Conservation and Recycling, 2010. **54**(10): p. 711-718.
31. Marwede, M., Berger, W., Schlummer, M., Mäurer, A., and Reller, A., *Recycling paths for thin-film chalcogenide photovoltaic waste - Current feasible processes.* Renewable Energy, 2013. **55**: p. 220-229.
32. Dodson, J.R., Hunt, A.J., Parker, H.L., Yang, Y., and Clark, J.H., *Elemental sustainability: Towards the total recovery of scarce metals.* Chemical Engineering and Processing: Process Intensification, 2012. **51**(0): p. 69-78.
33. Menezes, S., *Investigation of electrochemical processes for synthesis and removal of CuInSe2 thin films.* Mater. Res. Soc. Symp. Proc., 1996. **426**(Thin Films for Photovoltaic and Related Device Applications): p. 189-194.
34. Langer, J.M. and Heinrich, H., *Deep-Level Impurities: A Possible Guide to Prediction of Band-Edge Discontinuities in Semiconductor Heterojunctions.* Physical Review Letters, 1985. **55**(13): p. 1414-1417.
35. Greenwood, N. and Earnshaw, A., *Chemistry of the Elements, Second Edition*. 1997, Oxford, England: Butterworth-Heinemann.
36. Schlesinger, M.E., King, M.J., Sole, K.C., and Davenport, W.G., *Extractive Metallurgy of Copper (Fifth Edition)*, ed. M.E. Schlesinger, et al. 2011, Oxford: Elsevier. 1-12.
37. Fthenakis, V., Wang, W., and Kim, H.C., *Life cycle inventory analysis of the production of metals used in photovoltaics.* Renewable Sustainable Energy Rev., 2009. **13**(3): p. 493-517.
38. Alfantazi, A.M. and Moskalyk, R.R., *Processing of indium: a review.* Minerals Engineering, 2003. **16**(8): p. 687-694.
39. Downs, J.A., ed. *Chemistry of aluminium, gallium, indium and thallium*. 1993, Champman and Hall: Glasgow.

40. Felix, N., *Indium and Indium Compounds*, in *Ullmann's Encyclopedia of Industrial Chemistry*. 2000, Wiley-VCH Verlag GmbH & Co. KGaA.
41. Bautista, R.G., *Processing to obtain high-purity gallium.* JOM, 2003. **55**(3): p. 23-26.
42. Bawa, M.S., *Process for making hyperpure gallium*. 1975.
43. Hoffmann, J.E. and King, M.G., *Selenium and Selenium Compounds*, in *Kirk-Othmer Encyclopedia of Chemical Technology*. 2000, John Wiley & Sons, Inc.
44. Patnaik, P., *Handbook of Inorganic Chemicals*. 2003, New York: McGraw-Hill.
45. Clark, C.W. and Elkin, E.M., *Process for making selenium dioxide*. 1946.
46. Handwerk, E.C. and Monson, W.T., *Selenium recovery process*. 1960.
47. Rabjohn, N., *Selenium dioxide oxidation*, in *Organic chemistry*. 1949, John Wiley & Sons, Inc: New York. p. 331-446.
48. Riley, H.L., Morely, J.F., and Friend, N.A.C., *Selenium Dioxide, a New Oxidising Agent. Part I. Its Reaction with Aldehydes and Ketones.* Journal of the Chemical Society, 1932: p. 1875-1883.
49. Rabjohn, N., *Selenium dioxide oxidation*, in *Organic chemistry*. 1976, John Wiley & Sons, Inc: New York. p. 262-407.
50. Sharpless, K.B. and Gordon, K.M., *Selenium dioxide oxidation of ketones and aldehydes. Evidence for the intermediacy of β-ketoseleninic.* Journal of the American Chemical Society, 1976. **98**(1): p. 300-301.
51. Waitkins, G.R. and Clark, C.W., *Selenium Dioxide: Preparation, Properties, and Use as Oxidizing Agent.* Chemical Reviews, 1945. **36**(3): p. 235-289.
52. Rao, S.R., *Resource recovery and recycling from metallurgical wastes*. Waste Management Series. Vol. 7. 2006, London: Elsevier.
53. Sonoda, N., Kondo, K., Nagano, K., Kambe, N., and Morimoto, F., *CARBON-MONOXIDE WATER AS A REDUCING AGENT - FORMATION OF SELANE FROM SELENIUM.* Angewandte Chemie-International Edition in English, 1980. **19**(4): p. 308-309.
54. Smith, A.E., *Interferences in the determination of elements that form volatile hydrides with sodium borohydride using atomic-absorption spectrophotometry and the argon-hydrogen flame.* Analyst, 1975. **100**(1190): p. 300-306.
55. Wickstrom, T., Lund, W., and Bye, R., *Hydride generation atomic absorption spectrometry from alkaline solutions: determination of selenium in copper and nickel materials.* Journal of Analytical Atomic Spectrometry, 1991. **6**(5): p. 389-391.
56. Ayers, W.M., *Method and apparatus for constant composition delivery of hydride gases for semiconductor processing*. 1999.
57. Bastide, S., Hügel, P., Lévy-Clément, C., and Hodes, G., *Electrochemical preparation of H2S and H2Se.* Journal of The Electrochemical Society, 2005. **152**(3).
58. Gustafsson, A., Forman, M., and Ekberg, C., *Recycling of selenium from CIGS solar cell materials*, in *Industrial Materials Recycling*. 2012, Chalmers University of Technology: Gothenburg.
59. Kanari, N., Gaballah, I., and Allain, E., *A low temperature chlorination-volatilization process for the treatment of chalcopyrite concentrates.* Thermochimica Acta, 2001. **373**(1): p. 75-93.
60. Ojeda, M.W., Perino, E., and Ruiz, M.d.C., *Gold extraction by chlorination using a pyrometallurgical process.* Minerals Engineering, 2009. **22**(4): p. 409-411.
61. Nagasue, H., *Basic research for chlorination of copper and zinc in copper converter slag.* Transactions of the Japan Institute of Metals, 1979. **20**.
62. Fraissler, G., Jöller, M., Brunner, T., and Obernberger, I., *Influence of dry and humid gaseous atmosphere on the thermal decomposition of calcium chloride and its impact on the remove of*

heavy metals by chlorination. Chemical Engineering and Processing: Process Intensification, 2009. **48**(1): p. 380-388.

63. Campo, M.D., Bonnet, D., Gegenwart, R., and Beier, J., *Process for recycling CdTe/Cds thin film solar cell modules*. 2003.
64. Gaballah, I., Djona, M., Mugica, J.C., and Solozobal, R., *Valuable metals recovery from spent catalysts by selective chlorination.* Resources, Conservation and Recycling, 1994. **10**(1-2): p. 87-96.
65. Kubo, S., *Method of recovering gallium from scrap containing gallium*. 1987.
66. Ohwa, H., Yukinobu, M., Nabeshima, J., and Yasukawa, M., *High-Purity Metals Production of Sumitomo Metal Mining Co., Ltd.(SMM).* Extraction Metallurgy'89, 1989: p. 885-898.
67. Park, K.-S., Sato, W., Grause, G., Kameda, T., and Yoshioka, T., *Recovery of indium from In2O3 and liquid crystal display powder via a chloride volatilization process using polyvinyl chloride.* Thermochimica Acta, 2009. **493**(1-2): p. 105-108.
68. Shibasaki, T., Kimura, E., and Nishiyama, Y., *Process for recovering gallium trichloride from Gallium-containing waste*. 1990.
69. Siemens, R.E., Jong, B.W., and Russell, J.H., *Potential of spent catalysts as a source of critical metals.* Conservation & Recycling, 1986. **9**(2): p. 189-196.
70. Terakado, O., Iwaki, D., Murayama, K., and Hirasawa, M., *Indium Recovery from Indium Tin Oxide, ITO, Thin Film Deposited on Glass Plate by Chlorination Treatment with Ammonium Chloride.* Materials transactions, 2011. **52**(8): p. 1655-1660.
71. Terakado, O., Saeki, T., Irizato, R., and Hirasawa, M., *Pyrometallurgical recovery of indium from dental metal recycling sludge by chlorination treatment with ammonium chloride.* Materials transactions, 2010. **51**(6): p. 1136-1140.
72. Jena, P. and Brocchi, E., *Metal extraction through chlorine metallurgy.* Mineral Processing and Extractive Metallurgy Review, 1997. **16**(4): p. 211-237.
73. De Micco, G., Pasquevich, D.M., and Bohé, A.E., *Chlorination of aluminium-copper alloys.* Thermochimica Acta, 2007. **457**(1-2): p. 83-91.
74. Kanari, N., Gaballah, I., Allain, E., and Menad, N., *Chlorination of chalcopyrite concentrates.* Metallurgical and Materials Transactions B, 1999. **30**(4): p. 567-576.
75. Takahashi, K., Sasaki, A., Dodbiba, G., Sadaki, J., Sato, N., and Fujita, T., *Recovering Indium from the Liquid Crystal Display of Discarded Cellular Phones by Means of Chloride-Induced Vaporization at Relatively Low Temperature.* Metallurgical and Materials Transactions A, 2009. **40**(4): p. 891-900.
76. Túnez, F.M., Orosco, P., González, J.A., and Ruiz, M.D.C., *Kinetic study on the chlorination of indium oxide.* Thermochimica Acta, 2011. **524**(1-2): p. 151-156.
77. González, J., Ruiz, M., and Quiroga, O., *Kinetic study of the chlorination of gallium oxide.* Metallurgical and Materials Transactions B, 2005. **36**(4): p. 445-452.
78. Túnez, F.M., Gonzalez, J., and Ruiz, M.C., *GaAs chlorination study.* Latin American applied research, 2008. **38**(4): p. 369-375.
79. Tunez, F.M., Gonzalez, J.A., and Ruiz, M.d.C., *Thermogravimetric study of GaAs chlorination between -30 and 900 °C.* Thermochimica Acta, 2011. **523**(1-2): p. 124-136.
80. Poznański, J., *A study of the chlorination of copper(I) and copper(II) oxides.* Journal of the Less Common Metals, 1991. **169**(2): p. 181-186.
81. Bicerolu, O. and Gauvin, W.H., *The chlorination kinetics of zirconium dioxide in the presence of carbon.* The Canadian Journal of Chemical Engineering, 1980. **58**(3): p. 357-366.
82. González, J.A., Rivarola, J.B., and C. Ruiz, M., *Kinetics of chlorination of tantalum pentoxide in mixture with sucrose carbon by chlorine gas.* Metallurgical and Materials Transactions B, 2004. **35**(3): p. 439-448.

83. Ojeda, M.W., Rivarola, J.B., and Quiroga, O.D., *Study on chlorination of molybdenum trioxide mixed with carbon black.* Minerals Engineering, 2002. **15**(8): p. 585-591.
84. Pasquevich, D.M., Gamboa, J.A., and Caneiro, A., *On the role of carbon in the carbochlorination of refractory oxides.* Thermochimica Acta, 1992. **209**(0): p. 209-222.
85. Cao, Z.-f., Zhong, H., Liu, G.-y., and Zhao, S.-j., *Techniques of copper recovery from Mexican copper oxide ore.* Mining Science and Technology (China), 2009. **19**(1): p. 45-48.
86. Habbache, N., Alane, N., Djerad, S., and Tifouti, L., *Leaching of copper oxide with different acid solutions.* Chemical Engineering Journal, 2009. **152**(2-3): p. 503-508.
87. Bautista, R.G., *Gallium metal recovery.* JOM, 1989. **41**(6): p. 30-31.
88. Hoffmann, J., *Advances in the extractive metallurgy of selected rare and precious metals.* JOM Journal of the Minerals, Metals and Materials Society, 1991. **43**(4): p. 18-23.
89. Fang, Z. and Gesser, H.D., *Recovery of gallium from coal fly ash.* Hydrometallurgy, 1996. **41**(2–3): p. 187-200.
90. Li, J., Gao, S., Duan, H., and Liu, L., *Recovery of valuable materials from waste liquid crystal display panel.* Waste Management, 2009. **29**(7): p. 2033-2039.
91. Li, X.-h., Zhang, Y.-j., Qin, Q.-l., Yang, J., and Wei, Y.-s., *Indium recovery from zinc oxide flue dust by oxidative pressure leaching.* Transactions of Nonferrous Metals Society of China, 2010. **20**(Supplement 1): p. s141-s145.
92. Li, Y., Liu, Z., Li, Q., Liu, Z., and Zeng, L., *Recovery of indium from used indium–tin oxide (ITO) targets.* Hydrometallurgy, 2011. **105**(3–4): p. 207-212.
93. Yang, J., Retegan, T., and Ekberg, C., *Indium recovery from discarded LCD panel glass by solvent extraction.* Hydrometallurgy, 2013. **137**(0): p. 68-77.
94. Rao, S.R., *Chapter 4 Hydrometallurgical processes*, in *Resource recovery and recycling from metallurgical wastes*. 2006, Elsevier: London.
95. Wilson, A.M., Bailey, P.J., Tasker, P.A., Turkington, J.R., Grant, R.A., and Love, J.B., *Solvent extraction: the coordination chemistry behind extractive metallurgy.* Chemical Society Reviews, 2014. **43**(1): p. 123-134.
96. Lu, J. and Dreisinger, D., *Solvent extraction of copper from chloride solution I: Extraction isotherms.* Hydrometallurgy, 2013. **137**: p. 13-17.
97. Abisheva, Z.S., Blaida, I.A., Ponomareva, E.I., and Rozen, A.M., *Effect of amine structure on gallium extraction from hydrochloric acid solutions.* Hydrometallurgy, 1995. **37**(3): p. 393-399.
98. Ahmed, I.M., El-Nadi, Y.A., and El-Hefny, N.E., *Extraction of gallium(III) from hydrochloric acid by Cyanex 923 and Cyanex 925.* Hydrometallurgy, 2013. **131–132**(0): p. 24-28.
99. Bhat, T.R. and Sundararajan, S., *The extraction of gallium chloride by tributyl phosphate and the recovery of gallium from bayer liquor.* Journal of the Less Common Metals, 1967. **12**(3): p. 231-238.
100. Bhattacharya, B., Mandal, D., and Mukherjee, S., *Liquid–liquid extraction of gallium (III) with LIX 26.* Separation science and technology, 2003. **38**(6): p. 1417-1427.
101. Gupta, B., Mudhar, N., Begum, Z., and Singh, I., *Extraction and recovery of Ga (III) from waste material using Cyanex 923.* Hydrometallurgy, 2007. **87**(1): p. 18-26.
102. Mitchell, J.W. and Riley Jr, J.E., *Substoichiometric neutron-activation determination of gallium: Extraction from HCl with tri-n-octylphosphine oxide in cyclohexane.* Talanta, 1975. **22**(7): p. 567-570.
103. Sato, T., Nakamura, T., and Ishikawa, S., *Liquid-liquid extraction of gallium (III) from hydrochloric acid solutions by organophosphorus compounds and high-molecular weight amines.* Solvent Extraction and Ion Exchange, 1984. **2**(2): p. 201-212.

104. Zangen, M. and Rafaeloff, R., *Some mixed complexes of gallium—II: With ketones, chloride and bisulfate.* Journal of Inorganic and Nuclear Chemistry, 1970. **32**(8): p. 2753-2758.
105. Paiva, A.P., *Recovery of indium from aqueous solutions by solvent extraction.* Separation Science and Technology, 2001. **36**(7): p. 1395-1419.
106. Avila Rodriguez, M., Cote, G., and Bauer, D., *Recovery of Indium (III) from Mixed Hydrochloric Acid-Sulphuric Acid Media by Solvent Extraction with Cyanex 301®.* Solvent Extraction and Ion Exchange, 1992. **10**(5): p. 811-827.
107. Avila-Rodríguez, M., Cote, G., Navarro Mendoza, R., Saucedo Medina, T.I., and Bauer, D., *Thermodynamic trudy of the extraction of indium(III) and cadmium(II) by cyanex 301 from concentrated HCl media.* Solvent Extraction and Ion Exchange, 1998. **16**(2): p. 471-485.
108. Brunette, J.P., Taheri, M., Goetz-Grandmont, G., and Leroy, M.J.F., *Extraction of indium(III) from chloride medium with 1-phenyl-3-methyl-4-acylpyrazol-5-ones. Synergic effect with high molecular weight ammonium salts.* Polyhedron, 1982. **1**(5): p. 457-460.
109. Fischer, C., Wagner, H., Bagreev, V.V., and Stojanov, E.S., *On the extraction of In(III) with tri-n-octylamine from HCl solutions.* Journal of Inorganic and Nuclear Chemistry, 1977. **39**(3): p. 513-517.
110. Gupta, B., Deep, A., and Malik, P., *Liquid-liquid extraction and recovery of indium using Cyanex 923.* Analytica Chimica Acta, 2004. **513**(2): p. 463-471.
111. Maydan, D. and Marcus, Y., *ANION EXCHANGE OF METAL COMPLEXES. X.1 THE INDIUM—CHLORIDE SYSTEM. COMPARISON OF RESIN AND LIQUID ANION EXCHANGE.* The Journal of Physical Chemistry, 1963. **67**(5): p. 987-990.
112. Navrátil, O., Meindl, J., and Kos, J., *Extraction of indium (III) and antimony (III) from hydrochloric acid solutions by means of some neutral organophosphorus reagents.* Collection of Czechoslovak Chemical Communications, 1981. **46**(8): p. 1906-1912.
113. Nelson, A.D., Fasching, J.L., and McDonald, R.L., *Extraction of Fe (III) and In (III) from aqueous HCl by tri-n-octylamine in nitrobenzene.* Journal of Inorganic and Nuclear Chemistry, 1965. **27**(2): p. 439-447.
114. Rodríguez de San Miguel, E., Aguilar, J.C., and de Gyves, J., *An SLM system for the extraction of In(III) from concentrated HCl media using ADOGEN 364 as carrier.* Journal of Chemical Technology & Biotechnology, 1996. **66**(1): p. 56-64.
115. Rodríguez de San Miguel, E., de Gyves, J., Muñoz, M., and Valiente, M., *Solvent extraction of In(III) from concentrated HCl media with Adogen 364.* Solvent Extraction and Ion Exchange, 1995. **13**(1): p. 109-126.
116. Sato, T. and Sato, K., *Liquid-liquid extraction of indium (III) from aqueous acid solutions by acid organophosphorus compounds.* Hydrometallurgy, 1992. **30**(1–3): p. 367-383.
117. Virolainen, S., Ibana, D., and Paatero, E., *Recovery of indium from indium tin oxide by solvent extraction.* Hydrometallurgy, 2011. **107**(1–2): p. 56-61.
118. Irving, H. and Edgington, D.N., *The extraction of some metal chlorides into tri-n-butyl phosphate.* Journal of Inorganic and Nuclear Chemistry, 1959. **10**(3–4): p. 306-318.
119. De, A.K. and Sen, A.K., *Solvent extraction and separation of gallium(III), indium(III), and thallium(III) with tributylphosphate.* Talanta, 1967. **14**(6): p. 629-635.
120. Hasegawa, Y., Shimada, T., and Niitsu, M., *Solvent extraction of 3B group metal ions from hydrochloric acid with trioctylphosphine oxide.* Journal of Inorganic and Nuclear Chemistry, 1980. **42**(10): p. 1487-1489.
121. Kakade, S.M. and Shinde, V.M., *Extraction and spectrophotometric determination of gallium (III), indium (III) and thallium (III) in aluminium and aluminium alloys.* Analyst, 1993. **118**(11): p. 1449-1451.

122. Rafaeloff, R., *Separation of gallium from Group III elements, germanium, copper, arsenic, and iron.* Analytical Chemistry, 1971. **43**(2): p. 272-274.
123. Fortes, M.C.B., Martins, A.H., and Benedetto, J.S., *Indium recovery from acidic aqueous solutions by solvent extraction with D2EHPA: a statistical approach to the experimental design.* Brazilian Journal of Chemical Engineering, 2003. **20**: p. 121-128.
124. Nishihama, S., Hino, A., Hirai, T., and Komasawa, I., *Extraction and separation of gallium and indium from aqueous chloride solution using several organophosphorus componds as extractants.* Journal of Chemical Engineering of Japan, 1998. **31**(5): p. 818-827.
125. Nishihama, S., Hirai, T., and Komasawa, I., *Separation and Recovery of Gallium and Indium from Simulated Zinc Refinery Residue by Liquid-Liquid Extraction.* Industrial & Engineering Chemistry Research, 1999. **38**(3): p. 1032-1039.
126. Gupta, B., Mudhar, N., and Singh, I., *Separations and recovery of indium and gallium using bis(2,4,4-trimethylpentyl)phosphinic acid (Cyanex 272).* Separation and Purification Technology, 2007. **57**(2): p. 294-303.
127. Katsura, T. and Abe, H., *Solvent extraction of In and/or Ga*. 1975.
128. Good, M.L. and Holland Jr, F.F., *Extraction of In(III) and Ga(III) from aqueous chloride media by long chain alkyl amines and quaternary salts.* Journal of Inorganic and Nuclear Chemistry, 1964. **26**(2): p. 321-327.
129. Good, M.L. and Srivastava, S.C., *The nature of the halide complexes of Fe(III), Co(III), Ga(III) and In(III) extracted from aqueous chloride media by high molecular weight substituted alkyl ammonium compounds.* Journal of Inorganic and Nuclear Chemistry, 1965. **27**(11): p. 2429-2436.
130. Moats, M. and Free, M., *A Bright Future for copper electrowinning.* JOM, 2007. **59**(10): p. 34-36.
131. Oishi, T., Koyama, K., Alam, S., Tanaka, M., and Lee, J.-C., *Recovery of high purity copper cathode from printed circuit boards using ammoniacal sulfate or chloride solutions.* Hydrometallurgy, 2007. **89**(1): p. 82-88.
132. Lin, H.K., Wu, X.J., and Rao, P.D., *The electrowinning of copper from a cupric chloride solution.* JOM, 1991. **43**(8): p. 60-65.
133. Hoffmann, J.E., *Winning copper via chloride chemistry—An elusive technology.* JOM, 1991. **43**(8): p. 48-49.
134. Dalton, R.F., Diaz, G., Price, R., and Zunkel, A.D., *The cuprex metal extraction process: Recovering copper from sulfide ores.* JOM, 1991. **43**(8): p. 51-56.
135. Kekesi, T. and Isshiki, M., *Electrodeposition of copper from pure cupric chloride hydrochloric acid solutions.* Journal of Applied Electrochemistry, 1997. **27**(8): p. 982-990.
136. Napp, D.T., Johnson, D.C., and Bruckenstein, S., *Simultaneous and independent potentiostatic control of two indicator electrodes. Application to the copper(II)/copper(I)/copper system in 0.5M potassium chloride at the rotating ring-disk electrode.* Analytical Chemistry, 1967. **39**(4): p. 481-485.
137. Gray, D., *The Electrodeposition of Indium from Cyanide Solutions.* Transactions of The Electrochemical Society, 1934. **65**(1): p. 377-383.
138. Walsh, F. and Gabe, D., *The electrodeposition of indium.* Surface Technology, 1979. **8**(2): p. 87-99.
139. Westbrook, L.R., *Indium: Recovery by Electrodeposition.* Transactions of the American Electrochemical Society, 1930. **57**(1): p. 289-296.
140. Dennis, L.M. and Geer, W.C., *THE ATOMIC WEIGHT OF INDIUM.* Journal of the American Chemical Society, 1904. **26**(4): p. 437-438.

141. Fink, C.G. and Lester, R.H., *The Electrodeposition of Indium from Sulfate Baths.* Transactions of The Electrochemical Society, 1940. **78**(1): p. 349-372.
142. Markovoc, V. and Lovrecek, B., *Studies of the Electrochemical Kinetics of Indium: III . Systems and In + Combined Sulfate-Chloride Electrolyte.* Journal of The Electrochemical Society, 1966. **113**(8): p. 838-841.
143. Gunawardena, G., Pletcher, D., and Razaq, A., *The electrodeposition of indium onto vitreous carbon from acidic chloride media.* Journal of Electroanalytical Chemistry and Interfacial Electrochemistry, 1984. **164**(2): p. 363-367.
144. Lee, M.-S. and Sohn, K.-Y., *Comparison of indium purification between vacuum refining and electrowinning.* Journal of Materials Science, 2003. **38**(24): p. 4843-4848.
145. Mathers, F.C., *A study of the atomic weight of indium.* Journal of the American Chemical Society, 1907. **29**(4): p. 485-495.
146. Muñoz, A.G., Saidman, S.B., and Bessone, J.B., *Electrodeposition of Indium onto Vitreous Carbon from Acid Chloride Solutions.* Journal of The Electrochemical Society, 1999. **146**(6): p. 2123-2130.
147. Okamoto, H. and Takebayashi, K., *Method for recovering indium by electrowinning and apparatus therefor*. 1996.
148. Brown, R.W., *Recovery of gallium from alkali metal aluminate solutions*. 1952.
149. De la Breteque, P., *Method of recovering gallium from an alkali aluminate lye*. 1957.
150. Dorin, R. and Frazer, E.J., *The electrodeposition of gallium from synthetic Bayer-process liquors.* Journal of Applied Electrochemistry, 1988. **18**(1): p. 134-141.
151. Jelačić, Ć., Barišin, D., and Batinić-Haberle, I., *Method of obtaining gallium from aluminate solution by electrolysis.* Materials Science and Technology, 1986. **2**(4): p. 416-419.
152. Miyake, S., *Method for directly electrochemically extracting gallium from a circulating aluminate solution in the bayer process by eliminating impurities*. 1972, Google Patents.
153. Sebba, F. and Pugh, W., *281. Gallium. Part II. The extraction of gallium and germanium from germanite.* Journal of the Chemical Society (Resumed), 1937(0): p. 1371-1373.
154. Flamini, D.O., Saidman, S.B., and Bessone, J.B., *Electrodeposition of gallium onto vitreous carbon.* Journal of Applied Electrochemistry, 2007. **37**(4): p. 467-471.
155. Rafaeloff, R. and Yellin, E., *The electrodeposition of gallium.* Journal of the Less Common Metals, 1969. **19**(1): p. 63-65.
156. Stearns, R.I., *Electrolytic production of high-purity gallium*. 1969.
157. Sundararajan, S. and Bhat, T., *The electrodeposition of gallium from a chloride bath.* Journal of the Less Common Metals, 1966. **11**(5): p. 360-364.
158. Richards, T.W. and Boyer, S., *FURTHER STUDIES CONCERNING GALLIUM. Its Electrolytic Behavior, Purification, Melting Point, Density, Coefficient of Expansion, Compressibility, Surface Tension, and Latent Heat of Fusion.* Journal of the American Chemical Society, 1921. **43**(2): p. 274-294.
159. Fogg, H.C., *A Review of the Electrochemistry of Gallium.* Transactions of The Electrochemical Society, 1934. **66**(1): p. 107-115.
160. Roine, A., *HSC Chemistry for Windows, Version 5.1.* 2003, Outokumpu Research: Pori, Finland.
161. Erdey, L., Gál, S., and Liptay, G., *Thermoanalytical properties of analytical-grade reagents: Ammonium salts.* Talanta, 1964. **11**(6): p. 913-940.
162. De Micco, G., Bohé, A., and Pasquevich, D., *A thermogravimetric study of copper chlorination.* Journal of alloys and compounds, 2007. **437**(1): p. 351-359.

163. Kanari, N., Allain, E., Joussemet, R., Mochón, J., Ruiz-Bustinza, I., and Gaballah, I., *An overview study of chlorination reactions applied to the primary extraction and recycling of metals and to the synthesis of new reagents.* Thermochimica Acta, 2009. **495**(1-2): p. 42-50.

164. Jones, D.A., *Principles and prevention of corrosion, 2nd Edition*. 1996, Upper Saddle River, NJ: Prentice hall.

165. Sillén, L.G., Martell, A.E., and Bjerrum, J., *Stability constants of metal-ion complexes*. Vol. 17. 1964: Chemical Society London.

166. Rydberg, J., Cox, M., Musikas, C., and Choppin, G.R., *Solvent extraction principles and practice. Second edition, revised and expanded*. 2004, New York: Marcel Dekker.

167. Brugger, J., McPhail, D.C., Black, J., and Spiccia, L., *Complexation of metal ions in brines: application of electronic spectroscopy in the study of the Cu(II)-LiCl-H2O system between 25 and 90°C.* Geochimica et Cosmochimica Acta, 2001. **65**(16): p. 2691-2708.

168. Ferri, D., Salvatore, F., Vasca, E., and Miranda, R., *Complex Formation Equilibria at High Ligand Concentration: Indium (III)-Chloride Complexes.* Annali di chimica, 1994. **84**(3-4): p. 141-148.

169. Mihailov, M.H., *A correlation between the overall stability constants of metal complexes—I: Calculation of the stability constants using the formation function n.* Journal of Inorganic and Nuclear Chemistry, 1974. **36**(1): p. 107-113.

170. Scholz, F. and Pickett, C.J., eds. *Encyclopedia of Electrochemistry, Volume 7A, Inorganic Electrochemistry*. ed. A.J. Bard and M. Stratmann. 2006, Wiley-VCH.

171. Bard, A.J. and Faulkner, L.R., *Electrochemical methods: fundamentals and applications, 2nd edition*. Vol. 2. 2001: Wiley New York.

172. Antelman, M.S., *The encyclopedia of chemical electrode potentials*. 1982, New York: Plenum Press.

173. Schwartz, M., *Deposition from aqueous solutions: an overview*, in *Handbook of Deposition Technologies for Films and Coatings—Science, Technology and Applications*. 1994, William Andrew Publishing: Noyes. p. 506.

174. Nagy, Z., Blaudeau, J.P., Hung, N.C., Curtiss, L.A., and Zurawski, D.J., *Chloride Ion Catalysis of the Copper Deposition Reaction.* Journal of The Electrochemical Society, 1995. **142**(6): p. L87-L89.

175. Soares, D.M., Wasle, S., Weil, K.G., and Doblhofer, K., *Copper ion reduction catalyzed by chloride ions.* Journal of Electroanalytical Chemistry, 2002. **532**(1–2): p. 353-358.

176. Peters, D.G. and Cruser, S.A., *Cathodic chronopotentiometry of copper(I) and copper(II) in chloride media.* Journal of Electroanalytical Chemistry (1959), 1965. **9**(1): p. 27-40.

177. Miller, J.N. and Miller, J.C., *Statistics and chemometrics for analytical chemistry*. 2005: Prentice Hall.

178. Lindström, S., *Midsummer AB, Elektronikhöjden 6, 175 43 JÄRFÄLLA, SWEDEN*. +46-8-525 09 610.

179. Jaremalm, E., *Personal communication*. +46 8 525 09 610, Midsummer AB, Järfälla, Sweden.

180. Jagner, D., Sahlin, E., and Renman, L., *Experimental and computational study of species formed during electrochemical stripping oxidation of copper in chloride media determination of copper(II) in the ng l−1 range by stripping potentiometry.* Talanta, 1995. **42**(10): p. 1447-1455.

181. Ribeaucourt, L., Savidand, G., Lincot, D., and Chassaing, E., *Electrochemical study of one-step electrodeposition of copper–indium–gallium alloys in acidic conditions as precursor layers for Cu(In,Ga) Se$_2$ thin film solar cells.* Electrochimica Acta, 2011. **56**(19): p. 6628-6637.

182. Lincot, D., Guillemoles, J.F., Taunier, S., Guimard, D., Sicx-Kurdi, J., Chaumont, A., Roussel, O., Ramdani, O., Hubert, C., Fauvarque, J.P., Bodereau, N., Parissi, L., Panheleux, P., Fanouillere, P., Naghavi, N., Grand, P.P., Benfarah, M., Mogensen, P., and Kerrec, O., *Chalcopyrite thin film solar cells by electrodeposition.* Solar Energy, 2004. **77**(6): p. 725-737.
183. Külkens, H. and Fritzsche, P.E., *Verfahren zu galvanischen Abscheidung von Indium, insbesondere Indiumüberzügen*. 1960.
184. Bockris, J.O.M. and Enyo, M., *Electrodeposition of Gallium on Liquid and Solid Gallium Electrodes in Alkaline Solutions.* Journal of The Electrochemical Society, 1962. **109**(1): p. 48-54.
185. Fayram, T.S. and Anderson, C.G., *The development and implementation of industrial hydrometallurgical gallium and germanium recovery.* Journal of the South African Institute of Mining and Metallurgy, 2008. **108**(5): p. 261-272.
186. Sleppy, W.C. and Goheen, R.H., *Process for electrolytic recovery of metallic gallium*. 1975.
187. Smart, L.E. and Moore, E.A., *Solid State Chemistry An Introduction, 3rd edition*. 3 ed. 2005, Boca Raton (FL): CRC Press.
188. Markvart, T., Castañer, L., Tom, M., and Luis, C., *Principles of solar cell operation*, in *Solar Cells: Materials Manufacture and Operation* 2005, Elsevier Science: Oxford. p. 5-27.
189. Chopra, K.L., Paulson, P.D., and Dutta, V., *Thin-film solar cells: an overview.* Progress in Photovoltaics: Research and Applications, 2004. **12**(2-3): p. 69-92.
190. Shah, A., Torres, P., Tscharner, R., Wyrsch, N., and Keppner, H., *Photovoltaic Technology: The Case for Thin-Film Solar Cells.* Science, 1999. **285**(5428): p. 692-698.
191. Fathi, M. and Mougas, A., *Recycling of a defective metal insulator semiconductor solar cell by hot phosphoric acid.* Journal of Renewable and Sustainable Energy, 2011. **3**(1).
192. Frisson, L., Lieten, K., Bruton, T., De Clercq, K., de Moor, H., Goris, M., Benali, A., and Aceves, O. *Recent improvements in industrial PV module recycling*. in *16th European Photovoltaic Solar Energy Conference* 2000. Glasgow, Scotland.
193. Klugmann-Radziemska, E., Ostrowski, P., Drabczyk, K., Panek, P., and Szkodo, M., *Experimental validation of crystalline silicon solar cells recycling by thermal and chemical methods.* Solar Energy Materials and Solar Cells, 2010. **94**(12): p. 2275-2282.
194. Pa, P.S., *A Reclaiming Process for Solar Cell Silicon Wafer Surfaces.* Journal of Nanoscience and Nanotechnology, 2011. **11**(1): p. 691-695.
195. Bohland, J.R. and Anisimov, I.I. *Possibility of recycling silicon PV modules*. in *Proceedings of the 26th IEEE Photovoltaic Specialists Conference*. 1997. Anaheim, USA.
196. Yamashita, K., Miyazawa, A., and Sannomiya, H. *Research and Development on Recycling and Reuse Treatment Technologies for Crystalline Silicon Photovoltaic Modules*. in *Photovoltaic Energy Conversion, Conference Record of the 2006 IEEE 4th World Conference on*. 2006.
197. Fallavollita, J.A., *Methods and apparatus for recovery of silicon and silicon carbide from spent wafer-sawing slurry*. 2011.
198. Grabbe, A. and Ragan, T.M., *Method to recover and purify silicon from saw kerf.* 2010.
199. Hariharan, A.V. and Ravi, J., *Method to convert waste silicon to high purity silicon*. 2010.
200. Lin, Y.-C., Wang, T.-Y., Lan, C.-W., and Tai, C.Y., *Recovery of silicon powder from kerf loss slurry by centrifugation.* Powder Technology, 2010. **200**(3): p. 216-223.
201. Moro, L., Xiaobing, X., Perez-Mariano, J., Kai, L., Dubois, L.H., Lochtenberg, B., and Sanjurjo, A. *Low-cost solar-grade silicon: Purification and consolidation of silicon fines from wafering*. in *Photovoltaic Specialists Conference (PVSC), 2010 35th IEEE*. 2010.

202. Seo, K.H., Kang, B.H., and Kim, K.Y., *Fast melting and refining of recycled silicon powders from the wafer back grinding process for solar cell feedstock.* Materials Science Forum, 2012. **706-709**: p. 859-864.
203. Tai, Y.-D. and Lin, Y.-C., *Recovery of silicon and silicon carbide powder from kerf loss slurry using particle phase-transfer method*. 2010.
204. Tsai, T.-H., *Silicon sawing waste treatment by electrophoresis and gravitational settling.* Journal of Hazardous Materials, 2011. **189**(1-2): p. 526-530.
205. Zhang, L. and Ciftja, A., *Recycling of solar cell silicon scraps through filtration, Part I: Experimental investigation.* Solar Energy Materials and Solar Cells, 2008. **92**(11): p. 1450-1461.
206. Bombach, E., Müller, A., Wambach, K., and Röver, I., *Recycling of solar cells and modules-recent improvements*, in *Proceedings of the 20th European Photovoltaic Solar Energy Conference*. 2005: Barcelona, Spain.
207. Fthenakis, V.M., Morris, S.C., Moskowitz, P.D., and Morgan, D.L., *Toxicity of cadmium telluride, copper indium diselenide, and copper gallium diselenide.* Progress in Photovoltaics: Research and Applications, 1999. **7**(6): p. 489-497.
208. Goozner, R.E., Drinkard, W.F., Long, M.O., and Byrd, C.M. *A process to recycle thin film PV materials*. in *Proceedings of the 26th IEEE Photovoltaic Specialists Conference*. 1997. Anaheim, USA.
209. Goozner, R.E., Long, M.O., and Drinkard Jr, W.F., *Recycling of CdTe photovoltaic waste*. 1999.
210. Bohland, J., Anisimov, I., Dapkus, T., Sasala, R., Samigielski, K., and Kamm, K., *Recaliming metallic material from an article comprising a non-metallic friable substrate*. 2000.
211. Bradwell, D.J., Osswald, S., Wei, W., Barriga, S.A., Ceder, G., and Sadoway, D.R., *Recycling ZnTe, CdTe, and other compound semiconductors by ambipolar electrolysis.* Journal of the American Chemical Society, 2011. **133**(49): p. 19971-19975.
212. Fthenakis, V.M. and Wang, W., *Extraction and separation of Cd and Te from cadmium telluride photovoltaic manufacturing scrap.* Progress in Photovoltaics: Research and Applications, 2006. **14**(4): p. 363-371.
213. Menezes, S., *Electrochemical approach for removal, separation and retrieval of CdTe and CdS films from PV module waste.* Thin Solid Films, 2001. **387**(1-2): p. 175-178.
214. Mezei, A., Ashbury, M., Canizares, M., Molnar, R., Given, H., Meader, A., Squires, K., Ojebuoboh, F., Jones, T., and Wang, W., *Hydrometallurgical recycling of the semiconductor material from photovoltaic materials - Part one: Leaching*, in *Hydrometallurgy 2008: Proceedings of the Sixth International Symposium*, C.A. Young, Editor. 2008, Society for Mining, Metallurgy & Exploration Inc. p. 209.
215. Mezei, A., Ashbury, M., Canizares, M., Molnar, R., Given, H., Meader, A., Squires, K., Ojebuoboh, F., Jones, T., and Wang, W., *Hydrometallurgical recycling of the semiconductor material from photovoltaic materials - Part two: Metal recovery*, in *Hydrometallurgy 2008: Proceedings of the Sixth International Symposium*, C.A. Young, Editor. 2008, Society for Mining, Metallurgy & Exploration. p. 224.
216. Choi, J.-K. and Fthenakis, V., *Economic Feasibility of Recycling Photovoltaic Modules.* Journal of Industrial Ecology, 2010. **14**(6): p. 947-964.
217. Dean, J.R., *Practical Inductively Coupled Plasma Spectroscopy*. 2005: John Wiley & Sons, Ltd.
218. Harris, D.C., *Quantitative Chemical Analysis*. 7:th ed. 2007, New York: W. H. Freeman and Company.

219. Joint Committee of Powder Diffraction Standards, *JCPDS-ICCD: PDF-4 release 2010*. 2010, Philadelphia, USA.
220. Choppin, G.R., Liljenzin, J.-O., Rydberg, J., and Ekberg, C., *Radiochemistry and nuclear chemistry, 4th edition*. 3rd ed. 2013: Butterworth-Heinemann.
221. Hassfjell, S. +47 63 80 61 84, Institute of Energy Technology, Kjeller, Norway.

List of Abbreviations and Terms

CdS	Cadmium Sulphide
CdTe	Cadmium Telluride
CIGS	Copper Indium Gallium Selenide ($Cu(In,Ga)Se_2$)
Cyanex 272	di(2,4,4-trimethylpentyl)phosphinic acid
Cyanex 923	a mixture of four different trialkyl phosphine oxides
D2EHPA	di-(2-ethylhexyl) phosphoric acid
Gas-MS	Gas – Mass Spectroscopy
GC-MS	Gas Chromatography – Mass Spectroscopy
ICP-MS	Inductively Coupled Plasma – Mass Spectroscopy
ICP-OES	Inductively Coupled Plasma – Optical Emission Spectroscopy
LIX 84-I	2-hydroxy-5-nonylacetophenone oxime
LIX860	5-dodecylsalicylaldoxime
LIX984	mixture of LIX 84-I and LIX860 at a volume ration of 1:1
NAA	Neutron activation analysis
PV	Photovoltaic
TBP	tributylphosphate
TCO	Transparent Conductive Oxide
TOPO	trioctyl phosphine oxide
XRD	X-Ray Diffraction

Appendix A

Solar cells

The active material in a solar cell is a semiconductor. When sunlight hits the semiconductor material the absorbed energy promotes an electron to the conduction band, making the material conductive [187]. The construction of the device then ensures that the free electron can only be transported in one direction, thereby generating an electric current in an outer circuit connected to the device. The standard type of solar cell is the pn-junction solar cell [4], see Fig. A1.

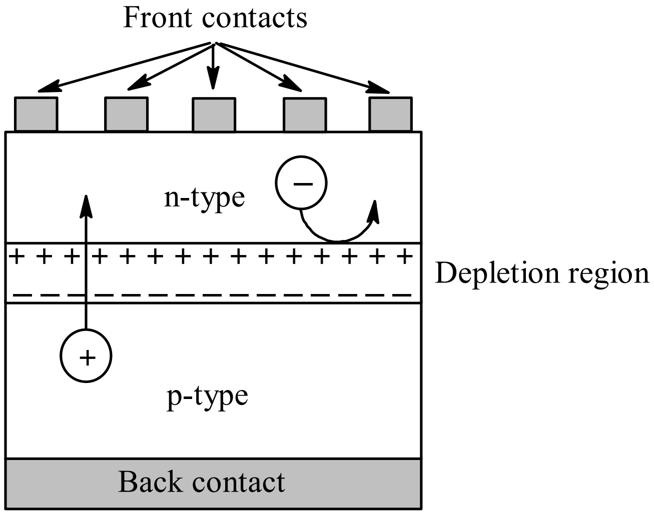

Fig. A1 Schematic cross-section of a standard pn-junction solar cell [187].

A semiconductor material that is deficient in electrons is called p-type (p for positive). One example of such a material is silicon doped with an element with fewer valence electrons, e.g. boron. Doping is the deliberate introduction of an impurity into a material. If, on the other hand, the material has an excess of valence electrons it is called n-type (n for negative). Doping of silicon with e.g. phosphorus, gives this kind of material. When regions of n-type and p-type doping meet in a semiconductor crystal electrons from the n-type will migrate into the p-type in order to balance the difference in electron concentration [187]. The migration of electrons into the p-type will give rise to a depletion region and a negative charge that counteracts further migration will be established. The electric field in the depletion region ensures that electrons can only be transported in one direction; from p-type to n-type [188]. If the same semiconductor is used as both p-type and n-type, as in the example with silicon above, the junction is called a homojunction. When different materials are used, e.g. CIGS/CdS, the junction is called a heterojunction [188].

In addition to the semiconductor, a solar cell consists of several different layers. The thickness of the absorber layer in thin film solar cells is typically <2 µm [27] which means that it is more than a 100 times thinner than silicon wafers [7]. Thus, while mono- and multicrystalline wafers are self-supporting (see Figure A1) thin film solar cells, e.g. amorphous silicon, CdTe and CIGS, need a supporting base called a substrate, see Fig. A2 [189].

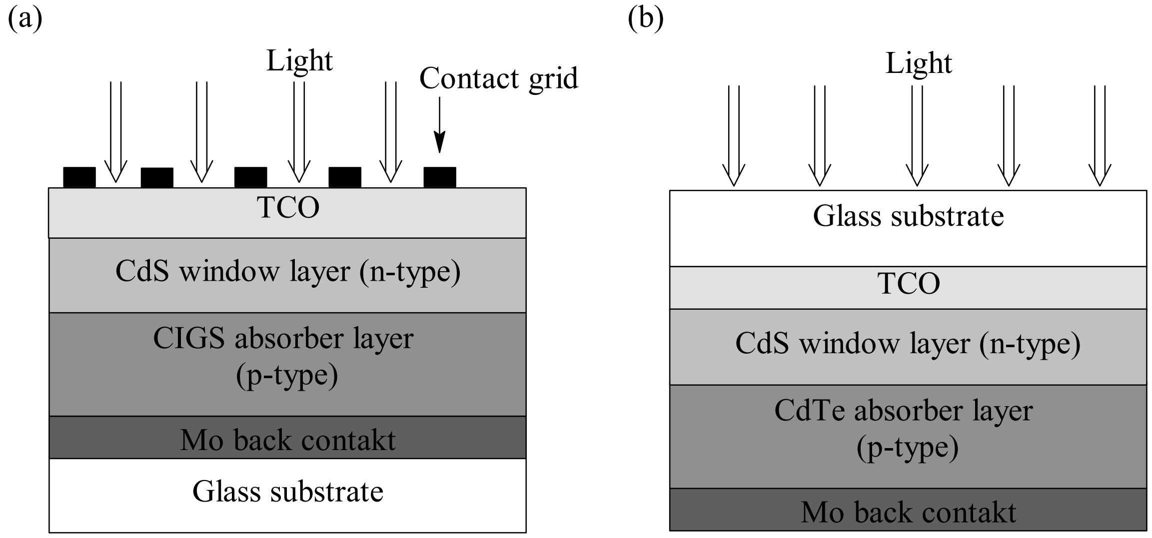

Fig. A2 Schematic cross-section of (a) a CIGS solar cell and (b) a CdTe solar cell [189].

For the solar cell to produce electricity it must be connected to an outer circuit. This is facilitated by contacts at the front and back of the semiconductor material. The back contact is usually a thin layer of molybdenum. The front contact can be provided by screen printing of a metal grid (Fig. A1), alternatively a transparent conductive oxide (TCO) can be used, e.g. zinc oxide (Fig. A2b) or a combination of the two (Fig. A2a) [14]. For energy production several solar cells are connected to form a solar cell module. Normally the module is laminated with EVA (ethylene-vinyl acetate) polymer onto a glass plate and encased in an aluminium frame for protection [21].

The top efficiency for different types of solar cells and solar cell modules are reviewed annually [28]. Currently the record holder for a small single-junction, laboratory device is a gallium arsenide cell with an efficiency of 28.8 % of the solar energy. This can be compared with 25.6 % for crystalline silicon, 20.5 % for CIGS and 19.6 % for CdTe. The corresponding numbers for solar cell modules are 22.9 % for crystalline silicon, 15.7 % for CIGS and 17.5 % for CdTe. The lower efficiency of the modules is due to the difficulty in scaling up the production methods. Modules made on an industrial scale seldom reach efficiencies over 10 % for thin film technologies and 16 % for silicon wafer technology due to the balance between efficiency and cost [13].

Recycling of silicon solar cells

Mono- and multicrystalline silicon are the dominating solar cell materials on the market with a market share of 81 % [12]. Over the past 15 years insufficient feedstock supply and the high price of silicon suitable for solar cell production [190] has made recycling an important issue. The focus on recycling of mono- and multicrystalline silicon solar cells has been mostly on the reuse of wafers with [191-194] or without [195, 196] removal of the pn-junction and other layers. There have also been considerable efforts made on the recycling of the waste material (kerf loss) from wafer production [197-205]. The only silicon solar cells recycling process that has been commercialized was developed by Deutsche Solar [30]. The process includes thermal delamination of the module, followed by manual separation of the glass and removal of contacts, anti-reflective coating and pn-junction by etching [206]. After the treatment intact silicon wafers are reused in new solar cells while broken wafers are melted and made into new wafers.

Recycling of CdTe solar cells

Considerable attention has been given to the recycling of CdTe solar cells, partly due to the toxicity of cadmium and partly because of the high cost and limited supply of tellurium [18, 207]. Two different approaches to the recycling of CdTe can be distinguished. The first approach includes removal of the semiconductor from the substrate and a purification step, but no separation of the elements [19, 208, 209]. In this case the challenge of separating the elements is transferred to the producers of solar cell semiconductor materials. The second approach includes separation of the elements into separate process streams [210-212]. In addition a completely different process, where an electrochemical cell is used to redeposit CdTe from an old solar cell onto a new substrate, has been developed by Menezes [213]. Of the processes that have been commercialized the most notable is the process developed by the CdTe solar cell producer First Solar [214-216]. The modules are dismantled and the semiconductor material is leached from the glass using a mixture of sulphuric acid and hydrogen peroxide [214, 216]. After leaching, the metals are precipitated with sodium hydroxide and form stable compounds, which makes further recycling of tellurium impossible [214, 216] or recovered with a combination of solvent extraction and electrodeposition [215].

Appendix B - Analytical techniques

ICP-OES

Inductively Coupled Plasma – Optical Emission Spectroscopy (ICP-OES) is used to analyze the concentration of different elements in solution. After passing through a nebulizer the analytes in the liquid sample are atomized in the plasma. The high excitation energy of the atoms in the plasma will cause them to emit electromagnetic radiation, which is detected in the optical emission detector. More information on ICP-OES is given by Dean (2005) [217]. A Thermo iCAP 6500 was used to analyze the composition of the different solar cell materials, before and after the experiments. All samples and standards were diluted using a solution of 0.1 M nitric acid made from Suprapur® nitric acid (65 %, Merck) and ultrapure water obtained from a Milli-Q® system (>18 MΩ·cm, Millipore Milli-Q Plus 185). The limit of detection (LOD) for each element was determined according to [218]

$\mathrm{LOD} = y_{\mathrm{blank}} + 3s_{\mathrm{blank}}$

where y_{blank} is the mean and s_{blank} is the standard deviation of 20 replicates measured on blank samples.

ICP-MS

Inductively Coupled Plasma – Mass Spectrometry (ICP-MS) is used to analyse the concentration of different elements in solutions. After atomization in the plasma the mass spectrometer measures the mass-to-charge ratio of the ions. The ions are separated by an electric field and detected with an electron multiplier detector. For further information on this technique see Dean (2005) [217]. A Perkin Elmer ELAN 6000 was used to determine the purity of the selenium from the selenium dioxide distillation experiments. All samples and standards were diluted with a solution of 1 M nitric acid made from Suprapur® nitric acid (65 %, Merck) and ultrapure water obtained from a Milli-Q® system (>18 MΩ, Millipore Milli-Q Plus 185).

GC-MS

Gas chromatography – Mass Spectrometry (GC-MS) is a combination of gas chromatography and mass spectroscopy. Gas chromatography is used to separate mixtures of chemicals in the gas phase into individual components prior to characterization in the mass spectrometer. Liquid samples are evaporated prior to analysis. This technique is described in more detail by Harris (2007) [218]. The purity of the organic product from the Riley oxidation was analysed with a GI800A GCD System from Hewlet Packard using a sp2330 column.

XRD

In X-ray powder diffraction (XRD) finely ground crystalline powder is exposed to monochromatic X-rays. The crystal planes in the crystallites will diffract the incoming X-rays according to Bragg’s law and the phase composition of the crystalline material in the sample can be determined. More details about this technique are given in Smart and Moore (2005) [187]. XRD was used to identify crystalline compounds in the CIGS materials, before and after the oxidation and chlorination experiments. A Bruker D2 Phaser diffractometer with a Cu Kα-source (λ=1.5418 Å) and a Lynxeye® silicon strip detector were used. The results were evaluated using the Joint Committee of Powder Diffraction Standards Database [219]. The detection limit for a crystalline compound using this method is approximately 2 % by weight. Non-crystalline compounds cannot be identified.

NAA

Neutron activation analysis (NAA) is a highly sensitive, non-destructive method used to determine concentrations of elements in a wide variety of samples. The atoms in a sample are bombarded with neutrons, causing the atoms to form radioactive isotopes. Detection of the gamma emission from the sample can then be used to determine the concentration of the elements. More information on this method is given in Choppin *et al.* [220]. The neutron activation analysis (NAA), which was used to determine the iron content in the recycled selenium, was performed using the 2MW JEEP II reactor at the Institute for Energy Technology in Kjeller, Norway. The neutron flux in the reactor was 10^{13} neutrons cm^{-2} s^{-1} with a relatively hard neutron spectrum where the epithermal neutron flux was 5 to 10 % of the thermal neutron flux [221]. After the irradiation the samples were analysed with high purity germanium detectors (HPGe, Canberra γ-analyst, ORTEC and Tennelec, respectively).